




5-2016

## **Novel Methods and Sensors for the Analysis of Trace Chemicals with Potential Environmental Applications**

Samuel Mason Rosolina

*University of Tennessee - Knoxville, srosolin@vols.utk.edu*

Follow this and additional works at: [https://trace.tennessee.edu/utk\\_graddiss](https://trace.tennessee.edu/utk_graddiss)

 Part of the [Analytical Chemistry Commons](#), and the [Environmental Chemistry Commons](#)

---

### **Recommended Citation**

Rosolina, Samuel Mason, "Novel Methods and Sensors for the Analysis of Trace Chemicals with Potential Environmental Applications. " PhD diss., University of Tennessee, 2016.  
[https://trace.tennessee.edu/utk\\_graddiss/3740](https://trace.tennessee.edu/utk_graddiss/3740)

This Dissertation is brought to you for free and open access by the Graduate School at TRACE: Tennessee Research and Creative Exchange. It has been accepted for inclusion in Doctoral Dissertations by an authorized administrator of TRACE: Tennessee Research and Creative Exchange. For more information, please contact [trace@utk.edu](mailto:trace@utk.edu).

To the Graduate Council:

I am submitting herewith a dissertation written by Samuel Mason Rosolina entitled "Novel Methods and Sensors for the Analysis of Trace Chemicals with Potential Environmental Applications." I have examined the final electronic copy of this dissertation for form and content and recommend that it be accepted in partial fulfillment of the requirements for the degree of Doctor of Philosophy, with a major in Chemistry.

Zi-Ling Xue, Major Professor

We have read this dissertation and recommend its acceptance:

Frank Vogt, Michael D. Best, Thomas A. Zawodzinski

Accepted for the Council:

Carolyn R. Hodges

Vice Provost and Dean of the Graduate School

(Original signatures are on file with official student records.)

**Novel Methods and Sensors for the Analysis of Trace  
Chemicals with Potential Environmental Applications**

**A Dissertation Presented for the  
Doctor of Philosophy  
Degree**

**The University of Tennessee, Knoxville**

**Samuel Mason Rosolina**

**May 2016**

Copyright © 2016 by Samuel M. Rosolina

All rights reserved.

# DEDICATION

To my parents, Kris and Larry  
my sister, Rachel  
and my wife, Erin.

Your belief in me has carried me so much further than I could have imagined.

Thank you.

## ACKNOWLEDGEMENTS

As this chapter in my life comes to a close, I cannot forget the many people that have helped me along the way. First and foremost I want to thank my advisor, Dr. Zi-Ling Xue for the work that he has put into me, the patience he has had with me, and the time he has given me. While first choosing a lab to join, the research projects that Dr. Xue had chosen resonated with me; but it was his kindness and excitement that lead me to join his group. I am truly glad that I made that decision, and truly thankful to have worked for, and with, Dr. Xue. Similarly, Dr. James Chambers has become a teacher, advisor, and friend over my time at UT. His knowledge of electrochemistry, his ability to give suggestions as well as praise, and his commitment to helping me and the rest of the Xue group has made him indispensable. For that, I will always be grateful.

I would also like to thank those who have served on my committee. Dr. Frank Vogt was a great professor to learn from, and a great professor to teach for. His love for his students is apparent, and his excitement as an educator is contagious. Dr. Michael Best has been a role model in the chemistry department. Seeing him interact with his graduate students, other faculty, and staff, I recognized early in my graduate career that he has perfected the balance of being personable and professional. I am especially thankful to Drs. Vogt and Best for joining my committee after past committee members were unable to serve. I am always struck by Dr. Thomas Zawodzinski's breadth of scientific knowledge, and his charismatic nature, and am honored to have his

electrochemistry expertise brought to the table. I am incredibly thankful for Drs Jon Camden and Robert Compton, both of whom served on my committee before leaving the University of Tennessee to begin their own new chapters in life. Dr. Camden was not only my professor (and choir director!), but he is still a role model to me. Dr. Compton, a fellow Berean, was always full of great stories, advice, and curiosity based questions that encouraged me to dig deeper in my studies. Thank you all for your time and help.

The members of the Xue group, past and present, have really made my time at UT more enjoyable, and easier to survive. I am especially grateful to the members who were present when I joined; they made my transition to Knoxville so much easier. Dr. Ruizhuo Ouyang was a very important resource to me when I began my research in electrochemistry. She is so kind and patient, attributes that made it so much easier for me to learn. Dr. Stefanie Bragg became such a good friend from the very beginning and was also willing to give her time, without complaint, to show me the ropes. Dr. Adam Lamb became a close friend as well, and always had the time when I needed to whine about something new. I could not have asked for a better teammate than Dr. Jonathan Fong when it came time to collect free stuff at the Pittcon expos. I was sad to see all of them leave Knoxville, as well as Drs. Seth Hunter and Bhavna Sharma, but I am so proud to see that they are all happy in life. Kendhl Witt, you were so great to have around the lab, and I'm glad that I still get to see you often. Hopefully that will continue to be the case. For the current members, Tabi Cook, Thomas Carpenter, Shelby Stavretis, Duncan Moseley and of course Roberto Federico-Perez, I'm so excited

to see where they will end up in life, I have no doubt they will be doing amazing things in the future. I would also like to recognize Dr. Jie Guo, and the year that she spent in Knoxville, TN to work with me on the Hg detection project. I look forward to seeing her again in the future, possibly in her home country of China! Kimbrah Johnson whom I mentored through the work on blood pretreatment was a great asset to have in the lab, even if just for the summer. I am extremely thankful for the work she put into the project and for her happy nature. Eric McAnly was another student that I am honored to have worked with, and has also become a good friend. I look forward to continuing all of these friendships in the future.

Thank you to Dr. Carlos Lee, and his willingness to team up with our small lab to solve a big problem in the pharmaceutical industry. I want to also thank all of the staff at UT who have assisted me along the way, particularly Bill Gurley for his friendship and willingness to help, and Art Pratt for his role in helping us create the H<sub>2</sub>S gas generator.

I want to recognize Dr. Marc Strand, my first chemistry teacher and the reason I have followed the path that I have. His love of chemistry and especially his love of research taught me to be excited as well. I will forever be grateful for the chance to be able to work with him, and learn from him, at Eastman Chemical Company. I would also like to recognize the amazing work that the professors at Berea College do every day. They see every single student as an individual, and they believe in each one of them. Many of the Berea faculty, from many different departments, have had profound effects on the way I write, approach situations,



research, think, and interact with others. The same is true for many of my fellow Berea students, many of whom I consider to be family. I would especially like to thank Christian Honce, David Bellnier, Matt Quarles, Laura Howard, Yousef Bashir, Ryan Camenisch, Lilly Belanger and Joshua Slaton for their constant support and encouragement. I can never repay the chance at life that they, and Berea as a whole, have given me.

Josh Schmeling and Marcus Griffey have been so important in my life for so long that it's hard to remember a time when they weren't a major part of it. I am forever grateful for their love, kindness, thoughtfulness, and honesty (even if it was tough to hear at the time) in my life. I am also amazed by the connections that I have made since moving to Knoxville. Tina Lephon, Matthew Dembo, Tyler and Cayce Anthony, Tanei Ricks, and Eunice Hong have all become something more akin to family than friends and I am so glad to have them in my life.

Similarly, I want to recognize the entire Church of the Savior congregation, whose tireless work toward social justice and never ending encouragement have made huge impacts on my life since finding them. All of these people have been major sources of support, love, and pure joy- gifts and qualities that have gotten me through the tough times in graduate school.

There have been many people who have stood by me throughout my life, but I especially want to highlight the entire Shanks family. Sue and Stephen are like an extra set of parents that I don't see often enough. Kathryn has always been like an older sister, and Myra has been one of my best friends since we were children. Their support and love has been constant and unflinching.

Lastly, I want to recognize all of my family members. There is no way that I could thank my parents, Kris and Larry Rosolina, enough. They have always been my support and my safety, and have taught me to be the same for others. Their kindness and love is contagious and given freely to everyone whom they come into contact with. My sister, Rachel Rosolina, is a role model of mine and I cannot wait to have the time to see her more often. Her love, support and care have been a constant throughout my life, except for that time that she stabbed me with a pencil. I will always take joy in knowing that I can approach her with any situation in the world and receive a listening ear, comfort, and thoughtful advice. To Casey Mumaw, Rishara Finsel, Ben Finsel, Emily Querin, and Emily and Dave Finsel: I could not ask for a better group of people to call my in-laws. And finally, thank you to Erin, my wife. She has dealt patiently with my lack of free time, my exhaustion, my frustrations, and my selfishness, without ever complaining. She makes my life so much easier than it would be without her. I am sincerely honored and humbled by the support that all of these people have given to me, and continue to give to me.

## ABSTRACT

The work in this dissertation focuses on the detection and analysis of trace chemicals in biological and environmental samples. Methods for the electrochemical detection of heavy metals Cd(II) [cadmium] and Pb(II) [lead], and the catalytic metal Pd(II) [palladium] in pharmaceutical ingredients have been optimized without the necessity of sample pretreatment. The metals can be analyzed simultaneously as well as individually, and the study includes the first known instance of the use of anodic stripping voltammetry (ASV) to detect metals in dimethyl sulfoxide (DMSO) solutions. Another method, based on ASV, has been optimized and evaluated for the purpose of mercury(II) analysis in a representative active pharmaceutical ingredient (API) and excipient. A pyridine-functionalized thin film has been fabricated to selectively preconcentrate hexavalent chromium [Cr(VI)] anions for electrochemical detection. Glassy carbon electrodes were modified through physical deposition of single-walled carbon nanotubes (SWNTs) on the electrode surface, followed by electrochemical deposition of a sol-gel containing a 2-pyridine functional group. The use of SWNTs has increased sensitivity for Cr(VI) detection in aqueous solutions, providing a detection limit of  $0.3 \mu\text{g L}^{-1}$  (micrograms per liter). Two new processes to pretreat blood samples have been developed. The treatments are based on a Fenton-like advanced oxidation process (AOP). The first method is performed with a simple convection oven over a period of five hours, while the second uses microwave irradiation for six minutes. These novel methods allow

for either cost-effective pretreatment through the use of the common lab oven, or time savings through the use of the synthesis microwave. The pretreated biological samples were further analyzed via anodic stripping for quantification of copper in the whole blood. A novel, disposable, Bi (bismuth)-based colorimetric sensor was developed for the detection of toxic hydrogen sulfide ( $\text{H}_2\text{S}$ ) gas. Using a simple laboratory setup to generate the  $\text{H}_2\text{S}$  in a total volume of 1.35 L (liters), the sensor was able to qualitatively detect the analyte down to 30 ppb (parts per billion), indicating its ability to be used in industrial settings and manufactured into an inexpensive product for the determination of bad breath.

# TABLE OF CONTENTS

1. Introduction and background.....	1
1.1. Foreword.....	2
1.2. Analysis techniques used in the research.....	3
1.2.1. Electrochemical techniques.....	3
1.2.2. Advanced oxidation process.....	6
1.2.2.1. Fenton process.....	6
1.2.2.2. Photo-Fenton process.....	7
1.2.3. Inductively coupled plasma-optical emission spectroscopy.....	7
1.2.4. Overview of sol-gel processes and their applications.....	8
1.2.5. Ultraviolet and visible spectroscopy.....	9
1.3. Summary of dissertation parts.....	9
1.3.1. Part 2.....	9
1.3.2. Part 3.....	10
1.3.3. Part 4.....	10
1.3.4. Part 5.....	11
1.3.5. Part 6.....	11
1.3.6. Part 7.....	12
References.....	13
2. Direct determination of cadmium and lead in pharmaceutical ingredients using anodic stripping voltammetry in aqueous and DMSO/water solutions...	15

Abstract.....	16
2.1. Introduction .....	17
2.2. Materials and methods.....	21
2.2.1. Chemicals and instruments .....	21
2.2.2. Sample preparation and SWASV analysis of Cd(II) and Pb(II)....	22
2.3. Results and discussion .....	23
2.3.1. Optimization of experimental conditions .....	24
2.3.1.1. Effect of supporting electrolyte .....	24
2.3.1.2. Effect of Bi(III) concentration.....	26
2.3.1.3. Effect of preconcentration potential .....	27
2.3.1.4. Effect of preconcentration time .....	27
2.3.2. Analytical results.....	29
2.3.2.1. Detection of Pb(II) and Cd(II) in aqueous media.....	29
2.3.2.2. Detection of Pb(II) and Cd(II) in 95/5 DMSO/H <sub>2</sub> O solutions.....	31
2.3.2.3. Organic matrix effect .....	34
2.3.2.4. Reproducibility and precision.....	36
2.3.3. Apparent recoveries <sup>79</sup> .....	38
2.4. Conclusion .....	39
References .....	41
3. Direct analysis of palladium in active pharmaceutical ingredients by anodic stripping voltammetry.....	48

Abstract.....	49
3.1. Introduction .....	50
3.2. Materials and methods.....	54
3.2.1. Chemicals and instruments .....	54
3.2.2. Sample preparation and SWASV analysis of Pd(II).....	55
3.3. Results and discussion .....	57
3.3.1. Analytical results.....	57
3.3.2. Detection of Pd(II).....	58
3.3.3. Interference effects .....	62
3.3.4. Apparent recoveries .....	64
3.4. Conclusion .....	65
References .....	67
4. Electrochemical study of trace mercury analysis in pharmaceutical ingredients through a classical anodic stripping approach .....	70
Abstract.....	71
4.1. Introduction .....	71
4.2. Materials and methods.....	75
4.2.1. Chemicals and instruments .....	75
4.2.2. Sample preparation and SWASV analysis of mercury(II) .....	76
4.3. Results and discussion .....	77
4.3.1. Optimization of experimental conditions .....	78
4.3.1.1. Effect of supporting electrolyte .....	78

4.3.1.2. Effect of preconcentration potential .....	78
4.3.1.3. Effect of preconcentration time .....	79
4.3.2 Analytical results.....	81
4.3.2.1. Detection of Hg(II) in the absence of organics.....	81
4.3.2.2. Effect of dissolved organics on analysis .....	82
4.3.2.3. Reproducibility and precision.....	83
4.3.3. Interference .....	83
4.4. Conclusions .....	84
References .....	86
5. Highly sensitive detection of hexavalent chromium utilizing a sol-gel/carbon nanotube modified electrode.....	90
Abstract.....	91
5.1. Introduction .....	91
5.2. Experimental .....	94
5.2.1. Apparatus and materials.....	94
5.2.2. Carboxylation of SWNTs .....	95
5.2.3. Preparation of electrode .....	96
5.2.4. Analysis procedure .....	97
5.3. Results and discussion .....	97
5.3.1. Surface analysis .....	97
5.3.2 Optimization.....	102
5.3.3. Cr(VI) detection .....	104



5.3.4. Real world sample .....	104
5.3.5. Reproducibility and the limit of detection .....	104
5.3.6. Interference studies .....	106
5.4. Conclusions .....	106
References .....	108
6. Novel methods for the pretreatment of whole blood using Fenton-like processes .....	112
Abstract.....	113
6.1. Introduction .....	113
6.2. Materials and methods.....	116
6.2.2. Chemicals and instruments .....	116
6.3. Experimental procedures .....	118
6.3.1. Swine blood sampling.....	118
6.3.2. Catalase deactivation .....	118
6.3.3. Laboratory-oven pretreatment .....	118
6.3.4. Microwave pretreatment .....	119
6.4. Results and discussion .....	120
6.4.1. Sample analysis .....	120
6.4.1.1. ASV analysis .....	121
6.4.1.2. ICP-OES analysis.....	123
6.4.1.3. Analysis of samples via UV-Vis spectroscopy .....	124
6.4.3. Discussion .....	125

6.5. Conclusion .....	125
References .....	127
7. Bismuth-based, disposable sensor for the detection of hydrogen sulfide gas .....	129
Abstract.....	130
7.1. Introduction .....	131
7.2. Experimental.....	135
7.2.1. Reagents and materials.....	135
7.2.2. Sensor preparation .....	136
7.2.3. Laboratory generation of 1.35-L, ppb-ppm H <sub>2</sub> S gas and its sensing .....	136
7.3. Results and discussion .....	140
7.4. Conclusion .....	144
References .....	146
8. Concluding remarks .....	151
Appendices .....	155
Appendix A .....	156
A.1 Apparent recoveries .....	157
A.1.1. Apparent recoveries of [Pb(II)] and [Cd(II)] in the presence of 1000 mg L <sup>-1</sup> caffeine (aqueous solution) .....	157

A.1.2. Apparent recoveries of [Pb(II)] and [Cd(II)] in 95/5 DMSO/H <sub>2</sub> O	
solutions .....	158
Appendix B .....	164
Appendix C .....	167
Appendix D .....	170
D.1. Laboratory generation of 1.35-L, ppb-ppm H <sub>2</sub> S gas and its	
sensing.....	170
VITA.....	173

## LIST OF TABLES

Table	Page
2.1. A comparison of Cd and Pb analyses and figures of merit.....	37
3.1. A comparison of Pd analyses and figures of merit.....	58
4.1. A comparison of Hg analyses and figures of merit.....	81
4.2. Comparison of interference effects.....	84
A.1. Calibration for Cd(II) and Pb(II) with 1000 mg L <sup>-1</sup> caffeine in 95/5 DMSO/H <sub>2</sub> O.....	159
A.2. Standard addition for Cd(II) and Pb(II) with 1000 mg L <sup>-1</sup> ketoprofen in 95/5 DMSO/H <sub>2</sub> O.....	161

## LIST OF FIGURES

Figure	Page
1.1. Waveform of square wave voltammetry.....	5
2.1. Effect of supporting electrolytes on the voltammetric behaviors of Cd(II) and Pb(II).....	25
2.2. Effect of Bi(III) concentrations on analysis.....	26
2.3. Accumulation time studies for Cd(II) and Pb(II).....	28
2.4. Individual analysis of Cd(II) and Pb(II) by ASV in aqueous solutions.....	30
2.5. Simultaneous detection of Cd(II) and Pb(II) by ASV in aqueous solutions.....	30
2.6. Individual analysis of Cd(II) by ASV in 95/5 DMSO/H <sub>2</sub> O.....	32
2.7. Individual analysis of Pb(II) by ASV in 95/5 DMSO/H <sub>2</sub> O.....	33
2.8. Simultaneous detection of Cd(II) and Pb(II) by ASV in 95/5 DMSO/H <sub>2</sub> O.....	33
3.1. Analysis of Pd(II) in aqueous solution.....	60
3.2. Analysis of Pd(II) in aqueous solutions in the presence of Bi(III), Cd(II), and Pb(II).....	60
3.3. Detection of Pd(II) with the assistance of a Bi(III) in 95/5 DMSO/ H <sub>2</sub> O solutions in the presence of Cd(II) and Pb(II).....	62
4.1. Effect of supporting electrolytes on the Hg(II) voltammetric behaviors.....	79
4.2. Studies on deposition potential for Hg(II).....	80

4.3.	Studies on accumulation times for Hg(II).....	80
4.4.	Increasing concentrations of Hg(II) in the absence of organics.....	82
5.1.	Schematic of the accumulation of chromate followed by its reduction.....	98
5.2.	SEM images of the sol-gel coated GCE surface.....	98
5.3.	Sol-gel film iridescence throughout the optimization of the deposition process.....	101
5.4.	Image of a bare GCE surface compared to optimized sol-gel film on the same electrode.....	101
5.5.	Square-wave voltammograms of various Cr(VI) concentrations collected at a pyridine-functionalized sol-gel electrode.....	103
5.6.	The detection of Cr(VI) is modeled by an exponential function.....	103
5.7.	Cr(VI) peak detected in an ashed swine blood solution.....	105
5.8.	Square wave voltammograms of individual 200 $\mu\text{g L}^{-1}$ Cr(VI) solutions.....	105
5.9.	Graphical representation of interference studies.....	107
6.1.	Swine blood solution before and after oven-based AOP.....	119
6.2.	Swine blood solution before and after microwave-based AOP.....	120
6.3.	Voltammograms of Cu in an oven pretreated blood solution.....	121
6.4.	Calibration curves of Cu oxidation in pretreated blood.....	122
6.5.	ICP-OES Standard calibration curve of copper in pretreated blood sample.....	123

6.6.	UV-Vis spectra comparing oven- and microwave-based results with dilute whole blood solutions, and porcine hemoglobin solution.....	124
7.1.	Schematic of H <sub>2</sub> S gas generation in a 1.35-L vessel.....	139
7.2.	Sensors after being exposed to 20 μL of pH 11 <i>solutions</i> of varying NaHS concentrations.....	142
7.3.	Six sensors after being exposed to 0 to 200 ppb H <sub>2</sub> S gas.....	142
7.4.	Test showing that Bi(III) is spread evenly throughout the sensor.....	144
A.1.	Voltammograms depicting the supporting electrolyte's effect on the sensitivity of detecting Cd(II) and Pb(II) in aqueous solutions.....	156
A.2.	Voltammograms depicting the supporting electrolyte's effect on Cd(II) and Pb(II) in 95/5 DMSO/water solutions.....	157
A.3.	Simultaneous standard additions of Cd(II) and Pb(II) in an aqueous solution containing caffeine.....	162
A.4.	Calibration plot of Cd(II) in the presence of ketoprofen and increasing Pb(II).....	162
A.5.	Linearized Cd(II) standard addition calibration.....	163
A.6.	Linear regression of Pb(II) through simultaneous standard additions of Cd(II) and Pb(II) in 95% DMSO containing ketoprofen.....	163
B.1.	Linear regression for the analysis of Pd(II), codeposited with Bi(III) in 95% DMSO/5% water.....	164
B.2.	Linear regression for the analysis of Pd(II) in aqueous solutions in the presence of caffeine.....	165
B.3.	Analysis of Pd(II), codeposited with Bi(III) in 95% DMSO/ 5% water	

in the presence of ketoprofen.....	165
B.4. Recovery of Pd(II) in aqueous solution.....	166
B.5. Recovery of Pd(II) 95% DMSO/ 5% water.....	166
C.1. Voltammograms depicting the supporting electrolyte's effect on the Hg(II) peak.....	167
C.2. Voltammograms collected from preconcentration potential optimization studies.....	168
C.3. Standard additions of Hg(II) in an aqueous solution containing caffeine.....	168
C.4. Standard additions of Hg(II) in an aqueous solution containing lactose.....	169
D.1. The system to generate H <sub>2</sub> S gas.....	172
D.2. Sensors containing differing amounts of Bi(III) after being exposed to 50 ppb gas equivalency NaHS solutions.....	172



## NOMENCLATURE AND ABBREVIATIONS

<i>A</i>	absorbance
A	amps
AA	atomic absorption
AOP	advanced oxidation process
API	active pharmaceutical ingredients
ASV	anodic stripping voltammetry
<i>b</i>	pathlength
C	concentration
°C	degrees Celsius
CPS	counts per second
CV	cyclic voltammetry
DI	deionized
DMSO	dimethyl sulfoxide
<i>E</i>	potential
EPA	Environmental Protection Agency
EtOH	ethanol
Et <sub>4</sub> NBF <sub>4</sub>	tetraethylammonium tetrafluoroborate
$\epsilon$	molar absorptivity
g	gram
GCE	glassy carbon electrode

h	hour
<i>h</i>	Planck's constant
Hz	hertz
ICP-OES	inductively coupled plasma optical emission spectrometer
ICH	International Conference on Harmonisation
<i>i</i>	current
L	liter
m	meter
MeOH	methanol
mM	millimolar
M	Molar
MΩ	megaohm
mA	milliamp
min	minutes
mg	milligram
mL	milliliter
NaOAc	sodium acetate
nm	nanometer
OSHA	Occupational Safety and Hazard Administration
ppb/μg L <sup>-1</sup>	parts per billion
ppm/mg L <sup>-1</sup>	parts per million
ppt/ng L <sup>-1</sup>	parts per trillion
<i>R</i> <sup>2</sup>	square of correlation coefficient

rpm	rotations per minute
RSD	relative standard deviation
s	second
SEM	scanning electron microscopy
SWNT	single-walled carbon nanotube
SWASV	square wave anodic stripping voltammetry
SWV	square wave voltammetry
<i>t</i>	time
TBAP	tetra(n-butyl)ammonium perchlorate
TMOS	trimethoxysilane
UV-Vis	ultraviolet-visible
USP	United States Pharmacopeia
V	volts
W	watts
μA	microamps
μg	microgram
μL	microliter
<i>ν</i>	frequency

# **PART 1**

## **Introduction and background**

## **1.1. Foreword**

In 2008, a waste containment area in Kingston, TN failed, releasing 1.1 billion gallons of coal ash slurry into the Emory and Clinch rivers. Coal ash contains a mix of many elements that do not combust with the coal, many of which (arsenic, cadmium, lead, mercury, copper, chromium, etc.) have negative effects on the environment and human health.<sup>1</sup> Despite changes in coal ash containment pond regulations, another spill occurred six years later in North Carolina, releasing 39,000 tons of ash and 27 million gallons of contaminated water into the Dan River. Similar catastrophes have occurred more recently, such as the high concentration of lead found in the water supply of Flint, MI and the massive southern California natural gas leak that released large amounts of mercaptan odorants into the surrounding community.

These same trace chemicals are found not only in large-scale environmental disasters, but also in foods, pharmaceuticals, human blood, and even human breath. Their analysis, requiring trace detection and regular sampling, can be applied to many areas from public health to industry. The development of new sensors and methods, potentially portable, simple to use, inexpensive, and remotely operated, is critical to the efforts.

This dissertation discusses the work of trace chemical detection using electrochemical and optical sensors that can have direct environmental applications. A method for the electrochemical detection of the heavy metals cadmium and lead, as well as the catalytic metal palladium in pharmaceutical

ingredients has been optimized without the necessity of sample pretreatment. The metals can be analyzed simultaneously as well as individually, and the study includes the first known instance of the use of anodic stripping voltammetry (ASV) to detect metals in a dimethyl sulfoxide (DMSO) solution. A novel, disposable, Bi (bismuth)-based colorimetric sensor was developed for the detection of toxic hydrogen sulfide (H<sub>2</sub>S) gas. Using a simple laboratory setup to generate the H<sub>2</sub>S in a total volume of 1.35 L (liters), the sensor was able to qualitatively detect the analyte down to 30 ppb (parts per billion), indicating its ability to be used in industrial and laboratory settings.

## **1.2. Analysis techniques used in the research**

### **1.2.1. Electrochemical techniques**

Voltammetry is a form of electrochemical measurement that utilizes a potential ramp or a potential shift to transfer electrons to or from the electrode and solution while the resulting current is recorded. The current response can then be utilized to extract useful chemical information including reaction kinetics, quantitative data, and qualitative data. Most voltammetry is performed with a three-electrode system. The first electrode is the *working electrode*, where the observed reaction takes place. Depending on the reaction, it can be either cathodic or anodic. The *counter electrode*, paired with the working electrode, provides current to maintain a set potential difference between the third electrode (the *reference electrode*) and the working electrode. The reference electrode

(typically Ag/AgCl, 3 M KCl) has no current flowing through it, and maintains a constant potential for use as a reference point.<sup>2,3</sup> The instrument used for such three-electrode electroanalytical experiments is the *potentiostat* which controls the voltage across the working electrode and the counter electrode. Based on programming, the potentiostat works to maintain a pre-determined potential difference between the working and reference electrode.<sup>2,3</sup>

The voltammetric technique used in the research herein was square wave voltammetry (SWV). SWV is a pulsed technique, which refers to a method in which the potential is pulsed, as opposed to linearly swept. Potential pulse techniques are commonly favored over potential sweep techniques because they are often more sensitive. This is due to the current sampling (the recording of the current) taking place at a time long enough after the potential change that the otherwise interfering charging current is negligible.<sup>4</sup> SWV can be described as a combination of a voltammetric square wave modulation (essentially quantized pulses in the potential) and a staircase potential waveform. When graphing the resulting potential versus time there is an obvious staircase waveform, each cycle of which contains two symmetrical pulses in opposite directions. Two current samples are taken during each cycle (one at the end of each half cycle), relating to the two respective pulses.<sup>2,3,5</sup>

As seen in Figure 1.1., a sample is taken at the end of the first pulse in the cycle. This pulse is referred to as the *forward pulse* because it is in the direction of the staircase scan. The reverse current sample is taken at the end of each *reverse pulse*, referring to the second pulse per cycle which is in the opposite

direction of the forward pulse. Thus, for each cycle, the *forward current sample*, and the *reverse current sample* are given. The difference in these two currents, the *net current*, is plotted to give a Gaussian peak rather than the usual voltammetric wave.<sup>3</sup> Additionally, since SWV applies pulses of equal amplitude, the net current cancels out all currents not related to the reactions of interest, further increasing sensitivity.<sup>6</sup>

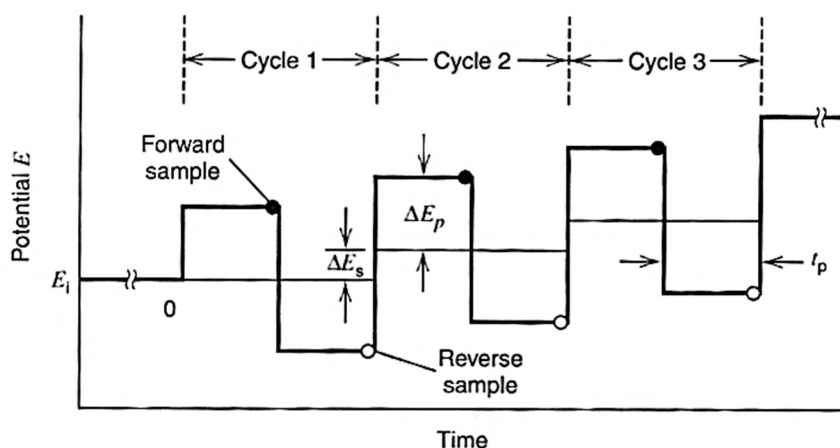


**Figure 1.1.** Waveform of square wave voltammetry. Also depicted here is the pulse width  $t_p$ , pulse height  $\Delta E_p$ , and the staircase potential shift  $\Delta E_s$ .<sup>3</sup>

Anodic stripping voltammetry (ASV) is a voltammetric method wherein the potential at the working electrode is held at a sufficiently negative potential to reduce the analyte (typically a metal) so that it deposits directly onto the electrode surface. Following the deposition step, the potential is swept in the anodic (positive) direction, oxidizing the analyte which strips it from the electrode



surface back into solution. This oxidation sweep, known as the stripping step, produces a Faradaic current that is directly proportional to the analyte concentration. ASV is a very sensitive method, due to the preconcentration of the analyte(s) during the deposition step. Throughout the work herein this method is paired with SWV, which further enhances sensitivity, and is able to detect metals at trace concentrations.

### **1.2.2. Advanced oxidation process**

Advanced oxidation processes (AOPs) are a type of treatment method to destroy organics through the formation of highly reactive hydroxyl radicals ( $\bullet\text{OH}$ ).<sup>7-10</sup> AOP methods are commonly used to pretreat wastewater because they are environmentally friendly alternatives to the use of strong chemical oxidizers.<sup>7-9</sup> The most common reactants used for AOPs are ozone ( $\text{O}_3$ ) and hydrogen peroxide ( $\text{H}_2\text{O}_2$ ).

#### **1.2.2.1. Fenton process**

The Fenton process uses a ferrous ion ( $\text{Fe}^{2+}$ ) alongside  $\text{H}_2\text{O}_2$  to form hydroxyl and hydroperoxyl radicals, which become the oxidants in the decomposition of organic compounds. The radical forming reactions involved in the Fenton process are given below.

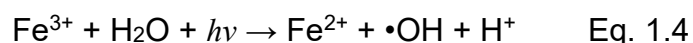




As shown in Eqs. 1.1-1.2,  $\text{Fe}^{2+}$  acts as a catalyst, cycling between the 2+ and 3+ oxidation states.<sup>11,12</sup>

#### 1.2.2.2. *Photo-Fenton process*

The Fenton process does not require irradiation. However, if irradiation is introduced, the formation of radicals is greatly increased. This is known as the Photo-Fenton Process and the increase in radicals is due to the direct hemolytic bond cleavage of the oxygen atoms in  $\text{H}_2\text{O}_2$  as well as the regeneration of  $\text{Fe}^{2+}$  ions through the reduction of  $\text{Fe}^{3+}$  ions by light-induced electron transfer.<sup>7-9,13</sup>



As the hydroxyl and hydroperoxyl radicals attack any organic compounds in solution, more radicals are generated that continue to further decompose the organics.

#### 1.2.3. *Inductively coupled plasma-optical emission spectroscopy*

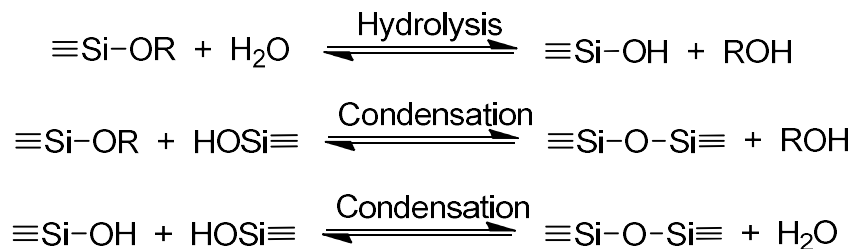
Inductively coupled plasma-optical emission spectroscopy (ICP-OES) is a powerful analytical technique for the detection of trace levels of metals in a

sample. In ICP, the sample is nebulized into a fine mist and introduced to the plasma cone via transport by argon gas. The plasma gas, usually argon, is ionized by a Tesla coil, and becomes a plasma by use of an induction coil that surrounds the torch. The plasma reaches temperatures in the 8,000-10,000 K range. Once in the plasma, the sample is mineralized and becomes high-energy atoms. As the atoms relax, their electrons move to a lower energy state, emitting photons at wavelengths that are specific to each element. Thus, ICP-OES is useful as a quantitative method (capable of detecting down to the parts per trillion range) as well as a qualitative method that can distinguish between elements.

#### ***1.2.4. Overview of sol-gel processes and their applications***

Sol-gel processes refer to a number of reactions involving the use of alkoxide precursors in solution (sol) to prepare gel-like glass and ceramic oxide materials.<sup>14</sup> The process generally involves the hydrolysis of an alkoxide precursor such as  $\text{Si}(\text{OR})_4$  or  $\text{R}'\text{Si}(\text{OR}'')_3$  (R = alkyl), followed by a condensation reaction, to produce a silica-based cross-linked polymer with a three dimensional porous structure. The sol-gel reactions (Scheme 1.1) can be adjusted to tailor the physical properties of the resulting gel by changing parameters such as pH, solvents, temperature and ligands.<sup>14-22</sup>

Sol-gels are easily paired with sensing techniques, such as optical and electrochemical sensing, due to their chemical inertness, robustness, and easy functionalization for selective analysis.



**Scheme 1.1.** The reactions in the sol-gel process.

### **1.2.5. Ultraviolet and visible spectroscopy**

Molecules with  $\pi$  bonding electrons or non-bonding electrons can absorb ultraviolet (UV) or visible light, exciting electrons from their ground states to excited states. Depending on the molecule, the energy absorbed can transfer to a nearby molecule or is expended through vibrational relaxation. As long as the molar absorptivity ( $\epsilon$ ) is known, the concentration of the absorbing species can be directly calculated using the Beer-Lambert Law (Eq. 1.5)<sup>23</sup>

$$A = \epsilon b C \qquad \text{Eq. 1.5}$$

Where  $A$  is absorbance,  $b$  is the pathlength, and  $C$  is the molar concentration of the species.

## **1.3. Summary of dissertation parts**

### **1.3.1. Part 2**

Part 2 of this dissertation describes the use of ASV for the determination of the toxic heavy metals Pb(II) and Cd(II) in active pharmaceutical ingredients

(API) and excipients. The metals can be detected simultaneously or individually and are performed directly in aqueous or DMSO solutions without pretreatment. The analysis requires the use of Bi(III) ions to co-deposit, forming an in-situ bismuth film and increasing the sensitivity. The method is simple, highly reproducible with the detection limits in the low ppb (parts per billion), indicating that voltammetry is a promising alternative to ICP-based approaches. This study also contains the first known use of ASV in DMSO solutions.

### **1.3.2. Part 3**

The third part of this dissertation involves the use of ASV to detect Pd(II), a catalytic metal, in API and excipients dissolved directly in aqueous or DMSO solutions using a simple glassy carbon electrode. The analysis does not *require* a Bi(III) co-deposition, but Bi(III) does not interfere with the Pd(II) detection. Thus it was determined that Pd(II), Pb(II), and Cd(II) can be analyzed simultaneously. This method was the first known detection of Pd in pharmaceutical ingredients using ASV, and had detection limits in the low ppb range.

### **1.3.3. Part 4**

Part 4 of this work reports the use of ASV to analyze Hg(II) in pharmaceutical matrices. The method uses a simple un-modified glassy carbon electrode and does not require pretreatment of the sample prior to the analysis. The method has limits of detection in the high ppt (parts per trillion) range in the

presence of a representative pharmaceutical and excipient. The performance has been evaluated in the presence of coexisting anions or cations. The good reproducibility and stability of the analytical platform and obviation of sample pretreatment show the promise of utilizing ASV as a sensitive, robust, and inexpensive alternative to inductively-coupled-plasma (ICP)-based approaches for the analysis of Hg in pharmaceutical matrices.

#### **1.3.4. Part 5**

The detection of carcinogenic Cr(VI) (hexavalent chromium) was studied using a sol-gel modified glassy carbon electrode doped with a pyridinium species. Through the use of single-walled carbon nanotubes (SWNTs) which increase conductivity, surface area, and the analyte preconcentration at the pyridinium sites, an LOD in the ppt range was reached. The analysis was applied to the determination of Cr concentrations in a dry-ashed swine blood sample.

#### **1.3.5. Part 6**

New pretreatment methods were optimized and are reported in Part 6 of this dissertation. The treatments are based on a Fenton-like advanced oxidation processes (AOPs). The first method is performed with a simple convection oven over a period of 5 h, while the second uses microwave irradiation for 6 min. These new methods allow for either cost effective pretreatment through the use of the common lab oven, or time savings through the use of a synthesis

microwave. The pretreated biological samples were further analyzed via anodic stripping for quantification of copper in the whole blood and validated by comparison with ICP-OES.

### **1.3.6. Part 7**

A novel optical sensor for the detection of hydrogen sulfide gas, the main contributor to bad breath and a toxic gas encountered in many mining and industrial occupations. The disposable sensor uses an alkaline bismuth species to react with the weakly acidic analyte, producing the solid  $\text{Bi}_2\text{S}_3$  and consequently a yellow-brown color on the otherwise white substrate. A laboratory setup for the generations of low-concentration  $\text{H}_2\text{S}$  gas at a set volume of 1.35 L is also described in this chapter. This volume was chosen to mimic the average volume of a human breath as a proof of concept that the sensor could be produced as a simple bad breath analyzer. The sensor was able to detect the analyte down to 30 ppb using the naked eye.

## References

1. Ruhl, L.; Vengosh, A.; Dwyer, G.S.; Hsu-Kim, H.; Deonarine, A.; Bergin, M.; Kravchenko, J. *Environ. Sci. Technol.* **2009**, *43*, 6326–6333.
2. Ellis, W.D. *J. Chem. Ed.* **1973**, *50*, A131.
3. Bard, A. J.; Faulkner, L. R. *Electrochemical Methods: Fundamentals and Applications*; 2<sup>nd</sup> ed.; Wiley: New York, NY, 2001.
4. Skoog, D. A.; Holler, F. J.; Nieman, T. A. *Principles of Instrumental Analysis, 6<sup>th</sup> Edition*; Brooks Cole, 2006.
5. Osteryoung, J.; Osteryoung, R. *Anal. Chem.* **1985**, *57*, 101A–110A.
6. Osteryoung, J. *Acc. Chem. Res.* **1993**, *26*, 77–83.
7. Parsons, S., Ed. *Advanced Oxidation Processes for Water and Wastewater Treatment*; IWA Publishing: London, 2004.
8. *Handbook on Advanced Photochemical Oxidation Processes*. EPA, 1998.
9. Legrini, O.; Oliveros, E.; Braun, A.M. *Chem. Rev.* **1993**, *93*, 671–698.
10. Symons, J.M.; Worley, K.L. *J. Amer. Wat. Works Assn.* **1995**, *87*, 66–75.
11. Bragg, S.A.; Armstrong, K.C.; Xue, Z.-L. *Talanta* **2012**, *97*, 118–123.
12. Yong, L.; Armstrong, K.C.; Dansby-Sparks, R.N.; Carrington, N.A.; Chambers, J.Q.; Xue, Z.-L. *Anal. Chem.* **2006**, *78*, 7582–7587.
13. Schulte, P.; Bayer, A.; Kuhn, F.; Luy, T.; Volkmer, M. *Ozone Sci. Eng.* **1995**, *17*, 119–134.
14. Brinker, C.J.; Scherer, G. W. *Sol-Gel Science: The Physics and Chemistry of Sol-Gel Processing*; 1<sup>st</sup> ed.; Academic Press: Boston, 1990.



15. Hench, L.L.; West, J.K. *Chem. Rev.* **1990**, *90*, 33–72.
16. Allain, L.R.; Sorasaene, K.; Xue, Z. *Anal. Chem.* **1997**, *69*, 3076–3080.
17. Lev, O.; Tsionsky, M.; Rabinovich, L.; Glezer, V.; Sampath, S.; Pankratov, I.; Gun, J. *Anal. Chem.* **1995**, *67*, 22A–30A.
18. Allain, L.R.; Canada, T.A.; Xue, Z. *Anal. Chem.* **2001**, *73*, 4592–4598.
19. Brinker, C.; Hurd, A.; Schunk, P.; Frye, G.; Ashley, C. *J. Non-Cryst. Solids* **1992**, *147*, 424–436.
20. Schubert, U.; Huesing, N.; Lorenz, A. *Chem. Mater.* **1995**, *7*, 2010–2027.
21. Carey, W.P.; DeGrandpre, M.D.; Jorgensen, B.S. *Anal. Chem.* **1989**, *61*, 1674–1678.
22. Carey, W.P.; Jorgensen, B.S. *Appl. Spectrosc.* **1991**, *45*, 834–838.
23. Harris, D.C. *Quantitative Chemical Analysis*, 8<sup>th</sup> ed.; W. H. Freeman, 2010.

## **PART 2**

**Direct determination of cadmium and lead in  
pharmaceutical ingredients using anodic stripping  
voltammetry in aqueous and DMSO/water solutions**

A version of this chapter was originally published by Samuel M. Rosolina, James Q. Chambers, Carlos W. Lee, and Zi-Ling Xue. Only minor revisions were made.

Samuel M. Rosolina, James Q. Chambers, Carlos W. Lee, and Zi-Ling Xue. "Direct determination of cadmium and lead in pharmaceutical ingredients using anodic stripping voltammetry in aqueous and DMSO/water solutions." *Anal. Chim. Acta* **2015**, 893, 25–33.

Additional materials for Part 2 are provided in Appendix A.

## Abstract

A new electrochemical method has been developed to detect and quantify the elemental impurities, cadmium(II) [Cd(II)] and lead(II) [Pb(II)], either simultaneously or individually in pharmaceutical ingredients and an excipient. The electro-analytical approach, involving the use of anodic stripping voltammetry (ASV) on an unmodified glassy carbon electrode, was performed in both aqueous and in a 95/5 dimethyl sulfoxide (DMSO)/water solutions, *without* acid digestion or dry ashing to remove organic matrices. Limits of detection (LODs) in the  $\mu\text{g L}^{-1}$  [or parts per billion (ppb), mass/volume] range were obtained for both heavy metals - in the presence and absence of representative pharmaceutical components. To the best of our knowledge, the work demonstrates the first analysis of heavy metals in DMSO/water solutions through ASV. The strong reproducibility and stability of the sensing platform, as well as

obviation of sample pretreatment show the promise of utilizing ASV as a sensitive, robust, and inexpensive alternative to inductively-coupled-plasma (ICP)-based approaches for the analysis of elemental impurities in, e.g., pharmaceutical-related matrices.

## **2.1. Introduction**

Toxic heavy metals such as cadmium and lead often exist in both inorganic and organic matrices. Electrochemical methods to analyze trace cadmium and lead have been mostly focused on their presence in aqueous systems,<sup>1-8</sup> such as drinking water, containing trace levels of organic matter without the need to consider the presence of dissolved organics. Electrochemical analyses of cadmium and lead in the presence of organic substrates have received less attention.<sup>1-8</sup> Determination of metal content in fish, honey and other organic/biological matrices often requires sample mineralization such as dry ashing or wet acid digestion.<sup>2,3,5,9,10</sup> There is a strong need to directly analyze the toxic metals in organic matrices without the mineralization.

Due to newly revised regulatory guidelines, the detection and quantification of elemental impurities within drug products and their ingoing components, including active pharmaceutical ingredients (API) and excipients, are being actively studied. The United States Pharmacopoeia (USP) is in the process of issuing updated guidelines for the control of elemental impurities in pharmaceutical products which are mainly organic in nature.<sup>11-13</sup> The

International Conference on Harmonisation (ICH) recently published new guidance (ICH Q3D) for the control of elemental impurities.<sup>14</sup> The proposed changes by USP provides for the replacement of USP <231> (Heavy Metals), the non-selective, wet-heavy metal test, which has been used by pharmaceutical manufacturers for well over 100 years, with two new chapters, USP <232> (Elemental Impurities-Limits) and USP <233> (Elemental Impurities-Procedures).<sup>12</sup> Of the elements listed in the new guidelines, we have focused on the analysis of cadmium and lead, two most toxic elemental impurities, each with oral Permissible Daily Exposure (PDE) values of 5 µg/day. USP <233> (Elemental Impurities-Procedures)<sup>12</sup> provides guidance on appropriate instrumentation and validation requirements, with a focus on inductively coupled plasma (ICP)-based approaches. While ICP-based techniques are known to detect to the parts per trillion (ppt, ng L<sup>-1</sup>) level for most metals, and therefore capable of addressing the requirements of the proposed new regulatory guidances,<sup>12,13</sup> they depend, however, on expensive instrumentation in a centralized, non-portable laboratory. ICP-based methods, like most trace-level, heavy metal analyses, often require time-consuming sample preparation, including acid digestion to remove organic matrices prior to analysis. It is highly desirable to develop lower cost, *portable field methods* to accurately detect and quantitate elemental impurities in APIs and excipients *before* they are fully processed into tablets or capsules. Methods that can accurately detect and quantify elemental impurities with minimal sample preparation would be ideal.

Electrochemical methods, specifically electrochemical techniques such as anodic stripping voltammetry (ASV), are attractive alternatives to ICP-based approaches. In addition to possessing multi-element detection capabilities, electroanalytical approaches require instrumentation of relatively low-cost maintenance and operation. Additionally, electrochemical techniques are extremely fast and sensitive, with limits of detection in the ppb ( $\mu\text{g L}^{-1}$ ) range. ASV is a common electroanalytical technique that utilizes the reduction of metal ions onto an electrode surface followed by rapid oxidation of the metals back into solution to produce the currents in the anodic peaks.<sup>15,16-19</sup> Square Wave Voltammetry (SWV) is one of the most sensitive voltammetric methods, making it especially useful when paired with ASV for trace analysis.<sup>17-19</sup>

Since the use of a Bi film electrode by Wang and coworkers,<sup>20</sup> Bi has found frequent applications in stripping voltammetry.<sup>21-46</sup> Bi shares many important electrochemical properties with Hg, including high hydrogen overpotentials and the ability to form alloys with other metals. But unlike Hg, Bi is non-toxic and more environmentally friendly.<sup>46</sup> Bi-assisted<sup>23-26,33,34</sup> and Bi-free<sup>47-53</sup> ASV analysis of Cd(II) and Pb(II), all in aqueous solutions, have been conducted by a variety of electrodes.

Electroanalysis of elemental impurities in organic matrices typically also requires sample preparation to remove the organic matrices prior to analysis,<sup>35,54-63</sup> as in the aforementioned ICP analyses of pharmaceuticals. Both wet- and dry-ashing require slow and careful work to reduce errors. Additionally, the elevated temperatures in the two approaches can result in low and inaccurate

measurement of more volatile metals such as mercury. Incomplete mineralization is also common.<sup>64,65</sup> For post wet-ashing samples, high acidity in the digested solutions may cause damage to electrodes and decrease the allowed potential window due to an enlarged hydrogen overpotential peak.

This work describes the use of square wave anodic stripping voltammetry (SWASV) to detect and quantitate Cd(II) and Pb(II) in representative pharmaceutical matrices. No sample pretreatment, either wet- or dry-ashing, was needed prior to the electrochemical analyses of the metals. The electrochemical analyses were conducted in both aqueous and 95%/5% DMSO/H<sub>2</sub>O (v/v) (hereinafter referred to as 95/5 DMSO/H<sub>2</sub>O) solutions with and without representative pharmaceutical substrates. The process uses a simple, unmodified glassy carbon electrode (GCE) to detect Cd(II) and Pb(II) in the low ppb ( $\mu\text{g L}^{-1}$ ) range while taking advantage of increased sensitivity through the use of in-situ bismuth co-deposition for each analysis. The co-deposition here is different from those using a Bi bulk or a pre-plated Bi film electrode. The importance of this method lies in its ability to be used in both aqueous and primarily non-aqueous (95/5 DMSO/water) solutions. Using either solvent system, representative APIs, excipients, and dietary supplements were easily dissolved with little to no prior sample pretreatment/digestion. We have chosen DMSO-based non-aqueous solutions for these studies because DMSO is known to be an excellent solvent for APIs.<sup>66</sup> DMSO also has fewer hydrogen bonding networks than water, allowing the formation of solvent cavities.<sup>66</sup> Prior work has indicated that it is important for pharmaceuticals to be soluble in DMSO because

biological testing is commonly performed with DMSO solutions.<sup>66</sup> Employment of the direct method herein allows for inexpensive, fast, and potentially portable analysis of Cd(II) and Pb(II) in low quantities of sample. The current work, to our knowledge, is the first work to analyze cadmium and lead in pharmaceutical matrices, demonstrating its potential. It also creates the opportunity to pre-screen many different organic products for heavy metal impurities throughout batch production. Results of our studies are discussed below.

## **2.2. Materials and methods**

### **2.2.1. Chemicals and instruments**

The following chemicals were used as received, and all but lactose monohydrate, were analytical grade: lactose monohydrate (Lab Grade, Thermo Fisher Scientific, Waltham, MA), caffeine (Thermo Fisher Scientific), ketoprofen (Sigma Aldrich Co., St. Louis, MO), tetra-*n*-butylammonium bromide (Bu<sub>4</sub>NBr, Thermo Fisher Scientific), NaNO<sub>3</sub> (Thermo Fisher Scientific), sodium acetate (NaOAc, Thermo Fisher Scientific), NaCl (Thermo Fisher Scientific), tetraethylammonium tetrafluoroborate (Et<sub>4</sub>NBF<sub>4</sub>, Sigma Aldrich), DMSO (Thermo Fisher Scientific), ethanol (95%, Decon Laboratories, Inc., King of Prussia, PA). Standard solutions of Bi(III), Cd(II), and Pb(II) with concentrations of 1000 mg L<sup>-1</sup> in 10% HNO<sub>3</sub> (Ricca Chemical Co., Arlington, TX) were diluted in supporting electrolytes to form stock solutions. Ultrapure water from a Millipore water purified system ( $\geq 18$  M $\Omega$ ·cm, Barnstead/Thermo Fisher Scientific) was used in all



assays. 95/5 DMSO/H<sub>2</sub>O solution was made by adding 1.0 mL ultrapure water to 19.0 mL of DMSO in the electrochemical cell prior to analysis.

Prior to use, GCEs were polished to a mirror-like surface on a standard electrode polishing kit (CH Instruments, Inc., Austin, TX) including a 1200 grit CarbiMet™ disk, 1.0 and 0.3 μm alumina slurry on a nylon cloth, and 0.05 μm alumina slurry on a microcloth polishing pad. After polishing, GCEs were successively sonicated with deionized (DI) water, ethanol, and DI water again for 5 min each. Electrochemical measurements were carried out on a CHI 440a Electrochemical Workstation (CH Instruments). A three-electrode configuration consisted of a bare, unmodified GCE (3 mm in diameter, BAS Inc., West Lafayette, IN), Ag/AgCl (saturated KCl solution, CH Instruments) and a platinum wire (CH Instruments) as working, reference, and counter electrodes, respectively.

### ***2.2.2. Sample preparation and SWASV analysis of Cd(II) and Pb(II)***

All experiments were conducted at room temperature without deaeration. The unmodified GCE, Ag/AgCl, and Pt wire electrodes were placed in an electrochemical cell containing 20 mL of 0.05 M Et<sub>4</sub>NBF<sub>4</sub> in ultrapure DI water or 0.05 M Et<sub>4</sub>NBF<sub>4</sub> in 95/5 DMSO/H<sub>2</sub>O. Prior to analysis, 50.0 μL of 1000 mg L<sup>-1</sup> Bi(III) standard solution was added to give 2.5 mg L<sup>-1</sup> of total Bi(III) in the aqueous samples, while 200.0 μL of 1000 mg L<sup>-1</sup> Bi(III) standard solution was added to give 9.9 mg L<sup>-1</sup> of total Bi(III) in the 95/5 DMSO/H<sub>2</sub>O solutions. For

detection in the aqueous system, co-deposition of Cd(II), Pb(II), and Bi(III) occurred by holding the potential at -1.0 V for 250 s and was then stripped back into solution by sweeping the potential from -1.0 to 0.6 V using a frequency of 15 Hz, a step potential of 4 mV, and amplitude of 25 mV. In 95/5 DMSO/H<sub>2</sub>O solutions, co-deposition took place at -1.4 V for 300 s followed by sweeping the potential from -1.4 to 0.6 V using a frequency of 25 Hz, a step potential of 4 mV, and amplitude of 25 mV. For all analyses stirring of the solution at 1200 rpm was required for the accumulation step, but was turned off prior to the stripping step. The electrode surface was regenerated between measurements by holding the potential at 0.6 V for 300 s for aqueous samples, and 0.6 V for 200 s in 95/5 DMSO/H<sub>2</sub>O solutions while stirring at high speed. In samples containing a dissolved organic compound, the solutions were stirred for one minute after spiking with the analyte of interest and before the first analysis. This was done to allow the metals to reach equilibrium throughout the matrix and to interact with the organics in solution. It should be noted that allowing spiked samples to sit for several days had no effect, either positive or negative, on the sensitivity of the detection as compared to allowing the sample to stir for one minute after spiking.

### ***2.3. Results and discussion***

Few studies have been performed using voltammetry to investigate or analyze metal ions in organic media. Research performed by Wang,<sup>67</sup>

Daniele,<sup>68,69</sup> and Rodríguez-López<sup>70</sup> are examples of previous work in this currently small field of research.

APIs and organic excipients often have -OH, -SH, -COOH, -NHR groups that can potentially bind/complex to Pb(II), Cd(II) and other ions, forming organic metal alkoxides, carboxylates, amine adducts and amides in the pharmaceutical matrices. Alkoxides of Pb(II) and Cd(II) have been reported to be easily hydrolyzed, forming inorganic metal oxides.<sup>71-73</sup> Carboxylates of the metals likely dissociate significantly at trace levels in water, as demonstrated by the acetates of lead and cadmium.<sup>74-76</sup> Few amide or amine adduct complexes exist with Cd(II) or Pb(II), none of which form spontaneously. Thus, for API or excipients soluble in aqueous or 95/5 DMSO/H<sub>2</sub>O, it is expected that the organic lead/cadmium complexes will dissociate in the solutions. However, if trace Pb-O/Cd-O or Pb-N/Cd-N species are left in aqueous or 95/5 DMSO/H<sub>2</sub>O solutions, the negative deposition potential (-1.2 and -1.4 V, respectively) would overcome the binding energies of ligands to metals, allowing for metal deposition on the electrode.

### **2.3.1. Optimization of experimental conditions**

#### **2.3.1.1. Effect of supporting electrolyte**

Voltammetric behaviors of Cd(II) and Pb(II) were investigated in several supporting electrolytes in both aqueous and organic (95/5 DMSO/H<sub>2</sub>O) solutions. For aqueous solution, NaOAc, NaNO<sub>3</sub>, NaCl, Bu<sub>4</sub>NBr, and Et<sub>4</sub>NBF<sub>4</sub> were

compared. Of these, only NaOAc, NaNO<sub>3</sub>, and Et<sub>4</sub>NBF<sub>4</sub> gave consistently good results. Figure 2.1A shows that NaOAc gave the strongest response for Pb(II), but a weaker response for Cd(II). Et<sub>4</sub>NBF<sub>4</sub> was chosen as the appropriate electrolyte because of its strong response to both Cd(II) and Pb(II). For the 95/5 DMSO/H<sub>2</sub>O organic solution, NaOAc, NaNO<sub>3</sub>, Bu<sub>4</sub>NBr, and Et<sub>4</sub>NBF<sub>4</sub> were tested, but only NaNO<sub>3</sub> and Et<sub>4</sub>NBF<sub>4</sub> produced consistent results. In the presence of an organic API/excipient, Et<sub>4</sub>NBF<sub>4</sub> showed the strongest response in peak area for both Cd(II) and Pb(II) (Figure 2.1B). The voltammograms for these optimization experiments are given in Figs. A1-A2.

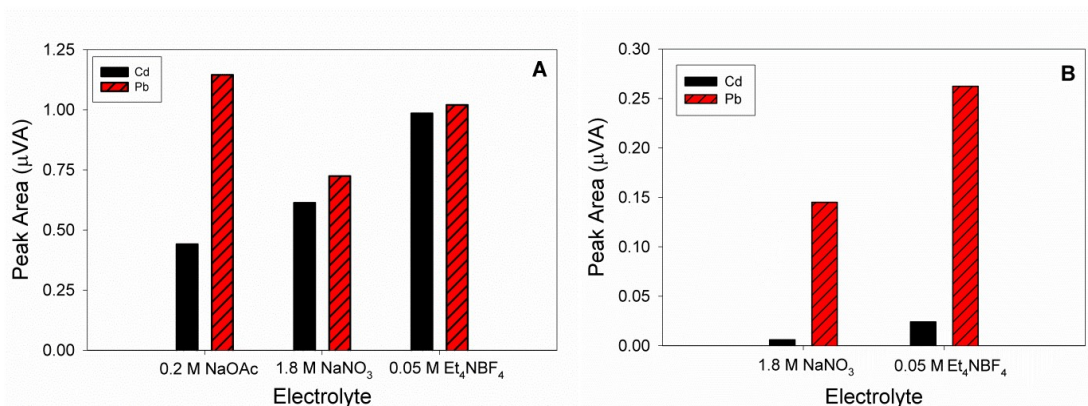


**Figure 2.1.** Effect of supporting electrolytes on the voltammetric behaviors of Cd(II) and Pb(II). [The best electrolyte was chosen through the comparison of Cd(II) (solid) and Pb(II) (hatched) peak areas (both at  $50 \mu\text{g L}^{-1}$ )]. In aqueous solutions (A), Et<sub>4</sub>NBF<sub>4</sub> was chosen due to the higher sensitivity of Cd(II). In 95/5 DMSO/H<sub>2</sub>O (B), both Pb(II) and Cd(II) showed better responses when using Et<sub>4</sub>NBF<sub>4</sub>.

### 2.3.1.2. Effect of Bi(III) concentration

In aqueous solutions without organic substrates, 1.0 mg L<sup>-1</sup> Bi(III) provided for the largest peak areas of Cd(II) and Pb(II). However, when representative pharmaceutical substrates were added, the peak areas for both analytes were reduced. Increasing [Bi(III)], however, allowed for improved signals of the analytes. This is shown nicely in Figure 2.2A, where, in the presence of 1,000 mg L<sup>-1</sup> lactose, [Bi(III)] had to be increased to 2.5 mg L<sup>-1</sup> to optimize the signals for both Cd(II) and Pb(II).

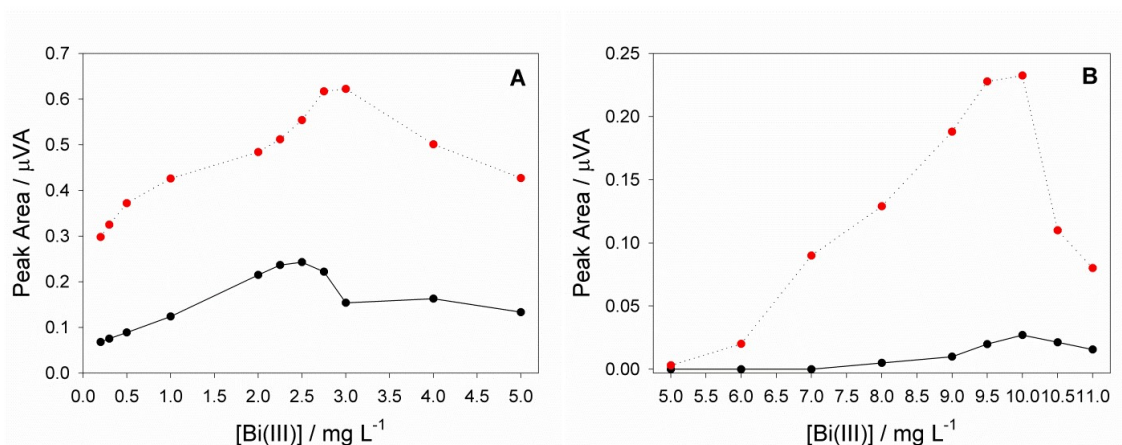


**Figure 2.2.** Effect of different Bi(III) concentrations in water (A) and 95/5 DMSO/H<sub>2</sub>O (B) by comparing Pb(II) (dotted line) and Cd(II) (solid line) peak areas. Both metals were held at 50  $\mu\text{g L}^{-1}$ . Tests in aqueous solutions were performed in the presence of 1,000  $\text{mg L}^{-1}$  lactose and 2.5  $\text{mg L}^{-1}$  Bi(III). In 95/5 DMSO/H<sub>2</sub>O, 10.0  $\text{mg L}^{-1}$  Bi(III) was chosen through optimization in the absence of a dissolved organic compound.

In 95/5 DMSO/H<sub>2</sub>O (Figure 2.2B), Cd(II) peaks were unobservable with [Bi(III)] below 7.0 mg L<sup>-1</sup>. Both Pb(II) and Cd(II) peaks increase with increasing [Bi(III)] until 10.0 mg L<sup>-1</sup> when both begin to drop. Once again, this reveals the importance of Bi(III) ions. Without Bi(III) codeposition, we would not be able to detect either analyte, especially when substrates are present.

#### *2.3.1.3. Effect of preconcentration potential*

Due to the fairly negative potential of the Cd oxidation peak, the hindrance from a possible hydrogen generation peak meant we needed to identify an optimized preconcentration potential. Though both Cd(II) and Pb(II) responded well to negatively increasing preconcentration potentials, -1.0 V was chosen for the aqueous solutions, allowing lower pH levels. Thus the system may allow for analysis in more acidic environments or if partial acid digestion were to be employed. On the other hand, because of the low water concentration in 95/5 DMSO/H<sub>2</sub>O, a preconcentration potential of -1.4 V was found to be the most effective.

#### *2.3.1.4. Effect of preconcentration time*

Figure 2.3A shows the electrochemical results for 50 µg L<sup>-1</sup> Cd(II) and Pb(II) in aqueous solutions. The peak area increased for both metals with increasing deposition time between 100 and 250 s. At deposition times greater than 250 s, Cd(II) experienced a decrease in signal intensity, likely due to

competition for active sites with Pb(II), whose peak continued to increase until 275 s after which it plateaued.

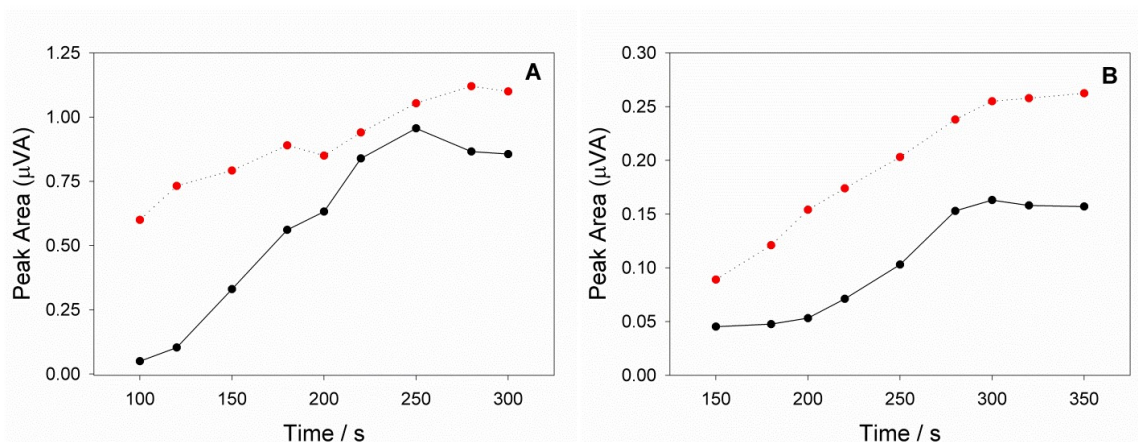


**Figure 2.3.** Studies on accumulation times for Cd(II) (solid line) and Pb(II) (dotted line) in (A) aqueous [0.05 M Et<sub>4</sub>NBF<sub>4</sub>, 2.5 mg L<sup>-1</sup> Bi(III)] and (B) 95/5 DMSO/H<sub>2</sub>O [0.05 M Et<sub>4</sub>NBF<sub>4</sub>, 10 mg L<sup>-1</sup> Bi(III)] solutions.

Figure 2.3B shows the results of preconcentration time on 100 µg L<sup>-1</sup> Cd(II) and Pb(II) in 95/5 DMSO/H<sub>2</sub>O. For both metals, the peak areas increased until 300 s, after which they began to level off. It is worth noting that the Cd(II) trend is non-linear, similar to the trend we have observed throughout concentration changes in the presence of DMSO/water. Our studies of the effect of wave frequency show that, in the 95/5 DMSO/H<sub>2</sub>O solution, a faster square wave stripping frequency produced sharper peaks observable at lower concentrations. Frequency larger than 25 Hz proved to be too high for our desktop computer. In comparison, changing the frequency above 15 Hz in the aqueous media did not increase the sensitivity.

### 2.3.2. Analytical results

Standard addition was used for all calibration curves. Thus it is important to note that all results are given *without* background subtraction. This approach was taken due to the importance of treating the analysis as if actually analyzing an unknown sample. Standard addition allows for the determination of an original concentration while keeping the matrix the same, which is necessary for analysis of un-ashed API. Results of the investigations, including the regression function, square of the correlation coefficient  $R^2$ , RSD (relative standard deviation) at  $50 \mu\text{g L}^{-1}$ , and LOD for each of the following studies ( $S/N = 3$ ), are listed in Table 2.1.

#### 2.3.2.1. Detection of Pb(II) and Cd(II) in aqueous media

Using the optimized parameters above, Cd(II) and Pb(II) were analyzed individually and simultaneously in the absence of representative pharmaceutical ingredients in aqueous solutions. When analyzed separately, the Cd(II) and Pb(II) peaks were observed at -0.73 and -0.49 V, respectively (Figure 2.4). Calculated LODs were  $0.76 \mu\text{g L}^{-1}$  for Cd(II) and  $1.9 \mu\text{g L}^{-1}$  for Pb(II) (Table 2.1).

When analyzed simultaneously (Figure 2.5), the Cd(II) and Pb(II) peaks were observed at -0.73 and -0.46 V, respectively. Calculated LODs were 3.2 and  $1.9 \mu\text{g L}^{-1}$  for Cd(II) and Pb(II), respectively (Table 2.1). The LOD for Pb(II) is identical to that when it was analyzed alone, indicating that its analysis is perhaps not affected by the presence of Cd(II).



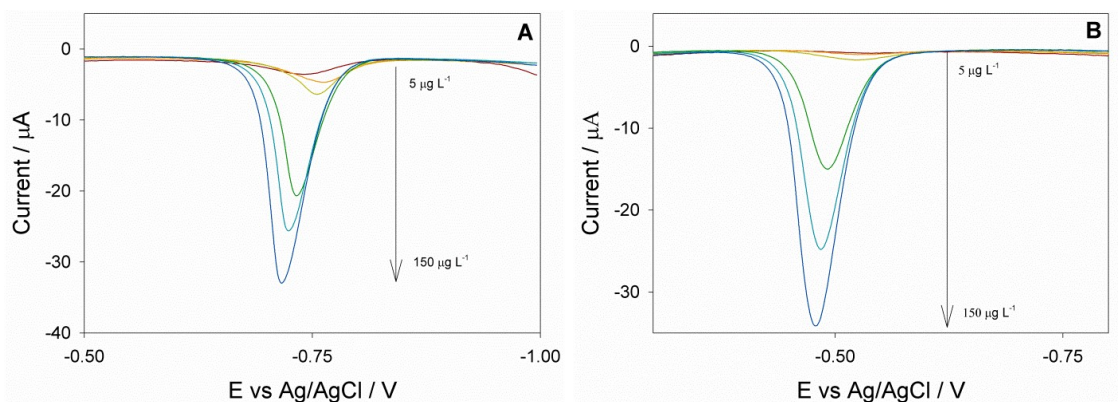


**Figure 2.4.** Increasing concentrations of: (A) Cd(II) ( $5\text{--}150\ \mu\text{g L}^{-1}$ ) in the absence of Pb(II) or an organic compound; (B) Pb(II) ( $5\text{--}150\ \mu\text{g L}^{-1}$ ) in the absence of Cd(II) or an organic compound [ $0.05\ \text{M Et}_4\text{NBF}_4$ ,  $2.5\ \text{mg L}^{-1}\ \text{Bi(III)}$ ].

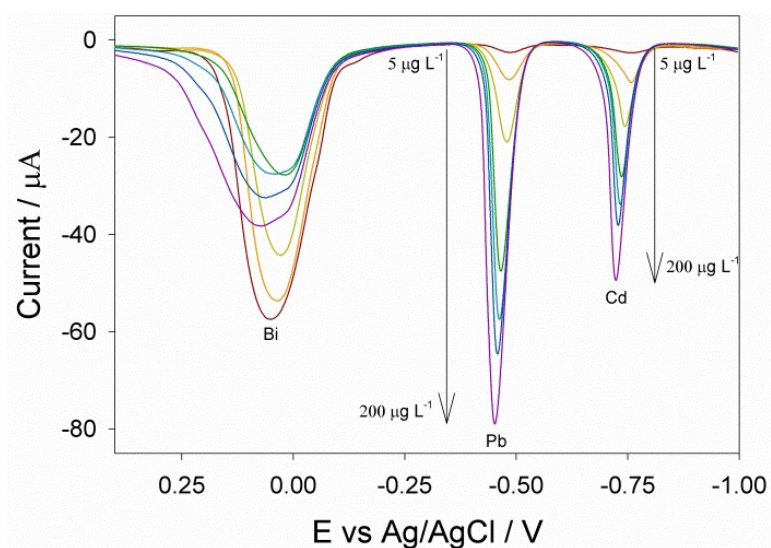


**Figure 2.5.** Simultaneous detection of Cd(II) and Pb(II) by ASV [ $5\text{--}200\ \mu\text{g L}^{-1}$  for each metal;  $0.05\ \text{M Et}_4\text{NBF}_4$ ,  $2.5\ \text{mg L}^{-1}\ \text{Bi(III)}$ ] in the absence of organic compounds.

The LOD of  $3.2 \mu\text{g L}^{-1}$  for Cd(II) is higher than  $0.76 \mu\text{g L}^{-1}$  observed when analyzed alone. During the stripping process, Cd(II) was removed first. It is not clear if the presence of Pb inside the Bi layer made it slightly more difficult to strip Cd, thus reducing the sensitivity of Cd analysis.

#### 2.3.2.2. *Detection of Pb(II) and Cd(II) in 95/5 DMSO/H<sub>2</sub>O solutions*

As indicated earlier, few studies have been performed to analyze these metals by ASV in organic solutions. Thus this is an especially significant part of the current work. Using the optimized parameters determined above, Cd(II) and Pb(II) were analyzed individually and simultaneously in the absence of representative pharmaceutical ingredients in 95/5 DMSO/H<sub>2</sub>O [0.05 M Et<sub>4</sub>NBF<sub>4</sub>, 10.0 mg L<sup>-1</sup> Bi(III)]. When analyzed separately, the Cd(II) and Pb(II) peaks were observed at -0.80 (Figure 2.6) and -0.58 V (Figure 2.7), respectively. The concentration range analyzed for Cd(II) was 50–250  $\mu\text{g L}^{-1}$  with a calculated LOD of  $18 \mu\text{g L}^{-1}$ . Interestingly, a non-linear relationship was observed between the Cd(II) concentration and its peak area. However, the data consistently fit a three parameter power function. This function, which could be converted to a linear form (Eqs. A1-A3, Appendix) was successfully used to determine Cd(II) levels in the presence of Pb(II) and representative pharmaceutical organic substrates such as ketoprofen. A possible explanation for this is the non-uniform deposition of Cd. Past studies have shown that in the presence of sulfides, Cd does not deposit in flat multilayer sheets, but deposits in nodes after the film thickness

reaches 600–700 Å.<sup>77,78</sup> These small nodular deposits increase the surface area, allowing for better Cd uptake and giving rise to the exponential increase in peak area. Trace sulfide from DMSO may have caused the uneven Cd deposition. The equation fit to the detection of solitary Cd(II) in 95/5 DMSO/H<sub>2</sub>O was  $y = 2.8e^{-5}x^{2.0} - 0.08$ ,  $R^2 = 0.997$  with a calculated LOD of 18  $\mu\text{g L}^{-1}$ . Unlike Cd(II), Pb(II) gives a linear response within a concentration range of 5–200  $\mu\text{g L}^{-1}$  with a calculated LOD of 0.80  $\mu\text{g L}^{-1}$  (Table 2.1).

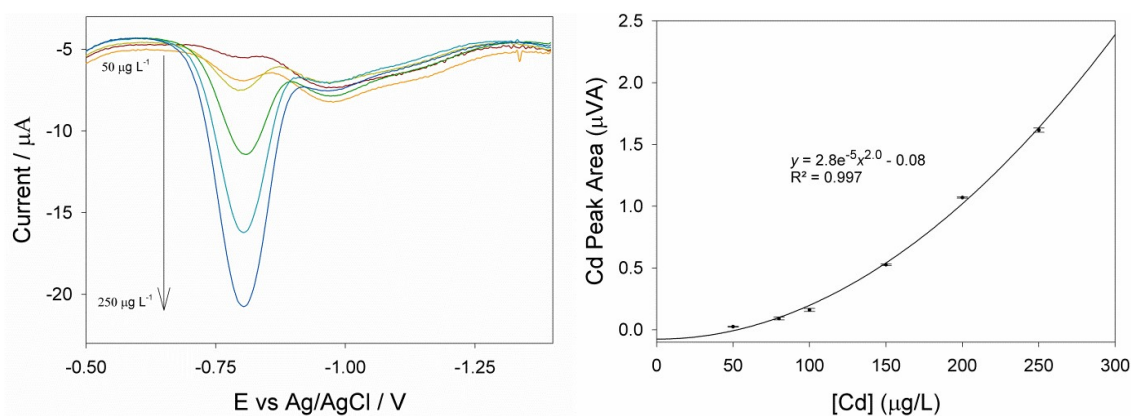


**Figure 2.6.** Voltammogram with increasing Cd(II) concentrations (50–250  $\mu\text{g L}^{-1}$ ) through standard addition in 95/5 DMSO/H<sub>2</sub>O [0.05 M Et<sub>4</sub>NBF<sub>4</sub>, 10.0 mg L<sup>-1</sup> Bi(III)] in the absence of Pb(II) and representative pharmaceutical substrates.

When detected simultaneously in 95/5 DMSO/H<sub>2</sub>O, the Cd(II) and Pb(II) peaks were observed at -0.80 and -0.58 V (Figure 2.8), respectively. The concentration range was 20–150  $\mu\text{g L}^{-1}$  with a calculated LOD of 2.9 and 25  $\mu\text{g L}^{-1}$  for Pb(II) and Cd(II), respectively.

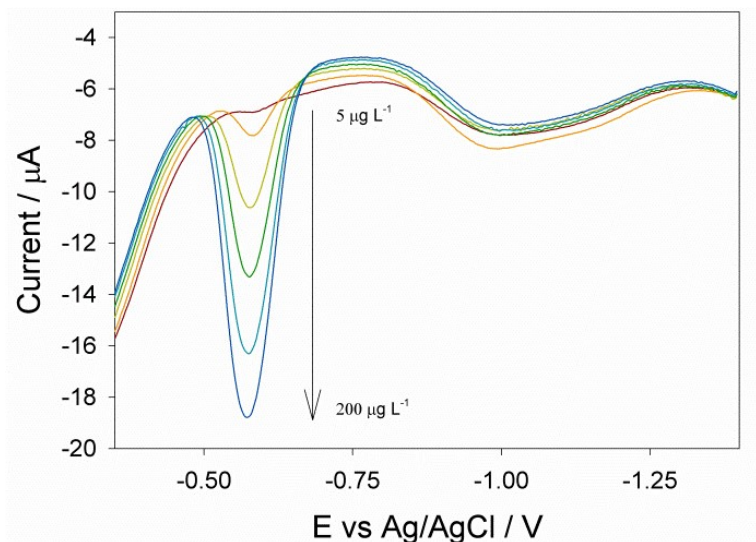


**Figure 2.7.** Increasing Pb(II) concentrations (5–200  $\mu\text{g L}^{-1}$ ) through standard addition in 95/5 DMSO/H<sub>2</sub>O [0.05 M Et<sub>4</sub>NBF<sub>4</sub>, 10.0 mg L<sup>-1</sup> Bi(III)] in the absence of Cd(II) or representative pharmaceutical substrate.

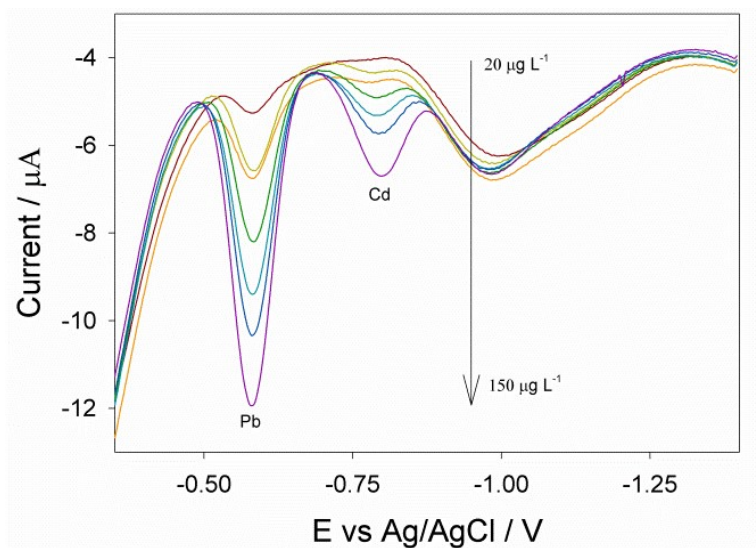


**Figure 2.8.** Detection of Cd(II) and Pb(II) through simultaneous standard additions (20–150  $\mu\text{g L}^{-1}$ ) in 95/5 DMSO/H<sub>2</sub>O [0.05 M Et<sub>4</sub>NBF<sub>4</sub>, 10.0 mg L<sup>-1</sup> Bi(III)] in the absence of representative pharmaceutical substrates.

Analysis of low-ppb Cd(II) in DMSO is the least sensitive of the detections (i.e., analyses of Cd(II) and Pb(II) in aqueous and DMSO, respectively) in the current work, and it is especially inhibited in the presence of Pb(II). However, due to the exponential nature of the Cd(II) regressions in DMSO, higher concentrations show stronger peaks than in the aqueous media. It is also interesting that the Pb(II) regression continues to stay linear even as the Cd(II) regression is not.

#### *2.3.2.3. Organic matrix effect*

The impact of organic substrates on the accuracy and sensitivity of the electroanalytical approach was investigated in aqueous solutions, using representative pharmaceutical organic components such as caffeine and lactose. Lactose and caffeine, both soluble in the aqueous solution, were evaluated separately, and added to the 0.05 M Et<sub>4</sub>NBF<sub>4</sub> solution at a concentration of 1000 mg L<sup>-1</sup>. These solutions were stirred until all organic compounds had fully dissolved. The solution also contained 2.5 mg L<sup>-1</sup> Bi(III) as well as the analytes of interest [Pb(II) and Cd(II)].

In the presence of lactose, the LODs of Cd(II) and Pb(II) were 2.7 and 3.3 µg L<sup>-1</sup>, respectively (Table 2.1). As indicated in Table 2.1, similar LODs were observed in the presence of 1000 mg L<sup>-1</sup> caffeine ([Cd(II)] = 4.4 µg L<sup>-1</sup>; [Pb(II)] = 3.0 µg L<sup>-1</sup>).

For the 95/5 DMSO/H<sub>2</sub>O solutions, ketoprofen was chosen as an

appropriate model API due to its low solubility in water. It was used at a concentration of 1000 mg L<sup>-1</sup> in 0.05 M Et<sub>4</sub>NBF<sub>4</sub> with 10.0 mg L<sup>-1</sup> Bi(III) solution while Cd(II) or Pb(II) was detected. LODs of Cd(II) (20–150 µg L<sup>-1</sup>) and Pb(II) (5–160 µg L<sup>-1</sup>) are 22 and 1.9 µg L<sup>-1</sup>, respectively (Table 2.1).

Addition of representative pharmaceutical ingredients to the electrolytic solutions resulted in weaker analyte detection with lower slopes and consequently higher LODs for both Cd and Pb. However, since the tests were conducted with high concentrations of the representative pharmaceutical ingredients, achieving the Cd(II) and Pb(II) detection in the low µg L<sup>-1</sup> range is remarkable, demonstrating the strength and potential of this method. In addition, two features of the method are particularly attractive. The first is that it is simple, using a bare, unmodified GCE. Thus there is little on the electrode for the organic compounds to interact with. For many modified electrodes, interactions between organic compounds and the electrode surface may limit the type of organic compounds to be analyzed. The second feature is the use of Bi(III) co-deposition, increasing detection sensitivity over pre-deposited Bi thin film electrodes.<sup>21,22</sup> In 95/5 DMSO/H<sub>2</sub>O, Bi(III) was required to see Pb(II) and Cd(II) in the low µg L<sup>-1</sup> range. In the aqueous solutions with an organic compound present, Bi(III) greatly increased the analyte peak areas (Figure 2.2A).

The effect of the organic substrates on the detection sensitivity is slight, but evident through comparisons of regression slopes and LODs. One example is the slight change in slope for Cd(II) detection in aqueous solutions, without and with lactose present: 0.0107 to 0.0042, respectively. Most likely, this decreased

response is due to the organic compounds hindering the mass transport of the metals to the surface during the deposition step, although the Bi(III) co-deposition helps to counteract this. In some instances, however, the addition of the organic compound causes little change in slope (such as detection of Cd(II) with caffeine in aqueous solution) or actually increases the detection response (Pb(II) with caffeine in aqueous solution), as shown in Table 2.1. Much of this variation, caused by the organic interference, can be combatted with standard addition as well as an increased deposition time. In all cases, the LODs are lower for the metals in the absence of representative pharmaceutical ingredients than in their presence. However the LODs are still comparable between these solutions. This comparison shows the selectivity and sensitivity of the analytical method, even in solutions with high concentrations of organic material, and portrays a sensing platform that can be pushed to even further limits. It also opens doors for future investigations of voltammetric methods that may be optimized around specific organic interferers in different media. Overall, these results certainly highlight the ability to analyze metals in pharmaceutical matrices through ASV without the use of pretreatment methods.

#### *2.3.2.4. Reproducibility and precision*

Tests of the current technique in both aqueous and 95/5 DMSO/H<sub>2</sub>O solutions show high reproducibility and consistency (Table 2.1). This is perhaps due, in part, to its simplicity and the optimized cleaning steps which allowed for a

**Table 2.1.** A Comparison of Cd and Pb analyses and figures of merit.

Analyte	Interference	Media	Regression	$R^2$	RSD at 50 $\mu\text{g L}^{-1}$ (n = 3)	LOD ( $\mu\text{g L}^{-1}$ ) (n = 3)	LOD in solid organic ( $\mu\text{g g}^{-1}$ )
Cd(II)	-	Water	$y = 0.0107x + 0.1173$	0.996	1.6%	0.76	-
Pb(II)	-	Water	$y = 0.014x - 0.1066$	0.989	1.3%	1.9	-
Cd(II)	Pb(II)	Water	$y = 0.0113x + 0.1449$	0.990	8.6%	3.2	-
Pb(II)	Cd(II)	Water	$y = 0.0216x + 0.077$	0.999	0.97%	1.9	-
Cd(II)	Lactose	Water	$y = 0.0042x + 0.0401$	0.994	4.7%	2.7	2.7
Pb(II)	Lactose	Water	$y = 0.0104x + 0.0276$	0.985	3.1%	3.3	3.3
Cd(II)	Caffeine	Water	$y = 0.0097x + 0.0093$	0.992	3.2%	4.4	4.4
Pb(II)	Caffeine	Water	$y = 0.0234x - 0.0767$	0.987	1.2%	3.0	3.0
Cd(II)	-	DMSO	$y = 2.8e^{-5}x^2 - 0.08$	0.997	11%	18	-
Pb(II)	-	DMSO	$y = 0.0041x - 0.0608$	0.999	0.46%	0.80	-
Cd(II)	Pb(II)	DMSO	$y = 2.1e^{-7}x^{2.7} - 2.7e^{-3}$	0.996	2.7%	25	-
Pb(II)	Cd(II)	DMSO	$y = 0.0041x - 0.0608$	0.996	2.7%	3.0	-
Cd(II)	ketoprofen	DMSO	$y = 3.7e^{-7}x^{2.7} - 3.9e^{-3}$	0.999	1.9%	22	22
Pb(II)	ketoprofen	DMSO	$y = 0.0022x - 0.007$	0.999	5.7%	1.9	1.9



fresh GCE surface each time. RSD was calculated through triplicate stripping analysis in a sample containing  $50 \mu\text{g L}^{-1}$  of the analyte, with cleaning between measurements. All but one RSD are below 9.0%. The table also shows that Cd(II) is much less responsive at low concentrations in DMSO than in water, but the exponential curve greatly increases the signal as the concentration increases.

The CHI software was used to determine the peak areas, which is calculated using a *linear* baseline between the two peak edges. Upon review of the regression equations in Table 2.1 which indicate the relationship between analyte concentration ( $x$ ) and the analyte peak area ( $y$ ), it was clear that statistical bias is present in many of them, as indicated by the large absolute values of the intercepts. It is the belief of the author that this error spawns from inadequate integration methods that do not take into account the often non-linear nature of the voltammogram baseline. For future studies, a more accurate method will be determined and employed.

### **2.3.3. Apparent recoveries<sup>79</sup>**

In an aqueous solution containing  $1000 \text{ mg L}^{-1}$  caffeine,  $10.0 \mu\text{g L}^{-1}$  Pb(II) and  $15.0 \mu\text{g L}^{-1}$  Cd(II) had apparent recoveries of 114% and 108%, respectively. In 95/5 DMSO/H<sub>2</sub>O solutions containing  $1000 \text{ mg L}^{-1}$  ketoprofen,  $5.0 \mu\text{g L}^{-1}$  Pb(II) and  $40.0 \mu\text{g L}^{-1}$  Cd(II) were recovered at 97.1% and 99.5%, respectively. These tests indicate that the method and platform used herein are sufficiently accurate

and can be used for the direct detection of both Cd(II) and Pb(II) as a quantitative or qualitative pre-screening method.

The response of Cd(II) in the presence of sulfide impurities in DMSO is non-linear. We have developed a method to derive the Cd(II) concentration by standard addition. The non-linear method was successfully used to determine the unknown [Cd(II)] in a solution. The method and experimental procedures for apparent recovery experiments are provided in Appendix A.

#### **2.4. Conclusion**

This work demonstrated the use of the classical electroanalytical method, ASV, by using an off-the-shelf, unmodified GCE, for the analysis of two of the most toxic elemental impurities, Cd(II) and Pb(II), at trace levels in representative pharmaceutical matrices. The analyses were successfully performed in both aqueous and DMSO/water solutions, allowing for the fast and simple dissolution of an active pharmaceutical ingredient, rendering ashing pretreatment techniques unnecessary. To the best of our knowledge, this is the first detection of heavy metals in DMSO-based solutions through ASV (with or without organic substrates). Detecting these heavy metals in pharmaceuticals is an important application of electrochemical analysis to an area of current interest.

While the detection limits are generally higher than the USP limits of cadmium and lead in pharmaceuticals, comparable LODs without and with the organic matrices indicate that detection of these impurities in the presence of an

API/excipient at even higher concentrations can still be maintained at trace levels. It can also be taken into account that acidifying the sample would allow for the analysis of a larger sample and lower organic interference, as well as increase the solubility of analytes in the form of metal oxides. Again, it is important to note that no data in the current studies were background-subtracted so as to replicate the determination of an unknown metal concentration in a real sample. Additional research and developments are needed to make this method meet the requirements of USP <233>. Future studies may be directed to increase sensitivity, include more analytes, and detect elements at higher API/excipient concentrations.

## References

1. Guzinski, M; Lisak, G.; Kupis, J.; Jasinski, A; Bochenska, M. *Anal. Chim. Acta* **2013**, *791*, 1-12.
2. *Analytical Chemistry of Cadmium: Sample Pre-Treatment and Determination Methods*, Moreda-Pineiro, A.; Moreda-Pineiro, J.; Eds.; Nova Science, Hauppauge, New York 2010.
3. Fitch, A. *Crit. Rev. Anal. Chem.* **1998**, *28*, 267-345.
4. Petrovic, S.C.; King, D.F.; Dewald, H.D. *Electroanal.* **1998**, *10*, 393-398.
5. Kasparova, L.; Navratil, T; Oieaoova, B.; Senholdova, Z. *Metals and Neurotoxicity*, Vojtisek, M.; Prakash, R.; Eds.; Society for Science and Environment, Jalgaon, India 2009. pp. 149-170/171-248.
6. Yantasee, W.; Lin, Y.; Hongsirikarn, K.; Fryxell, G.E.; Addleman, R.; Timchalk, C. *Environ. Health Perspect.* **2007**, *115*, 1683-1690.
7. Van Leeuwen, H.P.; Town, R.M. *Envir. Sci. Technol.* **2003**, *37*, 3945-3952.
8. Gissera, M.J.; Sevilla, M.T.; Procopio, J.R.; *Anal. Sci.* **2006**, *22*, 405-410.
9. Taylor, A.; Day, M.P.; Hill, S.; Marshall, J.; Patriarca, M.; White, M. *J. Anal. At. Spectrom.* **2015**, *30*, 542–579.
10. Pohl, P. *Trends Anal. Chem.* **2009**, *28*, 117-128.
11. Elemental Impurities: Standards-Setting Record, USP, December 20, 2012, [http://www.usp.org/sites/default/files/usp\\_pdf/EN/USPNF/2012-12-20\\_elemental\\_impurities\\_standards-setting\\_record-full.pdf](http://www.usp.org/sites/default/files/usp_pdf/EN/USPNF/2012-12-20_elemental_impurities_standards-setting_record-full.pdf) accessed on October 1, 2014.

12. <232> Elemental Impurities—Limits and <233> Elemental Impurities—Procedures, USP, <http://www.usp.org/usp-nf/official-text/accelerated-revision-process/accelerated-revision-history/elemental-impurities-limits-and-elemental> accessed on October 1, 2014.
13. Liba, A.; McCurdy, E., Proposed New USP General Chapters <232> and <233> for Elemental Impurities: The Application of ICP-MS for Pharmaceutical Analysis, [http://www.chem.agilent.com/Library/whitepaper/Public/5990-9382EN\\_WhitePaper\\_7700x\\_Pharma.pdf](http://www.chem.agilent.com/Library/whitepaper/Public/5990-9382EN_WhitePaper_7700x_Pharma.pdf) accessed on October 1, 2014.
14. Q3D (Impurities: Guideline for Metal Impurities), ICH, December 16, 2014, [http://www.ich.org/fileadmin/Public\\_Web\\_Site/ICH\\_Products/Guidelines/Quality/Q3D/Q3D\\_Step\\_4.pdf](http://www.ich.org/fileadmin/Public_Web_Site/ICH_Products/Guidelines/Quality/Q3D/Q3D_Step_4.pdf) accessed on February 3, 2015.
15. Kemula, W.; Strojek, J. *Chemia Analityczna* **1963**, *8*, 685–690.
16. Kemula, W.; Galus, Z.; Kublik, Z. *Nature* **1958**, *182*, 1228–1229.
17. Bard, A.J.; Faulkner, L.R. *Electrochemical Methods. Fundamentals and Applications*, 2<sup>nd</sup> ed., Wiley, Hoboken, New York, 2001, p. 458.
18. Compton, R.G.; Banks, C.E.; *Understanding Voltammetry*, 2<sup>nd</sup> ed., Imperial College Press, London, 2011.
19. Wang, J. *Analytical Electrochemistry*, Wiley-VCH, Hoboken, New York, 2000, p. 86.
20. Wang, J.; Lu, J.; Hocevar, S.B.; Farias, P.A.M.; Ogorevc, B. *Anal. Chem.* **2000**, *72*, 3218–3222.
21. Rico, M.A.G; Olivares-Marin, M.; Gil, E.P. *Electroanal.* **2008**, *20*, 2608–

- 2613.
22. Rico, M.A.G.; Olivares-Marin, M.; Gil, E. P. *Talanta* **2009**, *80*, 631–635.
  23. Hocevar, S.B.; Svancara, I.; Vytras, K.; Ogorevc, B. *Electrochim. Acta* **2005**, *51*, 706–710.
  24. Svancara, I.; Baldrianova, L.; Tesarova, E.; Hocevar, S.B.; Elsuccary, S.A.A.; Economou, A.; Sotiropoulos, S.; Ogorevc, B.; Vytras, K. *Electroanal.* **2006**, *18*, 177–185.
  25. Pauliukaite, R.; Brett, C.M.A. *Electroanal.* **2005**, *17*, 1354–1359.
  26. Rehacek, V.; Hotovy, I.; Vojs, M.; Mika, F. *Microsyst. Technol.* **2008**, *14*, 491–498.
  27. Lee, G.; Lee, H.; Rhee, C. *Electrochem. Commun.* **2007**, *9*, 2514–2518.
  28. Hwang, G.H.; Han, W.K.; Park, J.S.; Kang, S.G. *Talanta* **2008**, *76*, 301–308.
  29. Wu, Y.; Li, N.B.; Luo, H.Q. *Sens. Actuat. B.* **2008**, *133*, 677–681.
  30. Siriangkhawut, W.; Pencharee, S.; Grudpan, K.; Jackmune, J. *Talanta* **2009**, *79*, 1118–1124.
  31. Torma, F.; Kádár, M.; Tóth, K.; Tatár, E. *Anal. Chim. Acta* **2008**, *619*, 173–182.
  32. Kefala, G.; Economou, A. *Anal. Chim. Acta* **2006**, *576*, 283–289.
  33. Kachoosangi, R.T.; Banks, C.E.; Ji, X.; Compton, R.G. *Anal. Sci.* **2007**, *23*, 283–289.
  34. Toghill, K.E.; Wildgoose, G.G.; Moshar, A.; Mulcahy, C.; Compton, R.G. *Electroanalysis* **2008**, *20*, 1731–1737.
  35. Anastasiadou, Z.D.; Sipaki, I.; Jannakoudakis, P.D.; Girousi, S.T. *Anal.*

*Letters* **2011**, *44*, 761–777.

36. Qi, L.; Mei, L.H.; Hui, Z.Y.; Cong, R.M.; Xian, K.H.; Hua, T.X.; Xi, C *Sci. China Chem.* **2013**, *56*, 1749–1756.
37. Long, J.; Nagaosa, Y. *Intern. J. Environ. Anal. Chem.* **2008**, *88*, 51–60.
38. Wang, J.; Lu, J. *Electrochem. Comm.* **2000**, *2*, 390–393.
39. Wang, J.; Lu, J.; Hocevar, S.B.; Ogorevc, B. *Electroanal.* **2001**, *13*, 13–16.
40. Lin, L.; Lawrence, N.S.; Thongngamdee, S.; Wang, J.; Lin, Y. *Talanta* **2005**, *65*, 144–148.
41. Wang, J.; Lu, D.; Thongngamdee, S.; Lin, Y.; Sadik, O.A. *Talanta* **2006**, *69*, 914–917.
42. Armstrong, K.C.; Tatum, C.E.; Dansby-Sparks, R.N.; Chambers, J.Q.; Xue, Z.-L. *Talanta* **2010**, *82*, 675–680.
43. Ouyang, R.; Zhu, Z.; Tatum, C.E.; Chambers, J.Q.; Xue, Z.-L. *J. Electroanal. Chem.* **2011**, *656*, 78–84.
44. Yong, L.; Armstrong, K.C.; Dansby-Sparks, R.N.; Carrington, N.A.; Chambers, J.Q.; Xue, Z.-L. *Anal. Chem.* **2006**, *78*, 7582–7587.
45. Dansby-Sparks, R.N.; Chambers, J.Q.; Xue, Z.-L. *Anal. Chim. Acta.* **2009**, *643*, 19–25.
46. Wang, J.; Lu, J.; Kirgöz, Ü.A.; Hocevar, S.B.; Ogorevc, B. *Anal. Chim. Acta* **2001**, *434*, 29–34.
47. Lu, M.; Toghill, K.E.; Compton, R.G. *Electroanal.* **2011**, *23*, 1089–1094.
48. El Tall, O.; Jaffrezin-Renault, N.; Siguad, M.; Vittori, O. *Electroanal.* **2007**, *19*, 1152–1159.

49. McGaw, E.A.; Swain, G.M. *Anal. Chim. Acta* **2006**, *575*, 180–189.
50. Toghil, K.E.; Xiao, L.; Wildgoose, C.G.; Compton, R.G.; *Electroanal.* **2009**, *21*, 1113–1118.
51. Tesarova, E.; Baldrianova, L.; Hocevar, S.B.; Svancara, I.; Vytras, K.; Ogorevc, B. *Electrochim. Acta* **2009**, *54*, 1506–1510.
52. Bi, Z.; Salaun, P.; Van Den Berg, C.M.G. *Anal. Chim. Acta* **2013**, *769*, 56–64.
53. de Oliveira, M.F.; Saczk, A.A.; Okumura, L.L.; Fernandes, A.P.; de Moraes, M.; Stradiotto, N.R. *Anal. Bioanal. Chem.* **2004**, *380*, 135–140.
54. Mamani, M.C.V; Aleixo, L.M.; de Abreu, M.F.; Rath, S. *J. Pharm. Biomed. Anal.* **2005**, *37*, 709–713.
55. Matloob, M.H. *Mediterr. Health J.* **2003**, *9*, 28–36.
56. Mascarenhas, R.J.; Satpati, A.K.; Yellapa, S.; Sherigara, B.S.; Bopiah, A.K. *Anal. Sci.* **2006**, *22*, 871–875.
57. Lokesh, S.V.; Sherigara, B.S.; Naik, H.S.; Shivaraj, Y.; Satpati, A.K. India, J. *Environ. Sci. Eng.* **2008**, *50*, 69–74.
58. Holak, W.; Specchio, J.J.; *J. Assoc. Off. Anal. Chem.* **1988**, *71*, 857–859.
59. Gajan, R.J.; Capar, S.G.; Subjoc, C.A.; Sanders, M. *J. Assoc. Off. Anal. Chem.* **1982**, *65*, 970–977.
60. Coco, F.L.; Monotti, P.; Novelli, V.; Ceccon, L.; Adami, G.; Micali, G. *Food Addit. Contam.* **2004**, *21*, 441–446.
61. Pravda, M.; Vytrās, K. *J. Pharm. Biomed. Anal.* **1996**, *14*, 765–771.
62. Jyothi, N.V.V.; Mouli, P.C.; Reddy, S.R.J.; *J. Trace Elem. Med. Biol.* **2003**,



- 17, 79–83.
63. Melucci, D.; Torsi, G.; Locatelli, C. *Ann. Chim.-Rome*. **2007**, *97*, 141–145.
  64. Mester, Z.; Sturgeon, R. *Comprehensive Analytical Chemistry Volume XLI: Sample Preparation for Trace Metal Analysis*, Elsevier B.V., Amsterdam, 2003.
  65. Bragg, S.A.; Xue, Z.-L. *Am. J. Anal. Chem.* **2011**, *2*, 979–983.
  66. Lipinski, C. *Pharmaceutical Profiling in Drug Discovery for Lead Selection*; Borchardt, R; Kerns, E; Lipinski, C; Thakker, D; Wang, B. *Biotechnology: Pharmaceutical Aspects 1; American Association of Pharmaceutical Scientists*: Arlington, Texas, 2004; pp. 93–125.
  67. Wang, J.; Tuzhi, P.; *Anal. Chim. Acta* **1987**, *197*, 367-372.
  68. Daniele, S.; Corbetta, M.; Baldo, M.A.; Bragato, C. *J. Electroanal. Chem.* **1996**, *407*, 149-154.
  69. Baldo, M.A.; Daniele, S.; *Electroanal.* **2006**, *18*, 633-639.
  70. Barton, Z.J.; Rodríguez-López, J. *Anal. Chem.* **2014**, *86*, 10660–10667.
  71. Tohge, N.; Takahashi, S.; Minami, T. *J. Am. Ceram. Soc.* **1991**, *74*, 67–71.
  72. Bradley, D.C. *Chem. Rev.* **1989**, *89*, 1317–1322.
  73. Lennstrom, K.; Limmer, S.J.; Cao, G. *Thin Solid Films* **2003**, *434*, 55–61.
  74. West, C.J.; Hull, C. *International Critical Tables of Numerical Data, Physics, Chemistry and Technology*, Maple Press Co., York, Pennsylvania 1933.
  75. Jacques, A. *Complex Ions in Aqueous Solutions*, Longmans, Green and Co., London, 1914.
  76. Jacques, A. *Trans. Faraday Soc.* **1910**, *5*, 225–243.

77. Balakrishnan, K.S.; Rastogi, A.C. *Solar Energy Mat.* **1990**, *20*, 417–434.
78. Kadirgan, F.; Mao, D.; Song, W.; Ohno, T.; McCandless, B. *Turk. J. Chem.* **2000**, *24*, 21–33.
79. Burns, D.H.; Danzer, K.; Townshend, A. *Pure Appl. Chem.* **2002**, *74*, 2201–2205.

## **PART 3**

**Direct analysis of palladium in active pharmaceutical ingredients by anodic stripping voltammetry**

A version of this chapter was originally published by Samuel M. Rosolina, James Q. Chambers, and Zi-Ling Xue. Only minor revisions were made.

Samuel M. Rosolina, James Q. Chambers, and Zi-Ling Xue. "Direct analysis of palladium in active pharmaceutical ingredients by anodic stripping voltammetry." *Anal. Chim. Acta* **2016**, *914*, 47–52.

Additional materials for Part 3 are provided in Appendix B.

## Abstract

Anodic stripping voltammetry, a classical electroanalytical method has been optimized to analyze trace Pd(II) in active pharmaceutical ingredient matrices. The electroanalytical approach with an unmodified glassy carbon electrode was performed in both aqueous and 95% DMSO/5% water (95/5 DMSO/ H<sub>2</sub>O) solutions, *without* pretreatment such as acid digestion or dry ashing to remove the organics. Limits of detection (LODs) in the presence of caffeine and ketoprofen were determined to be 11 and 9.6  $\mu\text{g g}^{-1}$ , with a relative standard deviation (RSD) of 5.7% and 2.3%, respectively. This method is simple, highly reproducible, sensitive, and robust. The instrumentation has the potential to be portable and the obviation of sample pretreatment makes it an ideal approach for determining lost catalytic metals in pharmaceutical-related industries. Furthermore, the simultaneous detection of Pd(II) with Cd(II) and Pb(II) in the low  $\mu\text{g L}^{-1}$  range indicates that this system is capable of simultaneous multi-analyte analysis in a variety of matrices.

### **3.1. Introduction**

Platinum group metals are heavily used in catalysis pharmaceutical synthesis. Palladium-based catalysts are particularly useful for large scale synthesis of active pharmaceutical ingredients (APIs) mainly because many important organic reactions, including carbon-carbon cross-coupling, hydrogenations and cyclization reactions, rely on the catalysts.<sup>1</sup> Furthermore, palladium catalysts have been shown to be successful in the coupling of substrates with low reactivity, allow reactions to take place at lower temperatures, and often have the best turnover numbers in comparison to other catalysts.<sup>2</sup> Analysis of trace, residual palladium in pharmaceutical matrices is significant for several reasons. First, residual palladium may lead to unwanted side reactions during subsequent steps in synthesis, lowering the yields of final products. Second, palladium left in APIs has adverse effects on health of patients. Although it has a low acute oral toxicity, palladium is known to be a potent sensitizer, second only behind nickel.<sup>3</sup> Third, a consistent loss of palladium throughout the multi-step synthesis of APIs could quickly become costly. A quick and inexpensive analysis of the lost metal in API would help to determine inefficiencies in the system.

Detection and quantification of elemental impurities in pharmaceutical drug products (DPs) and their in-going components (APIs and excipients) to meet more stringent regulatory guidelines remain a major challenge. The International Conference on Harmonisation (ICH), which works to achieve greater harmonization of regulatory procedures in the world, recently published

new guidance (ICH Q3D) for the control of elemental impurities in pharmaceuticals products.<sup>4</sup> This new guideline has identified 24 elemental impurities, including previously unmonitored catalytic metals that must be controlled to the established Permissible Daily Exposure values (PDEs). Palladium, with an Elemental Impurity Classification of 2B, has a PDE of 100 µg/day, based on the oral route of administration. At the total oral daily intake of 10 g/day, palladium must be controlled down to 10 µg/g (ppm) in finished drug products.

ICP-based techniques, known to detect to the parts per trillion (ppt, ng L<sup>-1</sup>) level for most metals, are capable of addressing the requirements of the new proposed limits.<sup>5,6</sup> These techniques depend, however, on expensive instrumentation in a central laboratory, and are thus not portable. Many methods also require time-consuming sample pretreatment, including acid or microwave mineralization of the samples prior to analysis, in order to minimize interferences. Any extra sample handling increases the total error of the analysis and the time needed for sample shipment and pretreatment. It is highly desirable to develop lower cost, *portable field methods* to accurately detect and quantitate elemental impurities in APIs *without pretreatment*.

Electrochemical methods are attractive alternatives to ICP-based approaches. In addition to possessing high resolution, multi-element detection capabilities, electroanalytical approaches require instrumentation of relatively low-cost maintenance and operation. Several stripping voltammetric methods are in existence for the analysis of Pd(II) in aqueous solutions, most of which utilize

adsorptive stripping voltammetry (AdSV) on a hanging mercury drop electrode.<sup>7-11</sup> The method, relying on toxic mercury, raises safety and environmental concerns. An inexpensive, commercial, non-toxic electrode, requiring *no* modification, is an ideal probe for palladium analysis in APIs. A previous study used a bare glassy carbon electrode for the detection of Pd(II) in superficial nuclear wastes using anodic stripping voltammetry (ASV).<sup>12</sup>

ASV is a common electroanalytical technique first developed by Kemula in conjunction with his newly invented mercury-drop electrode.<sup>13,14</sup> Known for its speed and sensitivity, ASV utilizes the reduction of metal ions onto an electrode surface followed by rapid oxidation (stripping) of the metals off of the electrode back into solution, producing the currents in the anodic peaks.<sup>15-17</sup> Square wave voltammetry (SWV) is one of the most sensitive voltammetric methods, making it especially useful when paired with ASV for trace analysis.<sup>15-17</sup>

Electroanalysis of elemental impurities in organic matrices typically requires sample pretreatment to remove the organic matrices from the sample prior to analysis. Removal of the organic matrix is often conducted by acid digestions at elevated temperatures, using concentrated acids such as nitric acid, hydrochloric acid, sulfuric acid, and mixtures thereof.<sup>18-28</sup> Digestions are often performed in microwaves, in open and closed vessels. Removal of the organic matrix may also be conducted via dry-ashing, where the organic matrix is combusted at elevated temperatures, leaving the metal analytes behind.<sup>29,30</sup> Both pretreatments require slow and careful work to reduce errors during the process or sample transfer. Incomplete mineralization is also a common occurrence.<sup>29,30</sup>

For post wet-ashing samples, the low pH in the digest is not desirable in the subsequent electrochemical analysis. Aside from the potential to damage the electrode directly, the increased acidity may decrease the allowed potential window for detection due to the production of H<sub>2</sub> gas during the metal deposition.

This work describes the use of square wave anodic stripping voltammetry (SWASV) to detect and quantitate Pd(II) in pharmaceutical-like matrices. No sample pretreatment, either wet- or dry-ashing, is needed prior to the electrochemical analyses. The analyses conducted in both aqueous and 95/5 DMSO/ H<sub>2</sub>O solutions with and without pharmaceutical substrates. The process uses a simple, un-modified glassy carbon electrode (GCE) to analyze Pd(II) in the low ppb ( $\mu\text{g L}^{-1}$ ) range. An in-situ bismuth codeposition allows for the detection of Pd(II) in the 95/5 DMSO/ H<sub>2</sub>O solution, which is otherwise unobservable. No prefabrication of the off-the-shelf, commercial GCE is needed.

The stripping step, followed by a cleaning step, oxidizes and removes the metal analyte from the electrode, forming a fresh surface each time, allowing for more consistent results within the technique. The importance of this method lies in its ability to be used in both aqueous and DMSO-based media. Using either water or the DMSO solutions, representative APIs, excipients, and dietary supplements are easily dissolved with little to no prior workup, reducing the need for wet or dry-ashing of the sample.<sup>31</sup> We have chosen DMSO as our non-aqueous solvent, as DMSO, with fewer hydrogen bonding networks than water, is commonly used to dissolve many drug components.<sup>31</sup> The method reported here allows for inexpensive, fast, and portable analysis of Pd(II), thus creating



the opportunity to pre-screen many organic products for palladium impurities as well as pin-pointing stages where catalysts are deactivated throughout the API's synthesis. It also has the capability for simultaneous coanalysis of Cd(II) and Pb(II) along with Pd(II) in the same solutions. The work herein is, to our knowledge, the first work to detect palladium in pharmaceutical matrices using electroanalysis, as well as the first detection of palladium in DMSO solutions.

### **3.2. Materials and methods**

#### **3.2.1. Chemicals and instruments**

The following chemicals were used as received and of analytical grade: caffeine (Thermo Fisher Scientific, Waltham, MA), ketoprofen (Sigma Aldrich Co., St. Louis, MO), tetraethylammonium tetrafluoroborate ( $\text{Et}_4\text{NBF}_4$ , Sigma Aldrich Co.), DMSO (Thermo Fisher Scientific), ethanol (95%, Decon Laboratories, Inc., King of Prussia, PA). Standard solutions of Pd(II), Bi(III), Cd(II), and Pb(II) with concentrations of  $1000 \text{ mg L}^{-1}$  in 10%  $\text{HNO}_3$  (Ricca Chemical Co., Arlington, TX) were diluted in supporting electrolytes to form stock solutions. Ultrapure water from a Millipore water purified system ( $\geq 18 \text{ M}\Omega\cdot\text{cm}$ , Barnstead Thermolyne, Thermo Fisher Scientific) was used in all assays. 95/5 DMSO/ $\text{H}_2\text{O}$  was made by adding 1.0 mL ultrapure water to 19.0 mL of DMSO in the electrochemical cell prior to analysis.

Prior to use, GCEs were polished to a mirror-like surface on a standard electrode polishing kit (CH Instruments Inc., Austin, TX) including a 1200 grit

CarbiMet™ disk, 1.0 and 0.3  $\mu\text{m}$  alumina slurry on a nylon cloth, and 0.05  $\mu\text{m}$  alumina slurry on a microcloth polishing pad. After polishing, GCEs were successively sonicated with deionized (DI) water, ethanol, and DI water again for 5 min each. Electrochemical measurements were carried out on a CHI 440a Electrochemical Workstation (CH Instruments). A three-electrode configuration consisted of a bare, unmodified GCE (3 mm in diameter, BAS Inc., West Lafayette, IN), Ag/AgCl (saturated KCl solution, CH Instruments) and a platinum wire (CH Instruments) as working, reference, and counter electrodes, respectively.

### **3.2.2. Sample preparation and SWASV analysis of Pd(II)**

All experiments were conducted at room temperature without deaeration. The unmodified GCE, Ag/AgCl, and Pt wire electrodes were placed in an electrochemical cell containing 20 mL of 0.05 M  $\text{Et}_4\text{NBF}_4$  in ultrapure DI water or 0.05 M  $\text{Et}_4\text{NBF}_4$  in 95/5 DMSO/ $\text{H}_2\text{O}$ . In aqueous samples containing Bi(III), 50.0  $\mu\text{L}$  of 1000  $\text{mg L}^{-1}$  Bi(III) standard solution was added to give 2.5  $\text{mg L}^{-1}$  of total Bi(III), prior to analysis. For all 95/5 DMSO/ $\text{H}_2\text{O}$  samples, 200.00  $\mu\text{L}$  of 1000  $\text{mg L}^{-1}$  Bi(III) standard solution was added to give 9.9  $\text{mg L}^{-1}$  of total Bi(III) prior to analysis.

For analysis in aqueous solutions, the potential was held at -1.1 V for 250 s to pre-concentrate Pd onto the electrode surface via electrodeposition. This was followed by sweeping the potential from -1.1 to 0.9 V using a frequency of 15

Hz, a step potential of 4 mV, and amplitude of 25 mV for the stripping step. The solution was stirred at high speed during the accumulation, but the stirrer was turned off prior to the stripping step. The electrode surface was regenerated between measurements by holding the potential at 0.9 V for 200 s in the sample solution while stirring at high speed.

For analysis in 95/5 DMSO/H<sub>2</sub>O solutions, Pd (II) and Bi(III) were codeposited by holding the potential at -1.4 V for 300 s. For the stripping step, the potential was swept from -1.4 to 0.6 V using a frequency of 25 Hz, a step potential of 4 mV, and amplitude of 25 mV. Stirring of the solution at high speed was required for the accumulation step, but was turned off in time for the stripping step. In 95/5 DMSO/H<sub>2</sub>O, the electrode surface was regenerated between measurements by holding the potential at 0.8 V for 200 s while stirring the solution at high speed. All solutions were stirred at 1200 rpm during the accumulation step, but stirring was stopped 10 s prior to the stripping step.

Samples containing API were made by directly dissolving 20 mg of the organic compound (either caffeine or ketoprofen) in 20 mL of the media (water or 95/5 DMSO/H<sub>2</sub>O). During analysis of these samples, the solutions were allowed to stir for 1 min after spiking with Pd(II) in order to allow the metal to reach an equilibrium throughout the matrix, and to allow it to interact with the organics.

### 3.3. Results and discussion

#### 3.3.1. Analytical results

Standard addition was the chosen method for all calibration curves in this study. Thus it is important to note that all results are given *without* background subtraction. This approach was taken due to the importance of treating the analysis as if actually analyzing an unknown sample. Standard addition allows for the determination of an original concentration while keeping the matrix the same, which is necessary for analysis of an un-ashed API.

As a proof of concept for simultaneous multi-analyte detection, Pd(II) was analyzed in the presence of Bi(III), Cd(II), and Pb(II) which we have previously analyzed in pharmaceutical matrices.<sup>32</sup> Simultaneous analysis of all four metals was shown to be possible in both aqueous solutions as well as 95/5 DMSO/H<sub>2</sub>O solutions. Results, including the regression functions, square of the correlation coefficient  $R^2$ , RSD (relative standard deviation) at 80  $\mu\text{g L}^{-1}$ , and LOD for each of the following studies, are listed in Table 3.1. The classic equation for LOD was used:

$$LOD \equiv \frac{3s}{m} \quad \text{Eq. 3.1}$$

where  $s$  is the standard deviation of the peak area from the lowest observable concentration ( $n = 3$ ), and  $m$  is the slope of the linear regression.

In API solutions, API (20 mg) was dissolved in 20 mL solution, resulting in

API concentrations of  $1000 \text{ mg L}^{-1}$ . Thus, when calculating the LOD of Pd(II) as compared to the API sample,  $\mu\text{g L}^{-1}$  (mass analyte/volume solution) is directly converted to  $\mu\text{g g}^{-1}$  (mass analyte/mass API).

### **3.3.2. Detection of Pd(II)**

Using the optimized parameters listed above, Pd(II) was analyzed in aqueous solutions containing  $0.05 \text{ M Et}_4\text{NBF}_4$  as the supporting electrolyte. It was determined that addition of Bi(II) did not affect the sensitivity or selectivity of Pd(II), and was thus not necessary for analysis (Figure 3.1).

Analysis of Pd(II) was also performed in the presence of Bi(III) ( $2.5 \text{ mg L}^{-1}$ ), Cd(II) ( $80 \mu\text{g L}^{-1}$ ), and Pb(II) ( $80 \mu\text{g L}^{-1}$ ) (Figure 3.2), and in the presence of  $1000 \text{ mg L}^{-1}$  caffeine. Results are shown in Table 3.1.

Similarly, Pd(II) was analyzed in 95/5 DMSO/  $\text{H}_2\text{O}$  containing  $0.05 \text{ M Et}_4\text{NBF}_4$  as the supporting electrolyte. It was determined that a Bi codeposition using a Bi(III) concentration of at least  $8.0 \text{ mg L}^{-1}$  is required for the detection of Pd(II) in 95/5 DMSO/  $\text{H}_2\text{O}$ , otherwise no Pd(II) peak is observed at all. It is interesting to note that the addition of Bi leads to a new peak at  $-0.2 \text{ V}$  as a shoulder of the larger Bi stripping peak. Areas of the new peak show a linear correlation with Pd(II) concentrations in the solutions.

**Table 3.1.** Comparison of analyses performed and figures of merit

<b>Media</b>	<b>Interference</b>	<b>Regression</b>	<b>R<sup>2</sup></b>	<b>RSD at 50 µg L<sup>-1</sup> (n = 3)</b>	<b>LOD (µg L<sup>-1</sup>)</b>	<b>LOD (µg g<sup>-1</sup>)</b>
aqueous	-	$y = 0.0103x - 0.2110$	0.995	8.7%	5.8	-
aqueous	Cd(II), Pb(II), Bi(III)	$y = 0.0068x - 0.1579$	0.997	2.0%	4.7	-
aqueous	caffeine	$y = 0.0039x - 0.1034$	0.998	5.7%	11	11
DMSO	-	$y = 0.0046x + 0.1142$	0.992	4.6%	9.9	-
DMSO	Cd(II), Pb(II), Bi(III)	$y = 0.0047x - 0.0061$	0.997	4.2%	7.0	-
DMSO	ketoprofen	$y = 0.0044x - 0.0048$	0.996	2.3%	9.6	9.6

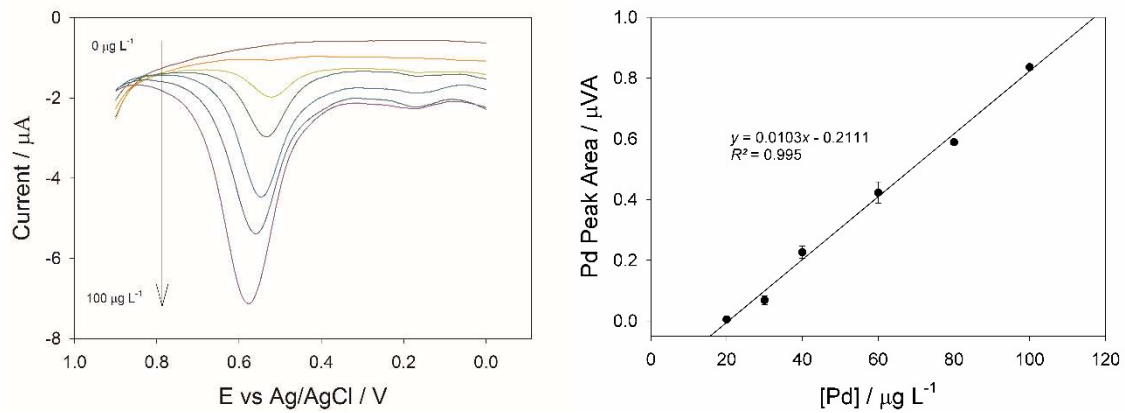


**Figure 3.1.** Analysis of Pd(II) (0–100 µg L<sup>-1</sup>) alone in aqueous solution.

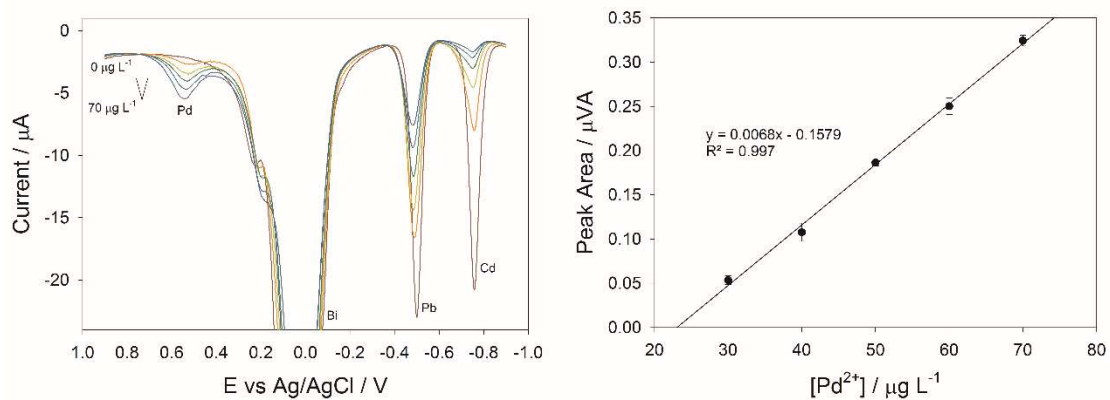


**Figure 3.2.** Analysis of Pd(II) (0–70 µg L<sup>-1</sup>) in aqueous solutions in the presence of Bi(III) (2.5 mg L<sup>-1</sup>), Cd(II) (80 µg L<sup>-1</sup>), and Pb(II) (80 µg L<sup>-1</sup>).

The nature of this peak shift is not clear. It is suspected that DMSO, a known stabilizer for nanoparticle formation,<sup>33,34</sup> may enable the reduction of Pd(II) onto the electrode surface as Pd-Bi alloy nanoparticles. Perhaps the bismuth in the Pd-Bi nanoparticles is more electropositive than the rest of bismuth in the bulk. Thus the bismuth in the Pd-Bi nanoparticles is oxidized into Bi(III) before bismuth in the bulk, forming the peak at -0.2 V. In other words, the oxidation of bismuth in the Pd-Bi nanoparticles may dislodge the Pd(0) nanoparticles from the electrode surface in the process. Thus no Pd(0) oxidation/stripping was subsequently observed at ca. +0.6 V. The higher the concentration of Pd(II) is, the more Pd-Bi nanoparticles form, leading to a larger area of the peak at -0.2 V. It has been reported that the electrooxidation of pure metal nanoparticles is shifted negatively in comparison to the electrooxidation of a bulk metal film.<sup>35</sup> Regardless of the nature of the peak, we have shown that the peak area has a direct relationship to the concentration of Pd(II) in solution before accumulation. The analysis of Pd(II) in 95/5 DMSO/ H<sub>2</sub>O was also performed in the presence of Cd(II) and Pb(II) (80 µg L<sup>-1</sup> each) using 10 mg L<sup>-1</sup> Bi(III) for codeposition (Figure 3.3), the optimized Bi(III) concentration for the detection of Cd(II) and Pb(II).<sup>32</sup> The analysis of Pd(II) was also performed separately, in the presence of ketoprofen, an API that is insoluble in water. All results are summarized in Table 3.1, with regression equations describing the relationship between Pd(II) concentration (x) and the Pd(II) peak area (y)

The CHI software was used to determine the peak areas, which is calculated using a *linear* baseline between the two peak edges. Upon review of



the regression equations in Table 3.1, it was clear that statistical bias is present in many of them, as indicated by the large absolute values of the intercepts. It is the belief of the author that this error spawns from inadequate integration methods that do not take into account the often non-linear nature of the voltammogram baseline. For future studies, a more accurate method will be determined and employed.

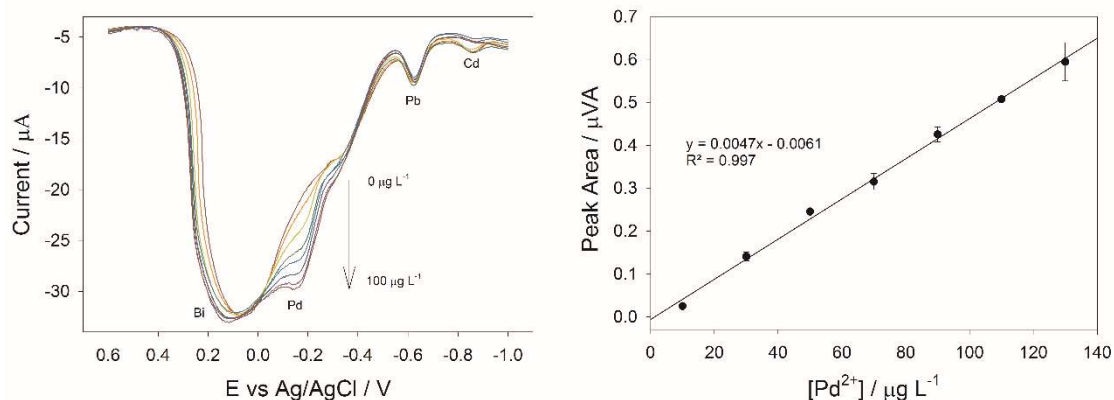


**Figure 3.3.** Detection of Pd(II) (0–100  $\mu\text{g L}^{-1}$ ) with the assistance of a Bi(III) (10.0  $\text{mg L}^{-1}$ ) codeposition in 95/5 DMSO/  $\text{H}_2\text{O}$  solutions in the presence of Cd(II) (80  $\mu\text{g L}^{-1}$ ) and Pb(II) (80  $\mu\text{g L}^{-1}$ ).

### 3.3.3. Interference effects

In aqueous solutions, interferences from the metals Cd(II), Pb(II) and Bi(III) as well as the organic caffeine have a negative effect on the sensitivity of

the Pd(II) analysis. This can be observed through a comparison of the regression model slopes summarized in Table 3.1. Increasing Pd(II) concentrations also appear to decrease the peak areas of both Cd(II) and Pb(II) (Figure 3.2). Although Cd(II) and Pb(II) were never treated as analytes in this study, it is clear that Pd(II) concentration would have an important effect on the analysis and consequent figures of merit if all three metals were to be detected simultaneously. Even so, it is apparent that all three can be qualitatively analyzed simultaneously, and quantitatively analyzed through individual standard additions. The effect of caffeine on Pd(II) analysis is strong and results in an LOD slightly higher than what will be required in the new ICH Q3D guidelines.<sup>4</sup> More work is required to decrease the lower limit, but may be as simple as increasing the amount of API being analyzed.

In 95/5 DMSO/ H<sub>2</sub>O, the dissolved ketoprofen has a much smaller effect on the slope of analysis than is seen in the caffeine/water system. Despite this slight decrease in sensitivity the LOD has not reached the new ICH guidance of 10.0 µg g<sup>-1</sup>; due in part to the high precision of the method. Contrary to the results observed in aqueous solutions, the metal interferers Cd(II), Pb(II) and Bi(III) had a positive effect on the regression slope, decreasing the LOD, as seen in Table 3.1. Furthermore, unlike the aqueous system, increasing Pd(II) concentrations do not appear to decrease the peak area of Pb(II) and only slightly decreases the peak area of Cd(II) (Figure 3.3).

### 3.3.4. Apparent recoveries

The accuracy of both the combined sensing platform and method was determined by apparent recovery of Pd(II) in the presence of organics after standard addition. This test was performed in the presence of 1000 mg L<sup>-1</sup> caffeine in an aqueous solution and also in the presence of 1000 mg L<sup>-1</sup> ketoprofen in 95/5 DMSO/ H<sub>2</sub>O. The definition for *apparent recovery* used here is based off of IUPAC recommendations which include the following equation:<sup>36</sup>

$$R'_A = \frac{x_{A(exp)}}{x_{A(theor)}} \quad \text{Eq. 3.2}$$

Where  $x_{A(exp)}$  is the value experimentally obtained from the standard addition method, and  $x_{A(theor)}$  is the known concentration value.

An aqueous solution containing 1000 mg L<sup>-1</sup> caffeine, and 0.05 M Et<sub>4</sub>NBF<sub>4</sub> was spiked to 20.0 µg L<sup>-1</sup> Pd(II). The sample was treated as an unknown and standard addition was performed by spiking the sample to added concentrations of 20.0, 40.0, 50.0, 80.0 and 90.0 µg L<sup>-1</sup> Pd(II). Between each of these spikes, SWASV was run in triplicate using the procedure previously described. By placing the original concentration at [Pd(II)] = 0, a linear regression was produced with the equation  $y = 0.0064x + 0.1202$  ( $R^2 = 0.987$ , Figure B.4 in Appendix B). Using this equation, the initial “unknown” concentration of Pd(II) was calculated to be 18.8 µg L<sup>-1</sup>, an apparent recovery of 93.9%.

A solution of 95/5 DMSO/ H<sub>2</sub>O water containing 1000 mg L<sup>-1</sup> ketoprofen, and 0.05 M Et<sub>4</sub>NBF<sub>4</sub> was spiked to an initial concentration of 20.0 µg L<sup>-1</sup> Pd(II). The sample was treated as an unknown and standard addition was performed by spiking the sample to added concentrations of 20.0, 40.0, 60.0 and 80.0 µg L<sup>-1</sup> Pd(II). After each spike, SWASV was run in triplicate using the procedure previously described. By placing the original concentration at [Pd(II)] = 0, a linear regression was produced with the equation  $y = 0.0033x + 0.0599$  ( $R^2 = 0.986$ , Figure B.5 in Appendix B). The initial “unknown” was calculated to be 18.1 µg L<sup>-1</sup>, an apparent recovery of 90.8%.

### **3.4. Conclusion**

This study has successfully demonstrated the use of SWASV using a simple GCE to detect Pd(II) in organic APIs. This important analysis can be performed in aqueous solutions or 95/5 DMSO/H<sub>2</sub>O solutions that contain dissolved APIs without pretreatment. An important finding of this work was the discovery that Pd(II) is not easily detectable in 95/5 DMSO/H<sub>2</sub>O by ASV unless co-deposited with Bi. To the best of our knowledge, this has been the first time that Pd(II) has been detected in DMSO solutions using voltammetry.

This work is particularly significant as palladium-based catalysts are among the most used in organic and pharmaceutical syntheses. Determination of palladium in the presence of directly dissolved organic compounds opens doors for industrial use and quality control. All LODs, except one, are well within the

limit. The exception, the highest LOD (in the presence of 1000 mg L<sup>-1</sup> caffeine) of 11 µg L<sup>-1</sup>, *i.e.*, 11 µg g<sup>-1</sup> of dissolved caffeine, is just outside of the newly revised ICH regulation limits. Comparable LODs in the presence and absence of organics indicate that trace level detection may still be maintained if the organic concentration is increased, allowing for lower LOD for the organics. The work reported here also indicates that Cd(II) and Pb(II) can be detected alongside Pd(II) with the aid of a Bi(III) codeposition. This work has the potential to open the doors for even more elements added to this multi-analyte simultaneous detection method in various industrial and environmental matrices.

## References

1. Recho, J.; Black, R.J.G.; North, C.; Ward, J.E.; Wilkes, R.D. *Org. Process Res. Dev.* **2014**, *18*, 626–635.
2. Magano, J.; Dunetz, J.R.; *Chem. Rev.* **2011**, *11*, 2177–2250.
3. Kielhorn, J.; Melber, C.; Keller, D.; Mangelsdorf, I. *Int. J. Hyg. Environ. Health*, **2002**, *205*, 417–432.
4. Q3D (Impurities: Guideline for Metal Impurities), ICH, December 16, 2014, [http://www.ich.org/fileadmin/Public\\_Web\\_Site/ICH\\_Products/Guidelines/Quality/Q3D/Q3D\\_Step\\_4.pdf](http://www.ich.org/fileadmin/Public_Web_Site/ICH_Products/Guidelines/Quality/Q3D/Q3D_Step_4.pdf) accessed on February 3, 2015.
5. Lewen, N.; Mathew, S.; Schenkenberger, M.; Raglione, T. *J. Pharm. Biomed. Anal.* **2004**, *35*, 739–752.
6. Wang, T.; Wu, J.; Hartman, R.; Jia, X.; Egan, R.S. *J. Pharm. Biomed. Anal.* **2000**, *23*, 867–890.
7. Sladkov, V.E.; Prokhorova, G.V.; Ivanov, V.M. *J. Anal. Chem.* **2000**, *99*, 889–892.
8. Georgieva, M.; Pihlar, B. *Fresenius J. Anal. Chem.* **1997**, *357*, 874–880.
9. Wang, J.; Varughese, K. *Anal. Chim. Acta* **1987**, *199*, (1987) 185–189.
10. Locatelli, C. *Electroanal.* **2005**, *17*, 140–147.
11. Locatelli, C. *Anal. Chim. Acta* **2006**, *557*, 70–77.
12. Bhardwaji, T.K.; Sharma, H.S.; Jain, P.C.; Aggarwal, S.K. *Nucl. Eng. Tech.* **2012**, *44*, 939–944.

13. Kemula, W.; Strojek, J. *Chemia Analityczna* **1963**, *8*, 685–690.
14. Kemula, W.; Galus, Z.; Kublik, Z. *Nature* **1958**, *182*, 1228–1229.
15. Bard, A.J.; Faulkner, L.R. *Electrochemical Methods. Fundamentals and Applications*, 2<sup>nd</sup> ed., Wiley, Hoboken, New York, 2001, p. 458.
16. R.G. Compton, C.E. Banks, *Understanding Voltammetry*, 2<sup>nd</sup> ed., Imperial College Press, London, **2011**.
17. Wang, J. *Analytical Electrochemistry*, Wiley-VCH, Hoboken, New York, 2000, p. 86.
18. Anastasiadou, Z.D.; Sipaki, I.; Jannakoudakis, P.D.; Girousi, S.T. *Anal. Letters* **2011**, *44*, 761–777.
19. Mamani, M.C.V; Aleixo, L.M.; de Abreu, M.F.; Rath, S. *J. Pharm. Biomed. Anal.* **2005**, *37*, 709–713.
20. Matloob, M.H. *Mediterr. Health J.* **2003**, *9*, 28–36.
21. Mascarenhas, R.J.; Satpati, A.K.; Yellapa, S.; Sherigara, B.S.; Bopiah, A.K. *Anal. Sci.* **2006**, *22*, 871–875.
22. Lokesh, S.V.; Sherigara, B.S.; Naik, H.S.; Shivaraj, Y.; Satpati, A.K. *J. Environ. Sci. Eng.* **2008**, *50*, 69–74.
23. Holak, W.; Specchio, J.J. *J. Assoc. Off. Anal. Chem.* **1988**, *71*, 857–859.
24. Gajan, R.J.; Capar, S.G.; Subjoc, C.A.; Sanders, M. *J. Assoc. Off. Anal. Chem.* **1982**, *65*, 970–977.
25. Coco, F.L.; Monotti, P.; Novelli, V.; Ceccon, L.; Adami, G.; Micali, G. *Food Addit. Contam.* **2004**, *21*, 441–446.
26. Pravda, M.; Vytřas, K. *J. Pharm. Biomed. Anal.* **1996**, *14*, 765–771.

27. Jyothi, N.V.V.; Mouli, P.C.; Reddy, S.R.J.; *J. Trace Elem. Med. Biol.* **2003**, *17*, 79–83.
28. Melucci, D.; Torsi, G.; Locatelli, C. *Ann. Chim.-Rome.* **2007**, *97*, 141–145.
29. Mester, Z.; Sturgeon, R. *Comprehensive Analytical Chemistry Volume XLI: Sample Preparation for Trace Metal Analysis*, Elsevier B.V., Amsterdam, 2003.
30. Bragg, S.A.; Xue, Z.-L. *Am. J. Anal. Chem.* **2011**, *2*, 979–983.
31. Lipinski, C. *Pharmaceutical Profiling in Drug Discovery for Lead Selection*; Borchardt, R; Kerns, E; Lipinski, C; Thakker, D; Wang, B. *Biotechnology: Pharmaceutical Aspects 1; American Association of Pharmaceutical Scientists*: Arlington, Texas, 2004; pp. 93–125.
32. Rosolina, S.M.; Chambers, J.Q.; Lee, C.W.; Xue, Z.-L. *Anal. Chim. Acta* **2015**, *893*, 25–33.
33. Liu, J.; Ruffini, N.; Pollet, P.; Llopis-Mestre, V.; Dilek, C.; Eckert, C.A.; Liotta, C.L.; Roberts, C.B. *Ind. Eng. Chem. Res.* **2010**, *49*, 8174–8179.
34. Duggan, J.N.; Bozack, M.J.; Roberts, C.B. *J. Nanopart. Res.* **2013**, *15*, 2089–2104.
35. Brainina, K.Z.; Galperin, L.G.; Vikulova, E.V.; Stozhko, N.Y.; Murzakaev, A.M.; Timoshenkova, O.R.; Kotov, Y.A. *J. Solid State Electrochem.* **2011**, *15*, 1049–1056.
36. Burns, D.H.; Danzer, K.; Townshend, A. *Pure Appl. Chem.* **2002**, *74*, 2201–2205.



## **PART 4**

**Electrochemical study of trace mercury analysis in  
pharmaceutical ingredients through a classical anodic  
stripping approach**

Research for this chapter was a collaborative work between visiting professor, Jie Guo, and Samuel M. Rosolina.

Additional materials for Part 4 are provided in Appendix C.

## **Abstract**

A simple method, based on anodic stripping voltammetry (ASV), has been optimized and evaluated for the purpose of mercury(II) analysis in a representative active pharmaceutical ingredient (API) and excipient. The method uses a simple un-modified glassy carbon electrode and does not require pretreatment of the sample prior to the analysis. The limits of detection (LODs) are 8.8 and 9.4  $\mu\text{g L}^{-1}$  [mass/volume, parts per billion (ppb)], respectively, in 1000  $\text{mg L}^{-1}$  aqueous caffeine and lactose solutions. In the absence of the organic API, LOD for Hg(II) is 4.7  $\mu\text{g L}^{-1}$ . The performance has been evaluated in the presence of coexisting anions or cations. The good reproducibility and stability of the analytical platform and obviation of sample pretreatment show the promise of utilizing ASV as a sensitive, robust, and inexpensive alternative to inductively-coupled-plasma (ICP)-based approaches for the analysis of mercury(II) in pharmaceutical matrices.

### **4.1. Introduction**

Mercury(II) [Hg(II)] is a highly toxic, accumulative and persistent heavy metal ion with adverse health effects on humans.<sup>1-3</sup> It is dangerous even at very

low concentrations.<sup>4,5</sup> For drinking water, 1 mg L<sup>-1</sup> (ca. 5 nM) is the guideline value by the World Health Organization.<sup>6</sup>

For drug products and their ingoing components, including active pharmaceutical ingredients (API) and excipients, residual mercury is among the most toxic and of top concern.<sup>7</sup> The International Conference on Harmonisation (ICH) has recently published new guidance (ICH Q3D) for the control of elemental impurities including mercury.<sup>7,8</sup> United States Pharmacopoeia (USP) has also proposed changes to replace non-selective, wet-heavy metal tests in the USP <231> (Heavy Metals), which has been used for over 100 years, by the new guidelines USP <232> (Elemental Impurities-Limits) and USP <233> (Elemental Impurities-Procedures).<sup>7,8</sup> We have focused on mercury analysis with oral Permissible Daily Exposure (PDE) values of 15 µg/day in the new guidelines. The detection and quantification of elemental impurities in pharmaceutical matrices, including APIs and excipients, have been actively studied to meet the new guidelines. Monitoring trace Hg(II) in pharmaceutical matrices is of critical importance and requires in situ, real-time, and highly-sensitive sensors.<sup>9</sup>

Mercury determination at low levels is mainly conducted by spectroscopic techniques<sup>10</sup> such as inductively coupled plasma-mass spectrometry (ICP-MS)<sup>11-14</sup> with good selectivity and sensitivity.<sup>15</sup> These techniques may analyze most metals and are thus capable of addressing the requirements of the proposed new regulatory guidelines.<sup>8,16</sup> They ICP-based methods, however, suffer important limitations such as the needs for pretreatment of pharmaceutical matrices, expensive instruments, and complex and time-consuming procedures,

thus limiting in-situ or on-line analysis. It would be ideal to develop methods that can accurately detect and quantify elemental impurities with no or minimal sample preparation. It is highly desirable to develop low-cost, portable field methods to accurately analyze elemental impurities in pharmaceutical matrices.

Anodic stripping voltammetry (ASV), a common electroanalytical technique,<sup>17,18</sup> is an attractive alternative to ICP-based approaches. In addition to possessing capabilities of multi-element analysis, the electroanalytical approach requires low-cost instrumentation/operation and minimum maintenance. In addition, it is fast and highly sensitive with limits of detection in the ppb ( $\mu\text{g L}^{-1}$ ) range. In ASV, the reduction of metal ions onto an electrode surface is followed by rapid oxidation of the metal back into solution to produce a characteristic current in the anodic peaks.<sup>19-21</sup> To date, electrochemical analyses of mercury have been mostly focused on their presence in drinking water with, to our knowledge, little work in pharmaceutical matrices. In fact, there have been few studies using voltammetry to investigate or analyze metal ions in organic media.<sup>22-25</sup>

We have recently reported a new electrochemical method, based on ASV on an unmodified glassy carbon electrode, to detect and quantify cadmium(II) [Cd(II)] and lead(II) [Pb(II)], either simultaneously or individually in pharmaceutical ingredients and an excipient. Cd(II) and Pb(II) are two other most toxic metals in pharmaceutical matrices.<sup>7,8</sup> No pretreatment, such as acid digestion or dry ashing to remove organics in solution, is needed prior to the ASV analysis. Through co-deposition of bismuth, limits of detection (LODs) in the  $\mu\text{g L}^{-1}$

<sup>1</sup> range were obtained for both heavy metals - in the presence and absence of representative pharmaceutical components.<sup>26</sup> However, mercury(II) analysis cannot be combined with our ASV analysis of cadmium(II) and lead(II), in part because different matrices are required for the analyses of Hg(II) and cadmium(II)/lead(II), as demonstrated below. The results have prompted us to develop the current, *separate* ASV analysis of Hg(II) in pharmaceutical matrices.

Electrochemical analysis of mercury has been conducted on modified electrodes such as copper<sup>27</sup> or iridium oxide films<sup>18</sup>, carbon-based materials,<sup>28-32</sup> and gold-nanoparticle-modified electrodes.<sup>33,34</sup> However, fabrications of these modified electrodes are time-consuming and costly. In addition, reproducibility of the mercury analyses at low concentrations on those modified electrodes is challenging, and a complexing ligand is needed for the process, adding to the complexity of the detection process.<sup>28,29,32,34</sup> It is thus highly desirable to develop an electrochemical method on commercial, unmodified glassy carbon electrodes which is not only sensitive, selective, and reliable but also simple, practical, and economical in its operation.

This work describes the use of square wave anodic stripping voltammetry (SWASV) to detect and quantitate mercury(II) in representative pharmaceutical matrices. The electrochemical analysis has been conducted in aqueous solutions with and without representative pharmaceutical substrates. No pretreatment of the samples is needed prior to ASV analyses. The process uses a simple, unmodified glassy carbon electrode (GCE) to detect Hg(II) in the low ppb ( $\mu\text{g L}^{-1}$ ) range. This direct method allows for inexpensive, fast, and potentially portable

analysis of Hg(II) in small amounts of the samples. The current work, to our knowledge, is the first study to analyze mercury in pharmaceutical matrices. It also creates the opportunity to pre-screen organic products for mercury, one of the top toxic elements in APIs and excipients.

## **4.2. Materials and methods**

### **4.2.1. Chemicals and instruments**

The following chemicals were used as received, and all but lactose monohydrate, were analytical grade: lactose monohydrate (Lab Grade, Thermo Fisher Scientific, Waltham, MA), caffeine (Thermo Fisher Scientific), sodium acetate (NaOAc, Thermo Fisher Scientific), tetra(n-butyl)ammonium perchlorate [ $\text{Bu}^n_4\text{N}(\text{ClO}_4)$ ], TBAP, for electrochemical analysis,  $\geq 99.0\%$ , Sigma Aldrich],  $\text{Na}_2\text{SO}_4$  and  $\text{NaNO}_3$  (Thermo Fisher Scientific), tetraethylammonium tetrafluoroborate ( $\text{Et}_4\text{NBF}_4$ , for electrochemical analysis,  $\geq 99.0\%$ , Sigma Aldrich), ethanol (95%, Decon Laboratories, Inc., King of Prussia, PA). Mercury atomic absorption standard solution of  $1000 \text{ mg L}^{-1}$  in 3%  $\text{HNO}_3$  (Ricca Chemical Co., Arlington, TX) was diluted in supporting electrolytes to form stock solutions. Fe(III), Cd(II), and Pb(II) atomic absorption standard solutions of  $1000 \text{ mg L}^{-1}$  in 10%  $\text{HNO}_3$  (Ricca Chemical Co., Arlington, TX) were diluted in supporting electrolytes to form stock solutions of the interference ions. Ultrapure deionized (DI) water from a Millipore water purified system ( $\geq 18 \text{ M}\Omega\cdot\text{cm}$ , Barnstead/Thermo Fisher Scientific) was used in all assays.

Prior to use, GCEs were polished to a mirror-like surface on a standard electrode polishing kit (CH Instruments, Inc., Austin, TX) including a 1200 grit CarbiMet™ disk, 1.0 and 0.3 μm alumina slurry on a nylon cloth, and 0.05 μm alumina slurry on a microcloth polishing pad. After polishing, GCEs were successively sonicated with DI water, ethanol, and DI water again for 5 min each. Electrochemical measurements were carried out on a CHI 440a Electrochemical Workstation (CH Instruments). A three-electrode configuration consisted of a bare, unmodified GCE (3 mm in diameter, BAS Inc., West Lafayette, IN) as working electrode and two platinum wires (CH Instruments) as quasi-reference and counter electrodes, respectively. A platinum wire quasi-reference electrode was used in place of an Ag/AgCl electrode to avoid the introduction of any Cl<sup>-</sup> into the system, as HgCl<sub>2</sub> is insoluble.

#### ***4.2.2. Sample preparation and SWASV analysis of mercury(II)***

All experiments were conducted at room temperature without deaeration. The unmodified GCE and Pt wire electrodes were placed in an electrochemical cell containing 20 mL of 0.01 M TBAP or another electrolyte in ultrapure DI water. For detection in the aqueous system, deposition of Hg(II) occurred by holding the potential at -1.1 V for 300 s and was then stripped back into solution by sweeping the potential from -1.1 to 0.6 V using a frequency of 25 Hz, a step potential of 4 mV, and amplitude of 25 mV. For all analyses, stirring of the solution at 1200 revolutions per min (rpm) was required for the accumulation step, but was turned

off prior to the stripping step. The electrode surface was regenerated between measurements by holding the potential at 1.0 V for 300 s for samples, while stirring at high speed. In samples containing an organic compound, the solutions were stirred for 1 min after spiking with the analyte of interest and before the first analysis. This was done to allow the metals to reach equilibrium throughout the matrix and to interact with the organics in solution. It should be noted that allowing spiked samples to sit for several days had no effect, either positive or negative, on the sensitivity of the detection as compared to allowing the sample to stir for 1 min after spiking.

#### **4.3. Results and discussion**

Functional groups such as -COOH, -NHR, -OH, and -SH are often present in APIs and organic excipients. These groups may bind/complex to Hg(II), forming organic mercury carboxylates, amine adducts, amides, alkoxides, and thiolates in the pharmaceutical matrices. Mercury(II) acetate, a carboxylate, for example, is highly soluble in water.<sup>35</sup> Thus mercury carboxylates likely dissociate significantly at trace levels in water. Many mercury(II) amine adducts and amides have also been reported to readily react with water, breaking the Hg-N bonds.<sup>36</sup> Thus, for API or excipients soluble in water that contain carboxylates, amine adducts and amides, it is expected that the organic mercury complexes will dissociate in the solutions. If trace Hg-O or Hg-N species are left in aqueous, the negative deposition potential (-1.1 V) would overcome the binding energies of



ligands to mercury(II), allowing for mercury deposition on the electrode. Few mercury(II) alkoxides/aryloxides have been reported.<sup>37</sup> Mercury thiolates (RS-Hg-) are likely less soluble in water. If they are present, the negative deposition potential (-1.1 V) is expected to overcome the Hg-S binding energies to make mercury deposition on the electrode.

### **4.3.1. Optimization of experimental conditions**

#### *4.3.1.1. Effect of supporting electrolyte*

Voltammetric behaviors of Hg(II) were investigated in several supporting electrolytes in water. NaOAc, NaNO<sub>3</sub>, Et<sub>4</sub>NBF<sub>4</sub>, and TBAP were compared. All gave consistently good results. Perchloric acid was often used as electrolyte in electrochemical analysis of trace mercury.<sup>28,38-40</sup> TBAP was chosen as the appropriate electrolyte because of its strong response to Hg(II) as shown in Figure 4.1. The voltammograms of these optimization experiments are given in Figure C.1 in Appendix C.

#### *4.3.1.2. Effect of preconcentration potential*

Using solutions containing 40 µg L<sup>-1</sup> Hg(II), the optimum preconcentration potential was determined through peak area comparisons. Due to the fairly negative potential of the Hg(II) oxidation peak and the possibility of forming hydrogen (H<sub>2</sub>), an optimized preconcentration potential is important. Depositing the Hg(II) at -1.1 V proved to produce the largest peak area. Figure 4.2 shows

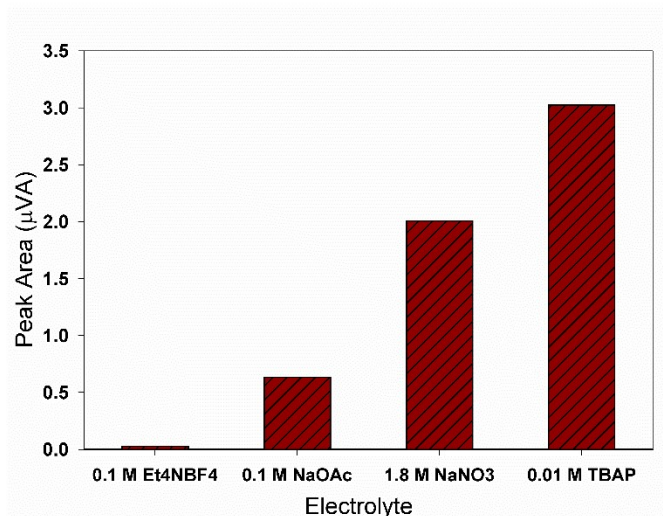


**Figure 4.1.** Effect of supporting electrolytes on the Hg(II) voltammetric behaviors. The best electrolyte was chosen through the comparison of the 100 µg L<sup>-1</sup> Hg(II) peak areas. The best response was obtained when using TBAP.

the results for these tests, and the voltammograms can be found in Figure C.2 in the Appendix C.

#### 4.3.1.3. Effect of preconcentration time

Figure 4.3 shows the electrochemical results for 50 µg L<sup>-1</sup> Hg(II) in aqueous solutions. The peak area increased for both metals with increasing deposition time between 100 and 300 s. For deposition times >300 s, Hg(II) began to level off. Thus a deposition time of 300 s was chosen.

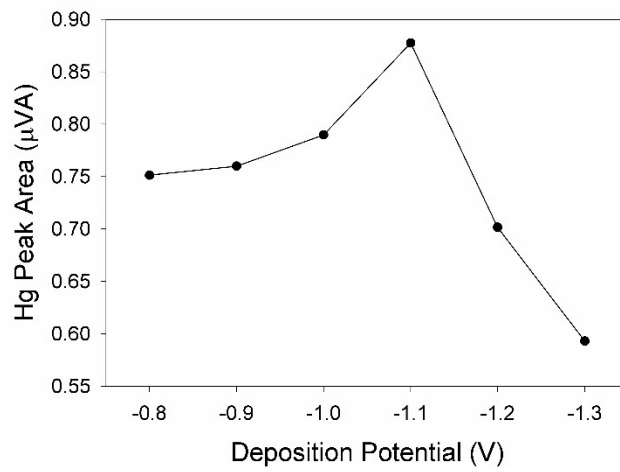


**Figure 4.2.** Studies on deposition potential for Hg(II) [0.01 M TBAP, 40 μg L<sup>-1</sup> Hg(II), 200 s]

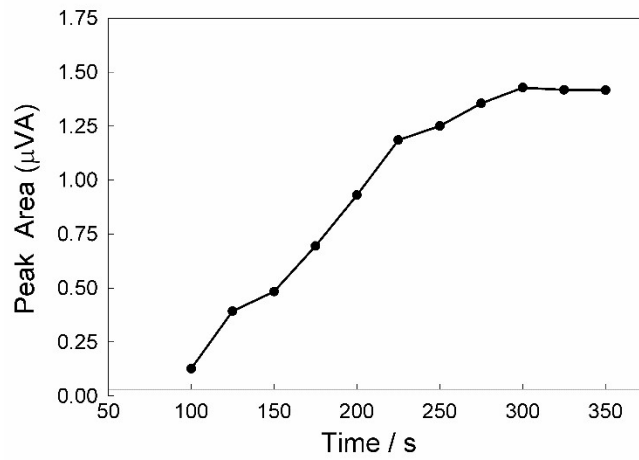


**Figure 4.3.** Studies on accumulation times for Hg(II) [0.01 M TBAP, 50 μg L<sup>-1</sup> Hg(II), -1.1 V].

### 4.3.2 Analytical results

Standard addition was used for all calibration curves. It is important to note that the results here are given without background subtraction. The method of standard addition allows for the determination of the original concentration without interference from the matrix, which is necessary for the analysis of unashed pharmaceuticals. Results of the investigations, including the regression function, square of the correlation coefficient  $R^2$ , RSD (relative standard deviation) at  $50 \mu\text{g L}^{-1}$  and LOD for each of the following studies ( $S/N = 3$ ), are listed in Table 4.1.

**Table 4.1.** Comparison of the Hg(II) analyses performed in the current study

Interference	Regression	$R^2$	RSD (n = 3) $50 \mu\text{g L}^{-1}$	LOD (n = 3) $\mu\text{g L}^{-1}$	LOD in solid organic ( $\mu\text{g g}^{-1}$ )
-	$y = 0.0318x - 0.1664$	0.998	1.5%	4.74	-
caffeine	$y = 0.0306x - 0.0368$	0.994	2.2%	8.77	8.77
lactose	$y = 0.0273x + 0.2342$	0.993	2.3%	9.40	9.40

#### 4.3.2.1. Detection of Hg(II) in the absence of organics

Using the optimized parameters above, Hg(II) was first analyzed in the absence of representative pharmaceutical ingredients. The Hg(II) peak was observed at  $-0.25 \text{ V}$  (Figure 4.4). Calculated LOD was  $4.74 \mu\text{g L}^{-1}$  (Table 4.1).

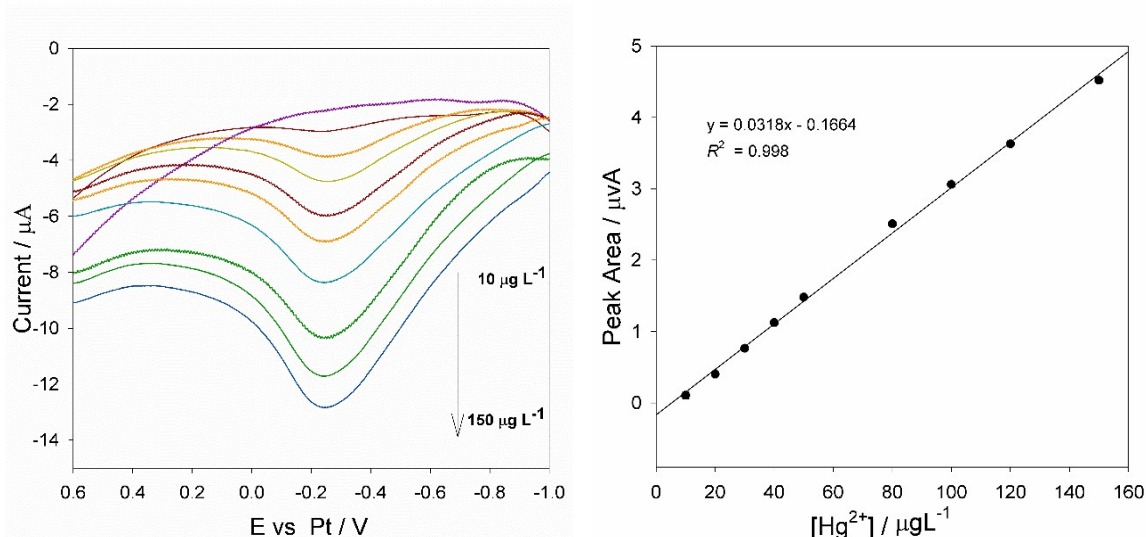


**Figure 4.4.** Increasing concentrations of Hg(II) (10-150  $\mu\text{g L}^{-1}$ ) in the absence of organics (0.01 M TBAP)

#### 4.3.2.2. Effect of dissolved organics on analysis

The impact of organic substrates on the accuracy and sensitivity of the electroanalytical approach was investigated in aqueous solutions, using representative pharmaceutical organic components such as caffeine and lactose. Caffeine and lactose, both soluble in the aqueous solution, were evaluated separately, and added to the 0.01 M TBAP solution at a concentration of 1000  $\text{mg L}^{-1}$ . These solutions were stirred until all organic compounds had fully dissolved. In the presence of lactose, the LODs of Hg(II) was 9.40  $\mu\text{g L}^{-1}$  (Table 4.1). As indicated in Table 4.1, similar LODs were observed in the presence of 1000  $\text{mg L}^{-1}$  caffeine ( $[\text{Hg(II)}] = 8.77 \mu\text{g L}^{-1}$ ).

Addition of representative pharmaceutical ingredients to the electrolytic solutions resulted in weaker analyte detection with lower slopes and

consequently higher LODs for Hg(II). However, since the tests were conducted with high concentrations of the pharmaceutical ingredients, achieving the Hg(II) detection in the low  $\mu\text{g L}^{-1}$  range is remarkable, demonstrating the strength and potential of this method. The effect of the organic substrates on the sensitivity is slight, but evident through comparisons of regression slopes and LODs.

#### *4.3.2.3. Reproducibility and precision*

Tests of the current technique show high reproducibility and consistency (Table 4.1). This is perhaps due, in part, to its simplicity and the optimized cleaning steps, which allowed for a fresh GCE surface each time. RSD was calculated through triplicate stripping analysis in a sample containing  $50 \mu\text{g L}^{-1}$  Hg(II), with cleaning between measurements. All but one RSD are below 2.5%.

#### **4.3.3. Interference**

A major challenge for Hg(II) detection in real samples is the elimination of interferences. In order to evaluate the performance of GCE toward Hg(II) change in the presence of coexisting anions or cations, including  $\text{SO}_4^{2-}$ ,  $\text{NO}_3^-$ ,  $\text{Pb}^{2+}$ ,  $\text{Cd}^{2+}$ , and  $\text{Fe}^{3+}$ , the effect of these ions on the cathodic peak current of Hg(II) change was examined (Table 4.2). The voltammetric response of the designed electrode toward  $100 \mu\text{g L}^{-1}$  Hg(II) was first measured, and then  $500 \mu\text{g L}^{-1}$  excess of the coexisting ions was subsequently added into the supporting electrolyte in the aqueous solution. Metals cations might form alloys with mercury, thus making the

peak area increase. Anion will influence the Hg(II) reduction kinetics, thus potentially decreasing the peak area.

**Table 4.2.** Comparison of the interference performance in 100 ppb Hg(II) solutions

<b>Interference/ Concentration</b>	<b>None</b>	<b>500 ppb NO<sub>3</sub><sup>-</sup></b>	<b>500 ppb SO<sub>4</sub><sup>2-</sup></b>	<b>500 ppb Pb<sup>2+</sup></b>	<b>500 ppb Cd<sup>2+</sup></b>	<b>500 ppb Fe<sup>3+</sup></b>
% Peak Area	100%	79%	86%	174%	179%	203%

#### **4.4. Conclusions**

This work demonstrated the use of the classical electroanalytical method, ASV, by using an off-the-shelf, unmodified GCE for the analysis of Hg(II), one of the most toxic elemental impurities, at trace levels in representative pharmaceutical matrices. The analyses were fast with just simple dissolution of the pharmaceutical ingredient and *no pretreatment*. To the best of our knowledge, this is the first detection of Hg(II) in aqueous solutions through ASV (with organic substrates). Detecting these heavy metals in pharmaceuticals is an important application of electrochemical analysis to an area of intensely current interest.

The detection limits are generally lower than the USP limits of mercury in pharmaceuticals. Comparable LODs in the absence and presence of organics indicate that Hg(II) detection in the presence of an API/excipient at even higher concentrations can be achieved at trace levels. Acidifying the API/excipient sample would allow for the analysis of a larger sample and lower organic

interference, as well as increase the solubility of analytes in the form of mercury oxides. Again, it is important to note that no data in the current studies were background-subtracted so as to replicate the determination of an unknown metal concentration in a real sample. Additional research and developments are needed to make this method meet the requirements of USP <233>.



## References

1. Renzoni, A.; Zino, F.; Franchi, E. *Environ. Res.* **1998**, *77*, 68–72.
2. Wiener, J.G.; Krabbenhoft, D.P.; Heinz, G.H.; Scheuhammer, A.M.;  
*Handbook of Ecotoxicology*, CRC Press LLC, Boca Raton, 2003. pp. 409–  
463.
3. Tchounwou, P.B.; Ayensu, W.K.; Ninashvili, N.; Sutton, D. *Environ. Toxicol.*  
**2001**, *18*, 149–175.
4. Wang, Q.; Kim, D.; Dionysiou, D.D.; Sorial, G.A.; Timberlake, D. *Environ.*  
*Pollut.* **2004**, *131*, 323–336.
5. Eisler, R. *Environ. Geochem.* **2003**, *25*, 325–345.
6. *Guidelines for Drinking-water Quality*, Vol. 1, 3<sup>rd</sup> ed., World Health  
Organization, Geneva, 2008,  
[http://www.who.int/water\\_sanitation\\_health/dwq/gdwq3rev/en/](http://www.who.int/water_sanitation_health/dwq/gdwq3rev/en/) accessed on  
November 23, 2015.
7. Thayer, A.M. *Chem. Eng. News.* **2013**, *91*, 10–13.
8. (a) Q3D (*Impurities: Guideline for Metal Impurities*), ICH on December 16,  
2014,  
[http://www.ich.org/fileadmin/Public\\_Web\\_Site/ICH\\_Products/Guidelines/Qu  
ality/Q3D/Q3D\\_Step\\_4.pdf](http://www.ich.org/fileadmin/Public_Web_Site/ICH_Products/Guidelines/Quality/Q3D/Q3D_Step_4.pdf) accessed on February 1, 2016. (b) <232>  
*Elemental Impurities—Limits* and <233> *Elemental Impurities—Procedures*,  
USP, [http://www.usp.org/usp-nf/official-text/accelerated-revision-  
process/accelerated-revision-history/elemental-impurities-limits-and-](http://www.usp.org/usp-nf/official-text/accelerated-revision-process/accelerated-revision-history/elemental-impurities-limits-and-)

[elemental](#) accessed on February 1, 2016.

9. Suib, S.L. *Frontiers Chem.* **2013**, *1*, 1–2.
10. Sánchez, R.; Snell, J.; Held, A. *Anal. Bioanal. Chem.* **2015**, *407*, 6569–6574.
11. Hsu, K.-C.; Lee, C.-F.; Tseng, W.-C.; Chao, Y.Y.; Huang, Y.L. *Talanta*. **2014**, *128*, 408–413.
12. Cattani, I.; Spalla, S.; Beone, G.M.; Boccelli, R.; Trevisan, M. *Talanta* **2008**, *74*, 1520–1526.
13. Pyhtilä, H.; Perämäki, P.; Piispanen, J.; Niemelä, M.; Suoranta, T.; Starr, M.; Nieminen, T.; Kantola, M.; Ukonmaanaho, L. *Microchem. J.* **2012**, *103*, 165–169.
14. Pontes, F.V.M.; Carneiro, M.C.; Vaitsmanb, D.S.; Monteiro, M.I.C.; Neto, A.A.; Tristão, M.L.B. *Fuel* **2014**, *116*, 421–426.
15. Pandey, S.K.; Kim, K.-H.; Brown, R.J.C. *Trends Anal. Chem.* **2011**, *30*, 899–917.
16. Liba, A.; McCurdy, E. Proposed new USP general chapters <232> and <233> for elemental impurities: The Application of ICP-MS for Pharmaceutical Analysis,  
[https://www.agilent.com/cs/library/whitepaper/Public/5990-9382EN\\_WhitePaper\\_ICP-MS\\_ICP-OES\\_Pharma.pdf](https://www.agilent.com/cs/library/whitepaper/Public/5990-9382EN_WhitePaper_ICP-MS_ICP-OES_Pharma.pdf) accessed on February 1, **2016**.
17. Kemula, W.; Strojek, J. *Chem. Anal. (Warsaw)*. **1963**, *8*, 685–690.
18. Salimi, A.; Alizadeh, V.; Hallaj, R. *Talanta* **2006**, *68*, 1610–1616.

19. Bard, A.J.; Faulkner, L.R. *Electrochemical Methods. Fundamentals and Applications*, 2<sup>nd</sup> ed., Wiley, Hoboken, New York, 2001, p. 458.
20. R.G. Compton, C.E. Banks, *Understanding Voltammetry*, 2<sup>nd</sup> ed., Imperial College Press, London, **2011**.
21. Wang, J. *Analytical Electrochemistry*, Wiley-VCH, Hoboken, New York, **2000**, p. 86.
22. Wang, J.; Tuzhi, P. *Anal. Chim. Acta.* **1987**, *197*, 367–372.
23. Miwa, T.; Mizuike, A. *Japan Analyst* **1968**, *17*, 448–452.
24. Xu, H.; Xu, Z. *Chem. Res. Appl.* **2001**, *13*, 187–188.
25. Barton, Z.J.; Rodríguez-López, J. *Anal. Chem.* **2014**, *86*, 10660–10667.
26. Rosolina, S.M.; Chambers, J.Q.; Lee, C.W.; Xue, Z.-L. *Anal. Chim. Acta* **2015**, *893*, 25–33.
27. Jovanovski, V.; Hrastnik, N.I.; Hočevar, S.B. *Electrochem. Commun.* **2015**, *57*, 1–4.
28. Rajabi, H.R.; Roushani, M.; Shamsipur, M. *J. Electroanal. Chem.* **2013**, *693*, 16–22.
29. Muntyanu, G.G. *J. Anal. Chem.* **2001**, *56*, 546–551.
30. Janegitz, B.C.; Figueiredo-Filho, L.C.S. *J. Electroanal. Chem.* **2011**, *660*, 209–216.
31. Shamsipur, M.; Tashkhourian, J.; Hemmateenejad, B.; Sharghi, H. *Talanta* **2004**, *64*, 590–596.
32. Ouafy, T.E.L.; Chtaini, A.; Oulfajrite, H.; Najih, R.; Ouafy, H.E.L. *Indian J. Inorg. Chem.* **2015**, *10*, 123–129.

33. Abollino, O.; Giacomino, A.; Malandrino, M.; Piscionieri, G.; Mentasti, E. *Electroanal.* **2008**, *20*, 75–83.
34. Safavi, A.; Farjami, E. *Anal. Chim. Acta* **2011**, *688*, 43–48.
35. Isbin, H.S.; Kobe, K.A. *J. Am. Chem. Soc.* **1945**, *67*, 464–465.
36. M.F. Lappert, P.P. Power, A.R. Sanger, R.C. Srivastava, *Metal and Metalloid Amides*, Wiley, Hoboken, New York, **1980**, p. 553.
37. Bradley, D.C.; Mehrotra, R.C.; Rothwell, I.P.; Singh, A. *Alkoxo and Aryloxo Derivatives of Metals*, Academic Press, Cambridge, MA, **2001**.
38. Kendall, D.R. *Anal. Lett.* **1972**, *5*, 867–873.
39. Andrews, R.W.; Larochelle, J.H.; Johnson, D.C. *Anal. Chem.* **1976**, *48*, 212–214.
40. Kiekens, P.; Mertens, M.; Bogaert, M.; Temmerman, E. *Analyst* **1984**, *109*, 909–911.

## **PART 5**

**Highly sensitive detection of hexavalent chromium  
utilizing a sol-gel/carbon nanotube modified electrode**

## Abstract

A pyridine-functionalized thin film has been fabricated to selectively preconcentrate Cr(VI) anions for electrochemical detection in the 5-300  $\mu\text{g L}^{-1}$  range. Glassy carbon electrodes were modified through physical deposition of single-walled carbon nanotubes (SWNTs) on the electrode surface, followed by electrochemical deposition of a sol-gel containing a 2-pyridine functional group. The use of SWNTs has increased sensitivity for Cr(VI) detection in aqueous solutions, providing a detection limit of 0.3  $\mu\text{g L}^{-1}$ .

Additional materials for Part 5 are provided in Appendix D.

### 5.1. Introduction

Chromium detection is of intense interest, as Cr(VI) is highly toxic even at trace (low  $\text{mg L}^{-1}$ ) levels. Due to the strong oxidizing nature of Cr(VI), exposure leads to health problems that include lung cancer, stomach cancer, nasal cancer, allergic dermatitis, and mutagenesis.<sup>1-5</sup> Despite its known effects on human health Cr(VI) species are found in many places including common anti-corrosive materials, paints, dyes, tanned leather, coal ash, wood preservatives, welding materials, and chrome plating.<sup>6-8</sup>

Trivalent chromium, on the other hand, is reported to be an essential trace element for mammals (ca. a few  $\text{mg L}^{-1}$  in blood samples), and detection of Cr(III) has been actively studied.<sup>9</sup> Little is known about the specific roles of Cr(III) in the biological system, but it has shown to help treat glucose intolerance and certain

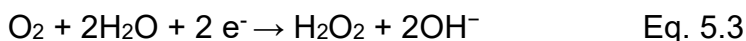
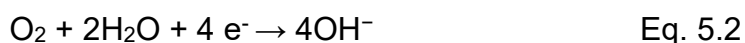
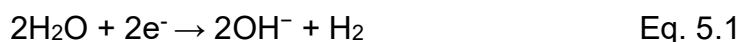
types of diabetes.<sup>10</sup> Often biological samples are pretreated by using e.g. H<sub>2</sub>O<sub>2</sub> before Cr analysis and the pretreatments convert Cr(III) to Cr(VI). In such cases, subsequent Cr quantification in the biological samples becomes the analysis of Cr(VI), and electrochemical methods have often been used.<sup>11</sup>

Detection of trace Cr(VI) requires sensitive techniques. Currently, these include ion chromatography, atomic absorption (AA) spectrophotometry, spectrofluorimetry, spectrophotometry, chemiluminescence, inductively coupled plasma optical emission spectroscopy (ICP-OES), inductively coupled plasma mass spectrometry (ICP-MS), and capillary zone electrophoresis.<sup>12-17</sup>

Electrochemical methods are attractive because of their sensitivity, portability, and relatively low cost in comparison to other common techniques.<sup>18-32</sup> One of the largest steps forward in electrochemical analysis has been the marriage of sol-gel thin films and electrodes.<sup>33-45</sup>

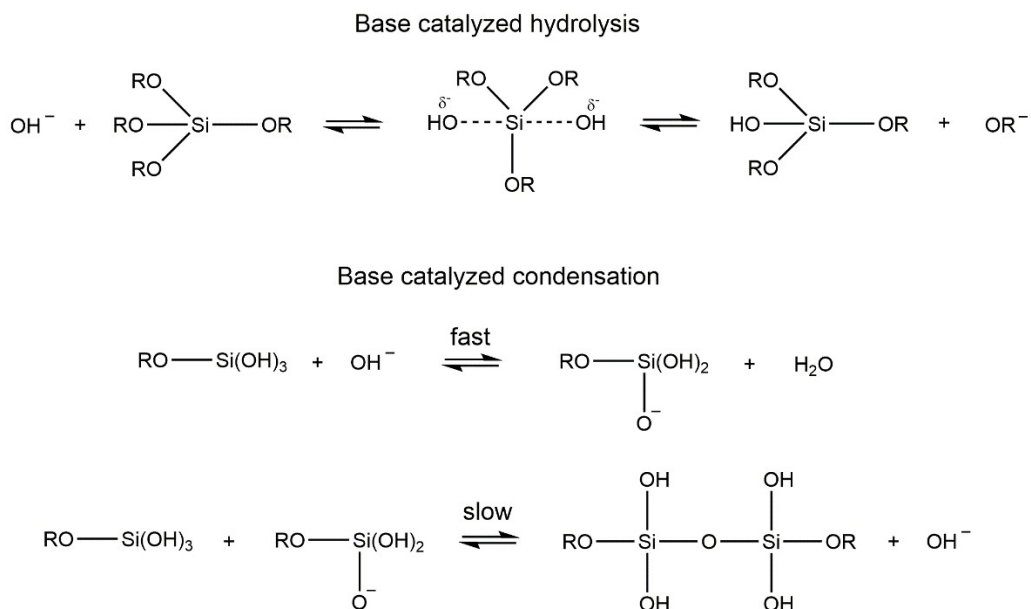
Sol-gel films are formed through the hydrolysis and condensation of metal alkoxides. These reactions can be catalyzed by either a base or an acid, each producing different porosities.<sup>45</sup> For trace analysis purposes, base catalysis tends to be favored over acid catalysis because it produces films with higher porosity and thus larger surface area.<sup>46</sup> This porosity as well as the electrochemical stability of the sol-gel films makes them ideal for electroanalytical purposes. Additionally, functional groups are easily trapped in the gel by simply adding them to the sol before hydrolysis, producing films tailored for specific analyses.<sup>33,35,37,38,41-44,47-50</sup> A very thin film is commonly desired because of a shorter diffusion pathlength of the analyte as well as a quicker response time.

Electrolytic sol-gel deposition is a fairly new development in the electroanalytical field and has been successfully employed to fabricate many new sensors.<sup>39-41,43,44,50</sup> By exposing an electrode to a sol consisting of alkoxy silane precursors and holding it at a sufficiently negative potential, hydroxide ions are generated at the electrode surface through the oxidation of water and oxygen (Eqs. 5.1-5.3). The localized increase in pH catalyzes the hydrolysis of the sol, which immediately begins to condense onto the electrode (Scheme 5.1.). Because the gelation and the drying do not occur at the same time, as they do in physical depositions, the porosity is much larger.<sup>51</sup> Electrodeposition has proven to produce sol-gel films with more consistent film thicknesses than through past deposition techniques such as spin coating and dip coating.<sup>52</sup> The original pH of the sol, as well as the deposition potential and time, directly affect the thickness of the sol-gel film and can thus be used as parameters to control it.



Previously, our group has developed a sol-gel based electrode containing pyridinium groups for Cr(VI) detection.<sup>43</sup> A new fabrication method has produced a more sensitive, Cr(VI) selective electrode. This new fabrication procedure reduces the limit of detection from 4.6 mg L<sup>-1</sup> in the earlier work to 0.3 µg L<sup>-1</sup>





**Scheme 5.1.** Base catalyzed hydrolysis and condensation of sol-gel precursors.

through the use of single-walled carbon nanotubes (SWNT), and through better control of the sol-gel film thickness. Films are deposited onto the glassy carbon electrode (GCE) using an electrodeposition technique and are believed to be between 75 and 100 nm thick due to their iridescence. Furthermore, the films are shown to remain completely intact and remain stable after many runs.

## 5.2. Experimental

### 5.2.1. Apparatus and materials

Scanning electronic microscopic (SEM) images were obtained with an LEO 1525 field emission scanning electron microscope. Electrochemical measurements were carried out on a modulated potentiostat (CHI 440a, CH

Instruments, Austin, TX). For the stripping step, a three-electrode configuration consisted of a modified glass encased GCE (3 mm in diameter, Cypress Systems, San Jose, CA), a fritted Ag/AgCl (saturated KCl solution, CH Instruments) and a platinum wire (CH Instruments) as working, reference and counter electrodes, respectively. For the analytical step, a Ag/AgCl wire electrode was prepared by soaking a silver wire in bleach. This was used in place of the fritted Ag/AgCl reference electrode.

The following chemicals were used as received: chromium standard solution (1000 mg L<sup>-1</sup>, Sigma Aldrich Co., St. Louis, MO), KCl (Certified ACS, Mallinckrodt, Dublin, Ireland), Tetramethyl orthosilicate (TMOS) (Sigma Aldrich), NaCl (Certified ACS, Thermo Fisher Scientific, Waltham, MA), 2-[2-(trimethoxysilyl)ethyl]-pyridine (Gelest, Morrisville, PA). Ultrapure water from a Millipore water purified system ( $\geq 18$  M $\Omega$ •cm, Barnstead/Thermo Fisher Scientific) was used in all solutions. Other reagents were of analytical grade and used as received. All glassware was soaked in 1 M nitric acid bath and thoroughly rinsed with deionized (DI) water before use.

### **5.2.2. Carboxylation of SWNTs**

SWNTs (40 mg) were added to a solution of 30% HNO<sub>3</sub> and then refluxed for 24 h at 140 °C to obtain carboxylic group-functionalized SWNTs. The resulting suspension was centrifuged, and the sediment was washed with deionized water.

Then, the oxidized SWNTs were dispersed in deionized water to a concentration of 0.5 mg mL<sup>-1</sup>.

### **5.2.3. Preparation of electrode**

Prior to fabrication, a GCE was polished carefully to a mirror-like surface on a standard electrode polishing kit (CH Instrument) including a 1200 grit Carbimet disk, 1.0 and 0.3 μm alumina slurry on a nylon cloth, and 0.05 μm alumina slurry on a microcloth polishing pad. After polishing, GCEs were successively sonicated with deionized (DI) water, ethanol and DI water for 5 min each. Carboxylated SWNTs were physically deposited by pipetting 4 μL (0.5 mg mL<sup>-1</sup>) of the SWNT suspension directly onto the GCE surface. This was allowed to dry under nitrogen gas flow at room temperature for a minimum of 3 h. Any water trapped under the SWNTs could cause structural instability of the SWNT layer and thus the sol-gel film. The working electrode was then exposed to a sol consisting of 8 mL of 0.2 M KCl, 8 mL of EtOH, 1.3 mL of 2-[2-(trimethoxysilyl)ethyl]-pyridine, and 1.4 mL of TMOS that was acidified with HCl to pH 5.0. A potential of -1.1 V was then applied for 1800 s, followed by a rinsing of the working electrode with a 1:1 mixture of EtOH and DI water. Finally, the GCE was dried in the oven for 24 h at 70 ° C.

#### **5.2.4. Analysis procedure**

Prior to analysis, the modified GCE was soaked in a 0.1 M HCl solution to ensure that all of the pyridinium groups are protonated. The electrode was then exposed to solutions containing varying Cr(VI) concentrations in an electrolytic buffer of 0.1 M KCl and 0.1 M HCl. Accumulation took place at open 0.6 V for 5 min while the solution was stirred. The electrode was then moved to a Cr(VI) free buffer (3.5% NaCl) solution and determination of the accumulated analyte took place by reduction to Cr(III) through cathodic stripping. This was done by sweeping from 0.6 V to -0.3 V using SWV with a frequency of 15 Hz, step potential of 4 mV and an amplitude of 25 mV (Figure 5.1). No stirring took place throughout the stripping step. The electrode was cleaned before every accumulation step by holding the potential at -0.2 V for 120 s in a buffer solution consisting of 0.1 M KCl and 0.1 M HCl while stirring.

### **5.3. Results and discussion**

#### **5.3.1. Surface analysis**

The surface was analyzed using a LEO 1525 field emission scanning electron microscope (Figure 5.2). An image taken at the border of the SWNT deposit area shows a contrast between the uniformity of the sol-gel coating on the bare GC surface versus the zone with SWNTs. This is strong evidence that the SWNT layer greatly increases the surface area of the electrodeposited sol-gel film.

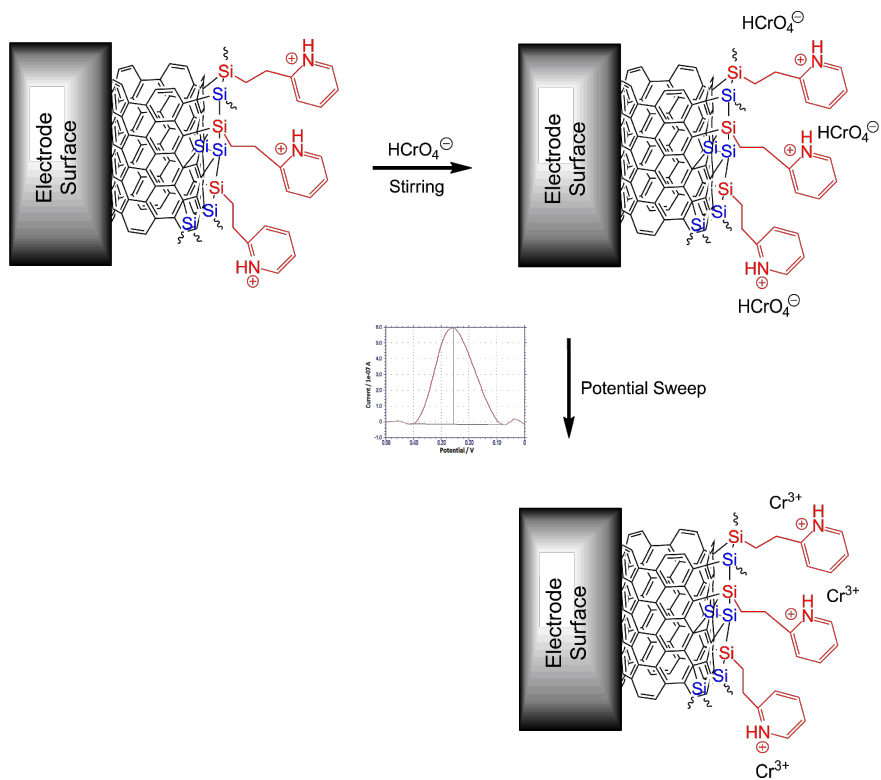


**Figure 5.1.** Schematic of the accumulation of chromate followed by its reduction, resulting in it being stripped off and detected through a change in current.

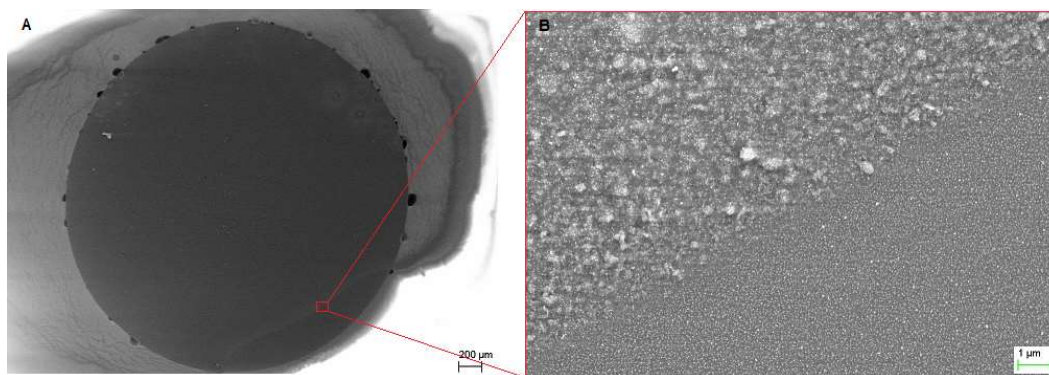


**Figure 5.2.** SEM images of the sol-gel coated GCE surface. Image B shows the strong difference in surface area that the sol-gel possesses between deposition on the bare GCE (bottom section) versus deposition on the SWNT-coated surface (top section).

The sol-gel film thickness and stability are controlled by the pH of the sol, the ratio of TMOS to 2-[2-(trimethoxysilyl)ethyl]-pyridine, the electrolytic content of the sol, the magnitude of the negative potential, and the deposition time. A sufficiently acidified sol helps to ensure that the deposited sol-gel film is thin. The low pH of the entire solution suppresses and localizes the high pH zone at the electrode surface where the OH<sup>-</sup> ions are generated. Because the hydrolysis and condensation of the alkoxysilanes are base catalyzed (Eqs. 5.4-5.6), less sol-gel is formed with lower amounts of hydroxide ions. This is directly related to the deposition potential and deposition time. Therefore, many parameters were experimentally determined during optimization. Nanometer-thick films have many advantages. As stated previously, shorter path lengths as well as quicker reduction response times are obtained through thinner films. The stability of the film also depends upon its thickness. If the film is too thick ( $\mu\text{m}$  range) it tends to crack and flake off while drying, or comes off in solution most likely due to physical forces caused by the stirring. Using electrochemical quartz crystal microbalance (EQCM) experiments, our group determined that a ratio of TMOS to 2-[2-(trimethoxysilyl)ethyl]-pyridine greater than 1 resulted in unstable films due to poor gelation at the electrode surface.<sup>43</sup>

One characteristic of a very thin film on a GCE is iridescent coloration. This is directly related to the film's thickness and differences in refractive indices between the air, film and GC surface. As the light travels to the electrode, certain wavelengths are reflected off of the film while other wavelengths are refracted at the air/film boundary and reflect off of the GC surface causing a change in the

color. The phase offset of the reflected light causes optical interferences which produce iridescence. This only occurs in very thin films, thus its appearance within this research is promising.<sup>41,53,54</sup>

Because the iridescent hue depends on thickness,<sup>41,53,54</sup> it is used to characterize the film. Not only is it a method for film thickness comparison, but it also reveals the uniformity of the film and thus aids in the formation of the experimental method. While this is unequal to imaging techniques such as SEM, it is a useful and cost-effective way to analyze the qualities of the film, as well as optimize the fabrication method.

Noting the changes in the color homogeneity of a film with respect to changes in the electrodeposition method led to the current parameters. A uniform, brown-hued iridescence is the most preferred in the films in this research. Brown films have shown to be the thinnest, followed by light blue. The thickest films that still show iridescence give yellow and red colorations.<sup>41,51</sup> Figure 5.3 displays the differences in film appearances throughout the optimization of the deposition process. Note the extreme variation in color and thus uniformity in Figure 5.3A as opposed to 5.3B. Also worth noting is the transition from generally thicker blue and yellow films (5.3A and 5.3B) to a very thin brown film (5.3C).<sup>51</sup> The areas of B and C that bare cortex patterns were located directly over the center of the stir bar during film deposition, causing less sol movement and thicker films in that area. Figure 5.4 shows a final product after optimization. Although research has shown that anodic treatment of a

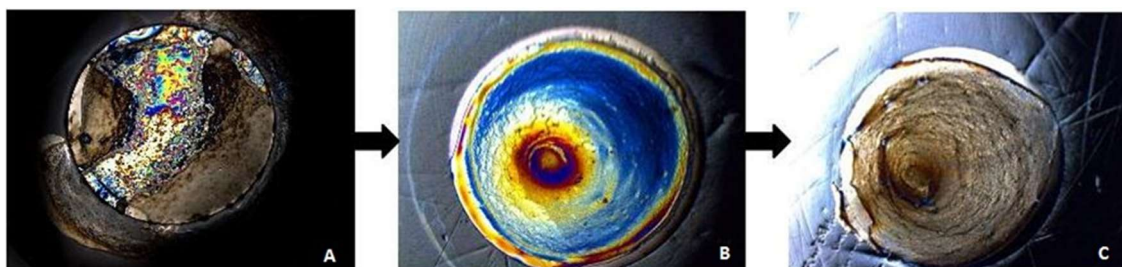


**Figure 5.3.** Sol-gel film appearances throughout the optimization of the deposition process.

Photographs were taken using a LEICA S8AP0 digital microscope.

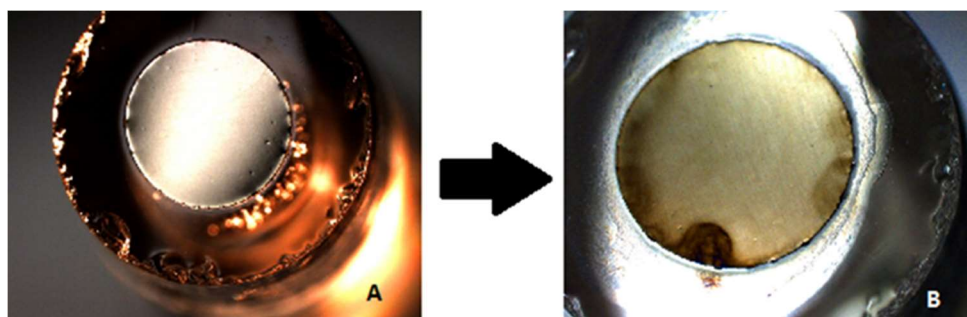


**Figure 5.4.** Image of a bare GCE surface (A) compared to sol-gel film on the same electrode after the deposition procedure was fully optimized (B). Photographs were taken using a LEICA S8AP0 digital microscope.



glassy carbon electrode in different silane-free electrolyte systems can lead to surface color changes, a KCl electrolytic system alone does not produce a color.<sup>55</sup>

### **5.3.2 Optimization**

Because of the importance of the electrode surface uniformity and reproducibility, optimized parameters were based on the consistency of the modified glassy carbon electrode. As previously stated, the sol-gel film formation employs a base-catalyzed hydrolysis and condensation. Thus, making the solution slightly acidic allows for a more controlled film deposition as the hydroxide formed at the electrode surface maintains a short local residence time before being neutralized or catalyzing the sol-gel reactions. It was determined that performing the electrodeposition at pH 5 allows for a higher degree of control over the film, and much better uniformity, as the sol-gel hydrolysis and condensation can only take place very near to the electrode itself. After optimizing the solution pH, the ideal deposition potential and time were determined based on the surface iridescence. Because the electrochemical reaction at the surface leads to the formation of one mole of H<sub>2</sub> gas to every two moles of OH<sup>-</sup> (eq. 1), it was discovered that too negative of a potential created enough bubbles on the electrode surface that it interfered with the film uniformity. A potential of -1.1 V was sufficient enough to catalyze the reactions without

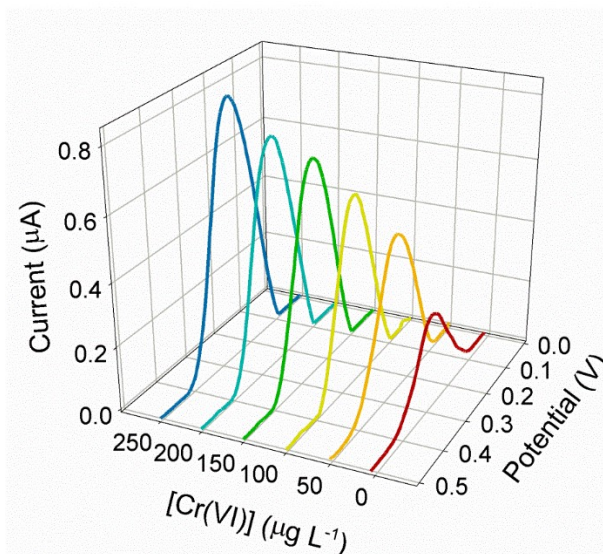


**Figure 5.5.** Square-wave voltammograms of various Cr(VI) concentrations collected at a pyridine-functionalized sol-gel electrode: 5, 50, 100, 150, 180, 200, and 250  $\mu\text{g L}^{-1}$ . Peaks are seen at 0.26 V.

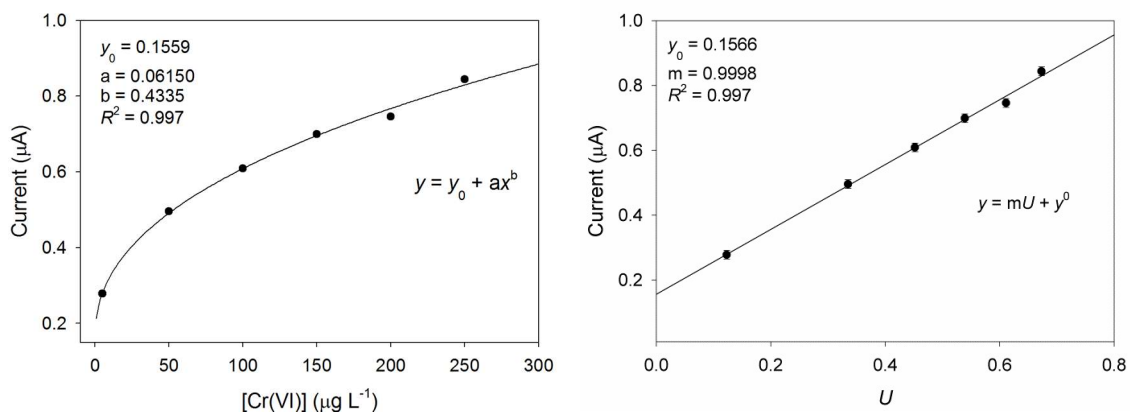


**Figure 5.6.** The detection of Cr(VI) is modeled by an exponential function due to saturation. This model can then be linearized as shown on the right where  $U = ax^b$ .

### **5.3.3. Cr(VI) detection**

The general process of Cr(VI) detection is outlined in Figure 5.1. The modified GCE is successfully preconcentrated with Cr(VI) by interactions between the positively charged 2-[2-(trimethoxysilyl)ethyl]-pyridinium groups and the chromate anions. The reduction of Cr(VI) to Cr(III) consistently produces a potential peak at 0.26 V, and a calibration model with a correlation greater than 99% (Figures 5.5 and 5.6).

### **5.3.4. Real world sample**

A diluted sample of dissolved swine blood ash was analyzed with the modified GCE, producing the potential peak seen in Figure 5.7. The average peak current ( $7.2 \times 10^{-7}$  A) after three potential sweeps correlates to a Cr concentration of  $165.1 \pm 0.1 \mu\text{g L}^{-1}$  through the calibration curve in Figure 5.6. The error is calculated using the standard deviation of the sample runs as the random error and the systematic error bars of the calibration curve. This value corresponds well with the ICP-OES analysis which determined that the same blood ash contains  $199.5 \pm 44.0 \mu\text{g L}^{-1}$  Cr.

### **5.3.5. Reproducibility and the limit of detection**

To investigate the reproducibility of the sol-gel/SWNT modified electrode, four successive square wave potential sweeps were carried out in separate  $200 \mu\text{g L}^{-1}$  Cr(VI) solutions at a freshly modified electrode (Figure 5.7). The scans had

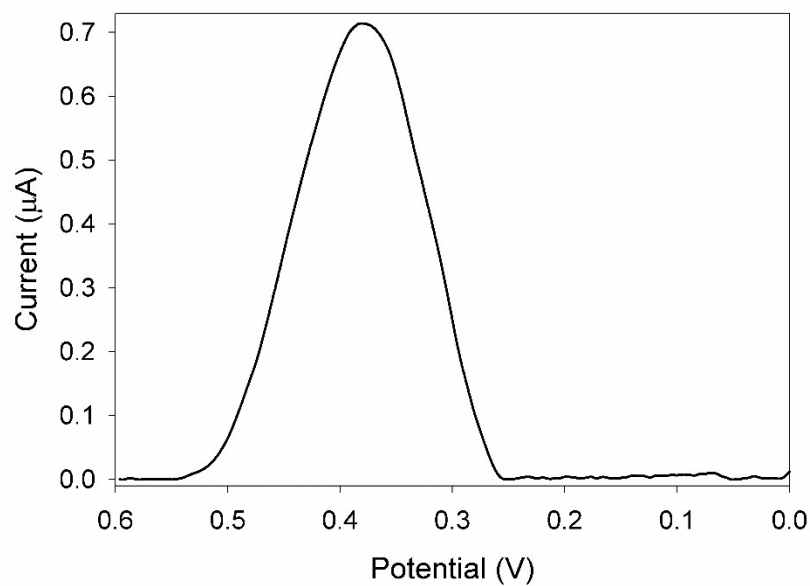


**Figure 5.7.** Cr(VI) peak detected in an ashed swine blood solution. The peak shift from 0.26 V to 0.38 V was experimentally determined to be caused by a lower pH in the sample.

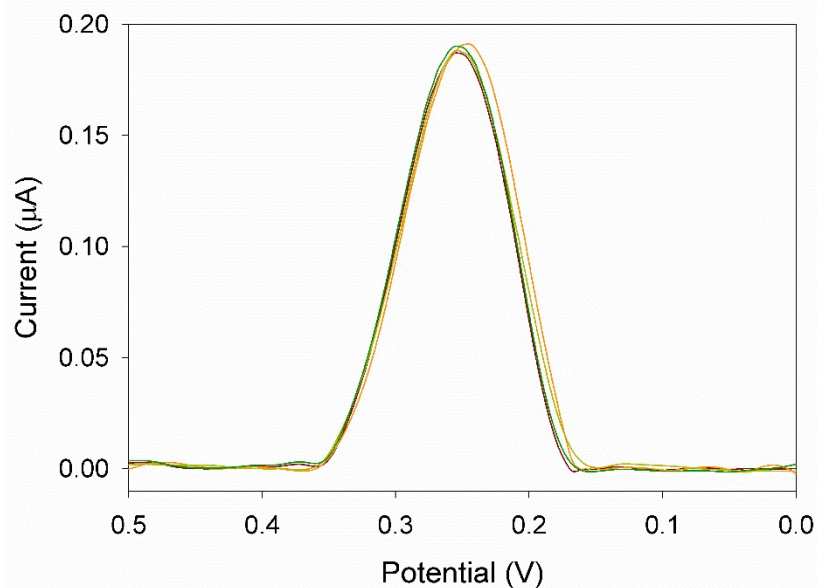


**Figure 5.8.** Square wave voltammograms of individual  $200 \mu\text{g L}^{-1}$  Cr(VI) solutions. The average standard deviation of the peak currents is calculated to be  $1.7 \times 10^{-3} \mu\text{A}$

a standard deviation of  $1.7 \times 10^{-3} \mu\text{A}$  and the limit of detection (LOD) was calculated to be  $0.3 \mu\text{g L}^{-1}$ , according to a signal-to-noise ratio of 3.

### **5.3.6. Interference studies**

Interference studies were performed in solutions of  $200 \mu\text{g L}^{-1}$  Cr(VI) spiked with metallic species and ions that are judged most likely to interfere ( $3.0 \times 10^{-6}$ ,  $1.0 \times 10^{-4}$ , and  $2.0 \times 10^{-2}$  M [interfering ion]). The Cr(VI) reduction peak current in the interference solutions are then compared to the Cr(VI) peak current in a non-spiked Cr(VI) solution. The ions chosen for study were  $\text{Na}^+$ ,  $\text{CH}_3\text{COO}^-$ ,  $\text{Cr}^{3+}$ ,  $\text{SO}_4^{2-}$ ,  $\text{Cu}^{2+}$ ,  $\text{Fe}^{3+}$ , and  $\text{VO}_4^{3-}$ . The only interferences observed were of  $\text{Cu}^{2+}$  and  $\text{Fe}^{3+}$  at concentrations of  $2.0 \times 10^{-2}$  M. Interestingly, the high concentrations of these metallic species increased the Cr(VI) peak current rather than decrease. Because both  $\text{Cu}^{2+}$  and  $\text{Fe}^{3+}$  are cations it is possible that they are becoming incorporated in the sol-gel film during the accumulation period, thereby attracting more chromate anions and increasing the peak height. More work is required to determine the true cause.

### **5.4. Conclusions**

A glassy carbon electrode modified with SWNTs and an electrodeposited pyridinium-functionalized sol-gel thin film was used to successfully preconcentrate Cr(VI). The reduction of Cr(VI) to Cr(III), using square wave

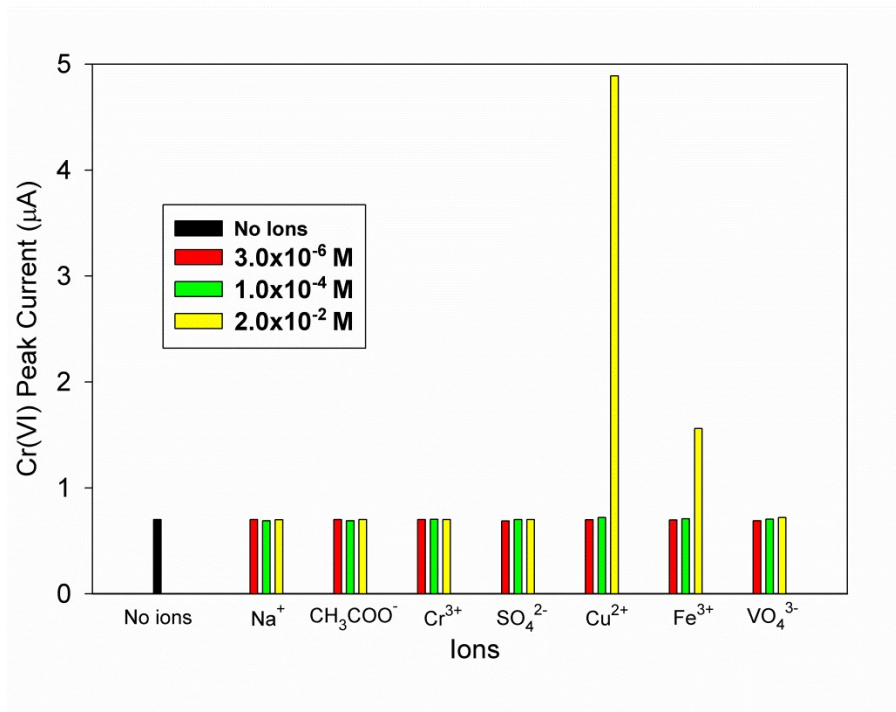


**Figure 5.9.** Graphical representation of interference studies. Note that the only interferences are  $\text{Cu}^{2+}$  and  $\text{Fe}^{3+}$  at levels higher than would be expected in environmental and biological samples.

voltammetry, produces a current peak at 0.26 V and does not require a complexing ligand. The highly reproducible detection has been successfully performed in the low  $\mu\text{g L}^{-1}$  range of Cr(VI) with a calculated LOD of  $0.3 \mu\text{g L}^{-1}$ . The analytical procedure here is unaffected by coexisting ions in expected biological and environmental concentrations. In comparison to earlier work from our group,<sup>43</sup> the addition of a SWNT base layer, as well as thinner sol-gel films, has allowed for a three orders of magnitude increase in sensitivity.

## References

1. Acharya, U.R.; Mishra, M.; Tripathy, R.R.; Mishra, I. *Reprod. Toxicol.* **2006**, *22*, 87–91.
2. Kotas, J.; Stasicka, Z. *Environ. Pollut.* **2000**, *107*, 263–283.
3. Norseth, T. *Environ. Health Perspect.* **1981**, *40*, 121–130.
4. Stohs, S.J.; Bagchi, D. *Free Radic. Biol. Med.* **1995**, *18*, 321–326.
5. Bagchi, D. *Toxicol.* **2002**, *180*, 5–22.
6. OSHA Instruction CPL 02-02-074, Inspection Procedures for the Chromium (VI) Standards, January 24, 2008.
7. OSHA Instruction CPL 02-02-076, National Emphasis Program – Hexavalent Chromium, February 23, 2010.
8. Hauber, C. Formation, Prevention & Determination of Cr(VI) in Leather, UNIDO, September 2000.
9. Vincent, J. *The Nutritional Biochemistry of Chromium(III)*, Elsevier Science, Amsterdam, The Netherlands, 2007.
10. Anderson, R.A. *J. Am. Coll. Nutr.* **1998**, *17*, 548–555.
11. Yong, L.; Armstrong, K.C.; Dansby-Sparks, R.N.; Carrington, N.A.; Chambers, J.Q.; Xue, Z.-L. *Anal. Chem.* **2006**, *78*, 7582–7587.
12. Bag, H.; Turker, A.R.; Lale, M.; Tunceli, A. *Talanta* **2000**, *51*, 895–902.
13. Hirata, S.; Honda, K.; Shikino, O.; Maekawa, N.; Aihara, M. *Spectrochim. Acta, B* **2000**, *55*, 1089–1099.

14. Tang, B.; Yue, T.; Wu, J.; Dong, Y.; Ding, Y.; Wang, H. *Talanta* **2004**, *64*, 955–960.
15. Kaneko, M.; Kurihara, M.; Nakano, S.; Kawashima, T. *Anal. Chim. Acta* **2002**, *474*, 167–176.
16. Muto, K.; Ohno, K.; Lin, J.M.; Yamada, M. *Jpn. J. Iron Steel* **2003**, *89*, 68–74.
17. Carrington, N.A.; Qiu, H.; Xue, Z.-L. *Am. Lab* **2007**, *39*, 37–41.
18. Paniagua, A.R.; Vazquez, M.D.; Tascon, M.L.; Sanchez Batanero, P. *Electroanal.* **1993**, *5*, 155.
19. Svancara, I.; Foret, P.; Vytras, K. *Talanta* **2004**, *64*, 844.
20. Welch, M.W.; Nekrassova, O.; Compton, R.G. *Talanta* **2005**, *65*, 74.
21. Yang, Y.-J.; Huang, H.-J. *Anal. Chem.* **2001**, *73*, 1377.
22. Lin, L.; Lawrence, N.S.; Thongngamdee, S.; Wang, J.; Lin, Y. *Talanta* **2005**, *65*, 144.
23. Turyan, I.; Mandler, D. *Anal. Chem.* **1997**, *69*, 894.
24. Ge, H.; Zhang, J.; Wallace, G.G. *Anal. Lett.* **1992**, *25*, 429.
25. Cox, J.A.; Kulesza, P.J. *Anal. Chim. Acta* **1983**, *154*, 71–78.
26. Crosmun, S.T.; Mueller, T.R. *Anal. Chim. Acta* **1975**, *75*, 199–205.
27. Boussemart, M.; Van den Berg, C.M.G.; Ghaddaf, M. *Anal. Chim. Acta* **1992**, *262*, 103–105.
28. Wang, J.; Lu, J.M.; Hocevar, S.B.; Farias, P.A.M.; Ogorevc, B. *Anal. Chem.* **2000**, *72*, 3218–3222.



29. Wang, J.J.; Lu, M.; Kirgoz, U.A.; Hocevar, S.B.; Ogorevc, B. *Anal. Chim. Acta* **2001**, *434*, 29–34.
30. Guo, S.J.; Wang, E.K. *Anal. Chim. Acta* **2007**, *598*, 81–192.
31. Yun, Y.H.; Dong, Z.; Shanov, V.N.; Doepke, A.; Heineman, W.R.; Halsall, H.B.; Bhattacharya, A.; Wong, D.K.Y.; Schulz, M.J. *Sens. Actuators B* **2008**, *133*, 208–212.
32. Ouyang, R.; Bragg, S.A.; Chambers, J.Q.; Xue, Z-L. *Anal. Chim. Acta* **2012**, *722*, 1–7.
33. Hsueh C., Collinson, M.M. *J. Electroanal. Chem.* **1997**, *420*, 243–249.
34. Petit-Dominguez, M. D.; Shen, H.; Heineman, W. R.; Seliskar, J. *Anal. Chem.* **1997**, *69*, 703–710.
35. Collinson, M.M.; Rausch, C.G.; Voigt, A. *Langmuir* **1997**, *13*, 7245–7251.
36. Wang, B.; Cheng L.; Dong, S. *J. Electroanal. Chem.* **2001**, *516*, 17–22.
37. Wang, H.; Xu, G.; Dong, S. *Anal. Chim. Acta* **2003**, *480*, 285–290.
38. Hu, Z.; Seliskar, C.J.; Heineman, W.R. *Anal. Chem.* **1998**, *70*, 5230–5236.
39. Collinson, M.M.; Moore, N.; Deepa, P.N.; Kanungo, M. *Langmuir* **2003**, *19*, 7669–7672.
40. Shacham, R.; Avnir, D.; Mandler, D. *Adv. Mater.* **384**, *11*, 384–388.
41. Deepa, P.N.; Kanungo, M.; Claycomb, G.; Sherwood, P.M.A.; Collinson, M.M. *Anal. Chem.* **2003**, *7575*, 5399–5405.
42. Collinson, M.M.; Novak, B. *J. Sol–Gel Sci. Technol.* **2002**, *23*, 215–220.
43. Carrington, N.A.; Yong, L.; Xue, Z.-L. *Anal. Chim. Acta* **2006**, *572*, 17–24.
44. Carrington, N.A.; Qiu, H.; Xue, Z.-L. *American Laboratory* **2008**, *39*, 37–41.

45. Brinker, C.J.; Scherer, G.W. *Sol-gel Science*, Academic Press, Cambridge, Massachusetts, 1990.
46. Buckley, A.M.; Greenblat, M. *J. Chem. Educ.* **1994**, *71*, 599–602.
47. Carrington, N.A.; Xue, Z.-L. *Acc. Chem. Res.* **2007**, *40*, 343–350.
48. Dansby-Sparks, R.N.; Ouyang, R.; Xue, Z.-L. *Sci China Ser B-Chem.* **2009**, *52*, 1777–1788.
49. Wei, H.; Collinson, M.M. *Anal. Chim. Acta* **1999**, *397*, 113–121.
50. Shacham, R.; Avnir D.; Mandler, D. *J. Sol–Gel Sci. Technol.* **2004**, *31*, 329–334.
51. Collinson, M.M. *Anal. Chem.* **2008**, *80*, 651–656.
52. West, A.C.; Cheng, C.C.; Baker, B.C. *J. Electrochem. Soc.* **1998**, *145*, 3070–3074.
53. Schauer, C.L. *Thin Solid Films* **2003**, *434*, 250–257.
54. Berthier, S. *Iridescences: The Physical Colors of Insects*, Springer Science, New York, 2007
55. Lang, L.; Hu, J.-M.; Zhang, J.-Q.; Cao, C.-N. *Anal. Chem.* **2009**, *81*, 3199–3200.

## **PART 6**

### **Novel methods for the pretreatment of whole blood using Fenton-like processes**

Research for this chapter was a collaborative work between Kimberly N. Johnson and Samuel M. Rosolina.

## **Abstract**

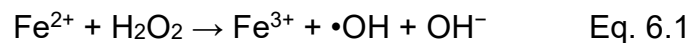
Two new processes to pretreat blood samples have been developed. The treatments are based on a Fenton-like advanced oxidation process (AOP) and use acid deactivation of the enzyme catalase in the blood. The first treatment is performed with a simple convection oven over a period of 5 h, while the second uses microwave irradiation for 6 min. These novel methods allow for either cost effective pretreatment through the use of the common lab oven, or time savings through the use of the synthesis microwave. The degradation of whole blood has been compared with that of pure hemoglobin samples through UV/Vis spectroscopy, and the copper concentration in the treated samples were analyzed via anodic stripping voltammetry (ASV).

### **6.1. Introduction**

Metal analysis in biological samples is an important and active area of study. As a useful method within many fields, such as biomedical, wastewater treatment, environmental, and even veterinary studies, there will always be a call for improving the processes involved in metal analysis.<sup>1-4</sup> One of the most important steps is the pretreatment method, especially when analyzing metals such as copper or chromium that form complexes or are bound in macromolecules.<sup>5,6</sup> Currently, the most common pretreatment methods include

dry ashing, chemical oxidation and advanced oxidation. In dry ashing, the sample is placed in an open vessel and the organics are destroyed through thermal decomposition under very high temperatures. This method can process large volumes of sample, but can have increased error due to the required amount of sample handled and the loss of volatile compounds such as Hg.<sup>7,8</sup> Chemical oxidation methods are often used in processes like wastewater treatment, but can require large quantities of oxidizing agents such as hypochlorite and potassium permanganate which can be costly and environmentally damaging.<sup>9</sup>

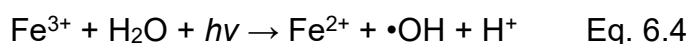
Advanced oxidation processes (AOPs) are a type of sample treatment method meant to destroy organics through the formation of highly reactive hydroxyl radicals ( $\bullet\text{OH}$ ).<sup>10-13</sup> The Fenton process is a common AOP that uses a ferrous ion ( $\text{Fe}^{2+}$ ) alongside  $\text{H}_2\text{O}_2$  to form hydroxyl and hydroperoxyl radicals, which become the oxidants in the decomposition of organic compounds. The radical forming reactions involved in the Fenton process can be seen below.



In Eq. 6.1–6.2,  $\text{Fe}^{2+}$  acts as a catalyst, cycling between the 2+ and 3+ oxidation states.<sup>14,15</sup>

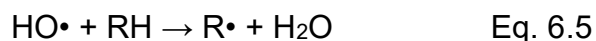
The Fenton process does not require irradiation. However, if irradiation is introduced, the formation of radicals is greatly increased. This is known as the

Photo-Fenton process and the increase in radicals is due to the direct homolytic bond cleavage of the oxygen atoms in H<sub>2</sub>O<sub>2</sub> as well as the regeneration of Fe<sup>2+</sup> ions through the reduction of Fe<sup>3+</sup> ions by light-induced electron transfer (Eqs. 6.3–6.4).<sup>10-12,16</sup>

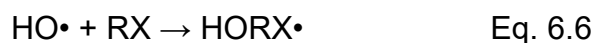


Three different reactions can take place between the hydroxyl ions and the organics in solution (Eqs. 6.5–6.6):

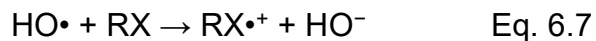
1) Hydrogen abstraction<sup>10,17</sup>



2) Electrophilic addition<sup>10</sup>



3) Electron transfer<sup>10</sup>



As the hydroxyl and hydroperoxyl radicals attack any organic compounds in solution, more radicals are generated that continue to further decompose the organics. For this reason, photo-Fenton processes require small quantities of

reagents, making them environmentally friendly alternatives to other methods.<sup>10,11</sup>

Past work in our group has successfully employed the photo-Fenton AOP method using UV irradiation as the photon source to mineralize swine blood samples.<sup>14</sup> The study utilized a four-cell reactor that was designed and built in-house, and was coupled with the electrochemical detection of Cr(III), an essential trace element in the body.

The work herein reports two separate Fenton-based methods using different irradiation methods. The first method, employing a common laboratory convection oven, is a novel, cost effective form of blood pretreatment. The second method, relying on irradiation from a synthesis microwave, requires only 6 min to perform. The pretreatment methods have been further validated via UV-Vis spectroscopy, comparing pre- and post-treated sample spectra with those of pure hemoglobin. Furthermore, the copper concentration in the treated samples were analyzed via anodic stripping voltammetry (ASV) and compared with results using inductively coupled plasma-optical emission spectroscopy (ICP-OES).

## **6.2. Materials and methods**

### **6.2.2. Chemicals and instruments**

Sodium hydroxide (NaOH, Certified ACS, Thermo Fisher Scientific, Waltham, MA), potassium oxalate ( $K_2C_2O_4$ , Certified ACS, Thermo Fisher Scientific), ammonium iron(II) sulfate  $[(NH_4)_2Fe(SO_4)_2 \cdot 6H_2O]$ , Acros/Thermo

Fisher Scientific], ethanol (95%, Decon Laboratories, Inc., King of Prussia, PA), porcine hemoglobin (Sigma Aldrich, St. Louis, MO), whole swine blood (Wampler's Farm, Lenoir City, TN), nitric acid (HNO<sub>3</sub>, 70%, Trace Metal Grade, Thermo Fisher Scientific) were used as received. Cu(II) ICP standard solutions (1000 mg L<sup>-1</sup>, Sigma Aldrich) were diluted prior to use.

Prior to use, GCEs were polished to a mirror-like surface on a standard electrode polishing kit (CH Instruments, Inc., Austin, TX) including a 1200 grit CarbiMet™ disk, 1.0 and 0.3 μm alumina slurry on a nylon cloth, and 0.05 μm alumina slurry on a microcloth polishing pad. After polishing, GCEs were successively sonicated with deionized (DI) water, ethanol, and DI water again for 5 min each. Electrochemical measurements were carried out on a CHI 440a Electrochemical Workstation (CH Instruments). A three-electrode configuration consisted of a bare, unmodified GCE (3 mm in diameter, BAS Inc., West Lafayette, IN), Ag/AgCl (saturated KCl solution, CH Instruments) and a platinum wire (CH Instruments) as working, reference, and counter electrodes, respectively. Microwave irradiation was carried out using a Biotage 2.5 synthesis microwave in 20 mL microwave reaction vials. The oven used was an Isotemp Standard Laboratory Oven (Thermo Fisher Scientific). UV-Visible spectra were collected using an Agilent 8453 photodiode array spectrophotometer and a 1.0 cm quartz cuvette. Blank spectra of deionized water were recorded and subtracted from those of the samples. pH measurements were carried out with a pH meter (Accumet Basic, Fisher Scientific).



### **6.3. Experimental procedures**

#### **6.3.1. Swine blood sampling**

Whole swine blood was obtained from Wampler's Farm (Lenoir City, TN). The sample was taken from a single pig that was freshly slaughtered and placed in a 1-L Nalgene bottle. Prior to this, the interior of the bottle was coated with 2 g of  $K_2C_2O_4$ , an anticoagulant. Using ultrapure DI water and trace metal grade  $HNO_3$ , the blood was diluted to 5.00% and acidified to pH 3. This solution was used for following studies.

#### **6.3.2. Catalase deactivation**

Catalase is a natural enzyme that decomposes hydrogen peroxide and prevents the formation of hydroxyl radicals.<sup>14</sup> In order for an AOP to reach its highest efficiency, the catalase must be inactive in the AOP. Low pH ( $\leq 3.0$ ) causes a temporary denaturation of catalase, allowing for the oxidation method to take place unimpeded.<sup>14,15</sup> Once the catalase has been permanently destroyed, the pH can be raised without consequence if necessary.

#### **6.3.3. Laboratory-oven pretreatment**

The optimized oven pretreatment method is carried out in a glass vial with a vented cap containing 15.0 mL of 5.00% whole blood (pH 3). Before placing it in the oven, 0.5 mg of  $(NH_4)_2Fe(SO_4)_2 \cdot 6H_2O$  is added to the solution and the vial is warmed on a hotplate to ensure that it is fully dissolved. Prior to pretreatment,

1.00 mL of 30% H<sub>2</sub>O<sub>2</sub> is added to the vial. The vial is then placed in the laboratory oven at 100 °C. After 1 h, 500 µL of 30% H<sub>2</sub>O<sub>2</sub> is added, and the solution is left in the oven for another 4 h. The final pretreated sample which is a clear, yellow tinted solution is then removed from heat and allowed to cool to room temperature (Figure 6.1).

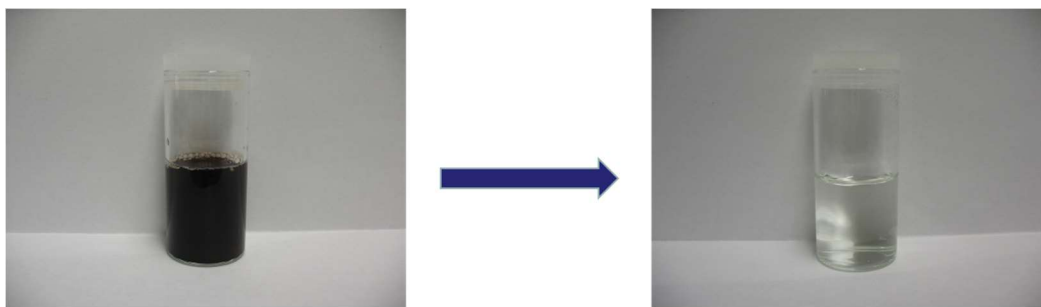


**Figure 6.1.** Swine blood solution before and after oven-based AOP.

#### **6.3.4. Microwave pretreatment**

The optimized microwave pretreatment method is carried out in a 20 mL microwave reaction vial containing 15 mL of 5.00% whole blood (pH 3). The microwave vial can be sealed with an aluminum cap that can withstand pressures up to 30 bar. Before irradiation, 0.2 mg of (NH<sub>4</sub>)<sub>2</sub>Fe(SO<sub>4</sub>)<sub>2</sub>•6H<sub>2</sub>O is added to the solution and the vial along with 1.00 mL of 30% H<sub>2</sub>O<sub>2</sub>. The vial is sealed and microwaved for 100 s at 150 W while being cooled with compressed N<sub>2</sub>. The vial is then removed from the microwave and allowed to cool to room temperature before adding 500 µL of 30% H<sub>2</sub>O<sub>2</sub>. The vial is then re-sealed and

microwaved again at 150 W for 160 s while cooling with compressed N<sub>2</sub>. The final pretreated sample which is a clear, yellow tinted solution is then removed from heat and allowed to cool to room temperature (Figure 6.2).

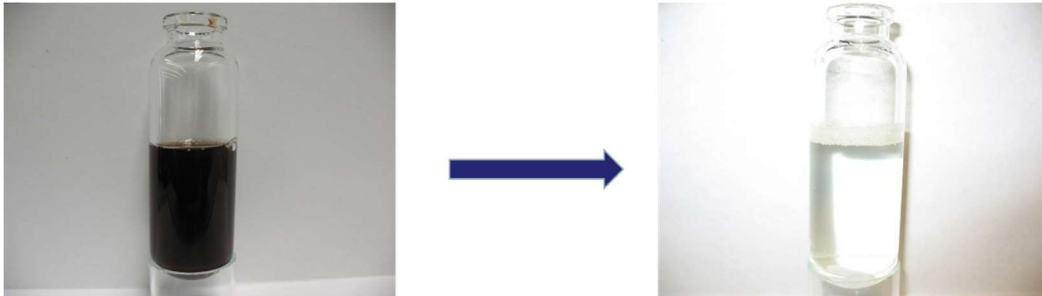


**Figure 6.2.** Swine blood solution before and after microwave-based AOP.

## **6.4. Results and discussion**

### **6.4.1. Sample analysis**

Using a laser and the Tyndall effect, the solutions were determined to be fully mineralized. This was further validated using a centrifuge and gravimetric analysis to ensure that no solids were left in the samples post treatment. Prior to analysis, pH was increased to 7 by adding 1.0 M NaOH solution dropwise. At this pH, the majority of Fe ions crash out as solid FeO(OH) which was separated via centrifugation. The sample solutions were then diluted in a 25.0 mL volumetric flask using ultrapure DI water.

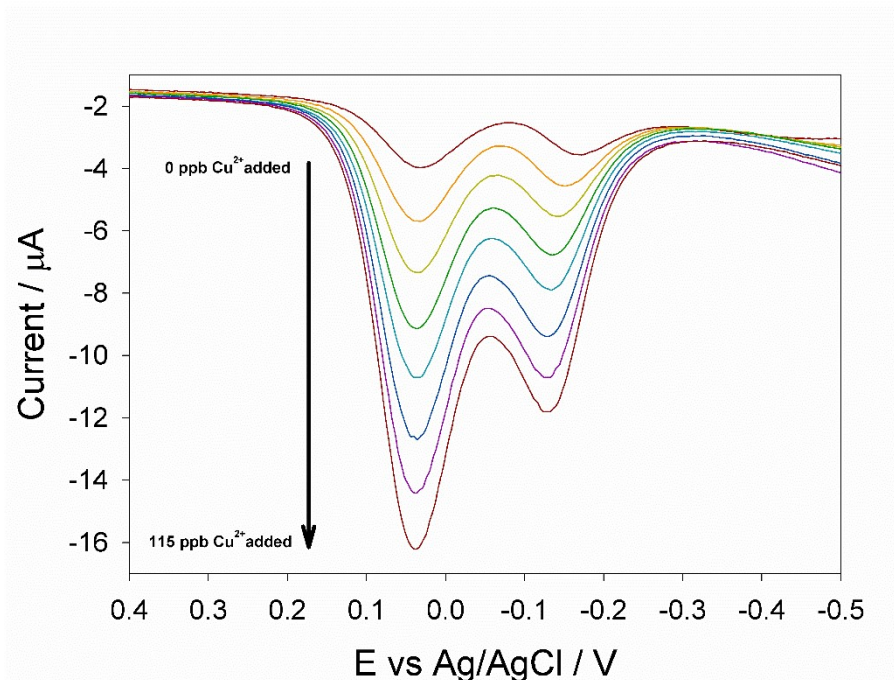


**Figure 6.3.** Voltammograms of Cu in an oven pretreated blood solution. Oxidation peaks for both Cu(I) and Cu(II) are observed.

#### 6.4.1.1. ASV analysis

Copper analysis in the pretreated sample (pH 7) was conducted without the addition of a supporting electrolyte given that ions left in solution were sufficient. Anodic stripping voltammetry (ASV) was paired with standard addition to determine the concentration of copper in the original whole swine blood sample. The bare glassy carbon working electrode was held at -1.2 V for 300 s before sweeping the anodic sweep to 0.9 V using a frequency of 25 Hz, a step potential of 4 mV, and amplitude of 25 mV. The standard addition method was used to add Cu(II) standard to total concentrations in the range of 0.0–115.2 ppb  $\text{Cu(II)}_{\text{added}}$  (Figure 6.3).

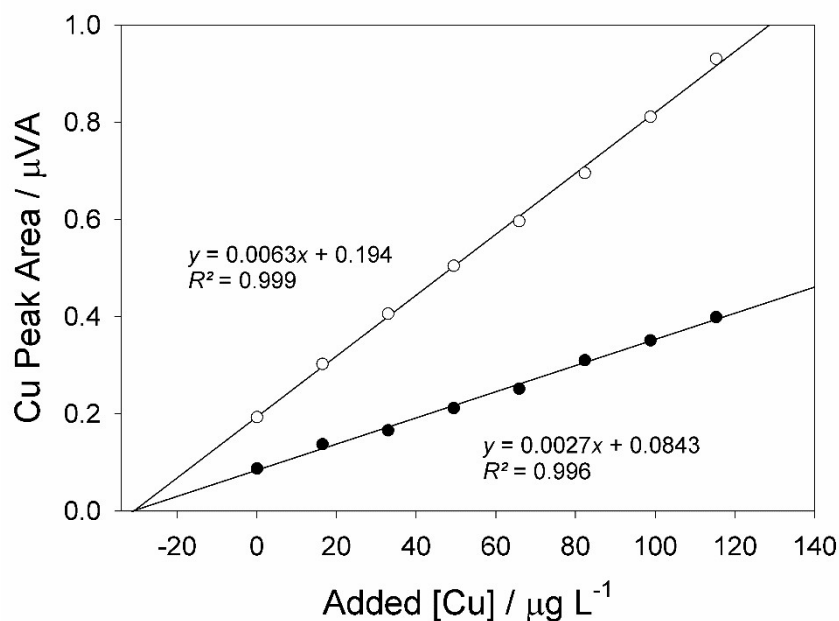


**Figure 6.4.** Calibration curves for the Cu(I) oxidation peak (black data points) and the Cu(II) oxidation peak (white data points) in pretreated blood.

The voltammograms show oxidation peaks for both Cu(I) (-0.16 V) and Cu(II) (0.04 V). The calibration curves for both peaks are given in Figure 6.3. Using the linear equations for the Cu(I) and Cu(II) peak (Figure 6.4), an original Cu concentration of 31.2 ppb and 30.8 ppb can be calculated, respectively, in the sample. The %RSDs at the highest concentration (the only concentration run as a replicate [ $n = 5$ ]) for the Cu(I) and Cu(II) peak were determined to be 5.2% and 3.9%, relatively. The average of these concentrations translates to  $1033 \pm 9.4$  ppb Cu in the original whole blood. This is calculated based on the known dilution factors: 15.0 mL of 5% whole blood was diluted to 25.0 mL and analyzed after mineralization.

#### 6.4.1.2. ICP-OES analysis

The calculated original concentration of Cu was further validated using ICP-OES. By creating a calibration curve using standards (Figure 6.5) followed by analysis of the sample solution, the Cu concentration was determined to be  $32.9 \pm 0.135$  ppb, corresponding to  $1097 \pm 4.50$  ppb Cu in the original whole blood. This concludes that the ASV analysis has a 5.8% error when compared to the ICP-OES data.

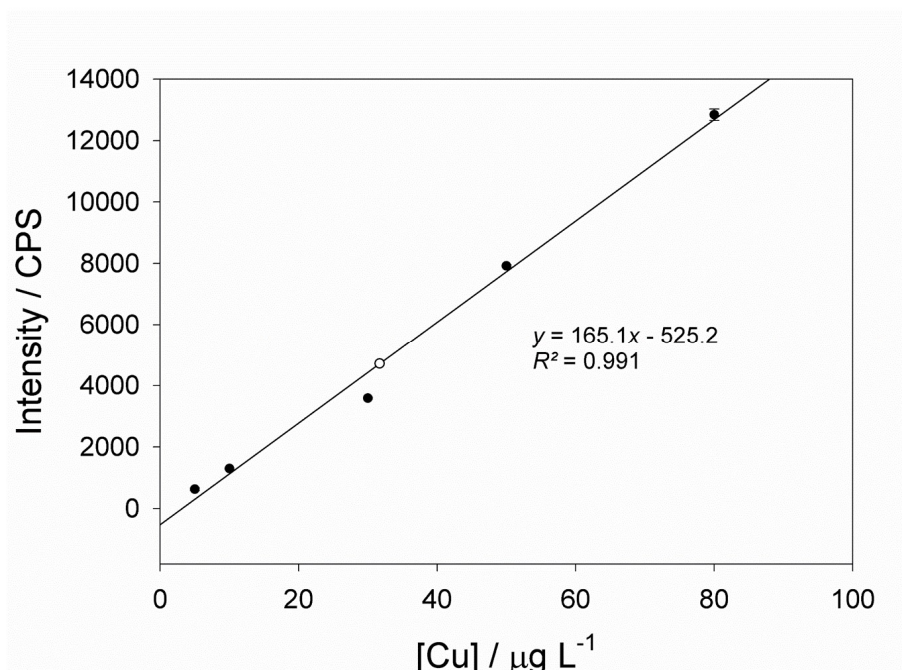


**Figure 6.5.** ICP-OES standard calibration curve of copper in pretreated blood ( $\lambda = 327.393$  nm). The white data point was collected from the sample solution which was determined to be  $32.9 \pm 0.135$  ppb.

### 6.4.1.3. Analysis of samples via UV-Vis spectroscopy

UV-Vis spectra were taken of diluted whole-blood solution acidified to pH 3, a solution made from porcine hemoglobin and acidified to pH 3, oven-based AOP treated blood, and microwave-based AOP treated blood (Figure 6.6). The spectra illustrate the destruction of organics in the blood, as the hemoglobin peak at 380 nm no longer appears in the pretreated samples.

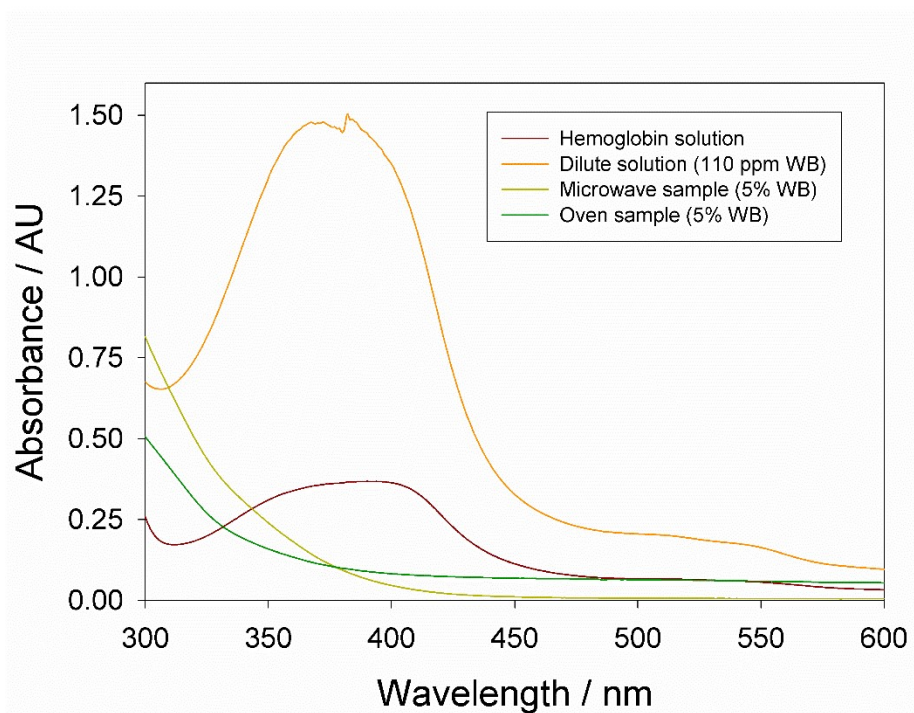


**Figure 6.6.** UV-Vis spectra comparing oven- and microwave-based results with a dilute whole blood (WB) solution, and porcine hemoglobin solution.

### **6.4.3. Discussion**

Direct analysis of the pretreated oven sample via ASV illustrates, in several ways, the success of this method. Since ASV is a sensitive method, organics in solution can easily interfere with the voltammetry, either by interacting with the electrode surface, or by inhibiting mass transfer of the analyte. Due to the clean, sharp peaks, these interferences are clearly absent. The fact that the voltammograms were smooth without the requirement of adding an electrolyte is another indication of complete, or near complete, sample mineralization.

Furthermore, the ability to detect the original Cu concentration by ASV with 5.8% error, which was validated by ICP-OES, indicates that the majority of Cu was free in the solution.

The Cu concentration in healthy pigs is ~1.1 ppm,<sup>19,20</sup> which agrees with the data we extracted through ASV and ICP-OES. While very low, the 5.8% error of the ASV Cu analysis, when compared to the ICP-OES Cu analysis, indicates that the mineralization may not have been complete. More studies are required to truly determine the validity of these new methods, including analysis of the microwave treated sample through ASV and ICP-OES, and reproducibility studies.

### **6.5. Conclusion**

The work in this part provides two novel methods for the pretreatment of whole blood. One utilizes a convection oven allowing for an inexpensive method,



and the other is based on microwave irradiation for quick treatment. Analyses of the oven-treated sample using UV-Vis spectroscopy, ASV, and ICP-OES all indicate that the method was successful. While the microwave-treated sample has not yet been analyzed by ASV, the UV-Vis spectra also indicate that the organics have been destroyed. Further studies will examine whether the 5.8% error between the ASV and ICP-OES data are caused by the AOP or the analysis techniques themselves. It is the belief of the author that the two new mineralization procedures will open new avenues for research and medical laboratories.

## References

1. Miller, N.J.; Rice-Evans, C.; Davies, M.J.; Gopinathan, V.; Milner, A. *Clin. Sci.* **1993**, *84*, 407–412.
2. Knahr, K.; Karamat, L.; Pinggera, O. *Ceramics in Orthopaedics (Bioceramics and Alternative Bearings in Joint Arthroplasty)*, Springer, 2005; pp. 39–44.
3. Lewis, S.A.; O'Haver, T.C.; Harnly, J.M. *Anal. Chem.* **1984**, *56*, 1066–1070.
4. Wang, J. *J. Electroanal. Chem.* **1982**, *139*, 225–232.
5. Rodman, D.L.; Carrington, N.A.; Xue, Z.-L. *Talanta* **2006**, *70*, 668–675.
6. Yong, L.; Armstrong, K.C.; Dansby-Sparks, R.N.; Carrington, N.A.; Chambers, J.Q.; Xue, Z.-L. *Anal. Chem.* **2006**, *78*, 7582–7587.
7. Mester, Z.; Sturgeon, R. *Comprehensive Analytical Chemistry Volume XLI: Sample Preparation for Trace Metal Analysis*, Elsevier B.V., Amsterdam, 2003.
8. Bragg, S.A.; Xue, Z.-L. *Am. J. Anal. Chem.* **2011**, *2*, 979–983.
9. Szpyrkowicz, L.; Juzzolino, C.; Santosh, N.K. *Water Res.* **2001**, *35*, 2129–2136.
10. Parsons, S., Ed. *Advanced Oxidation Processes for Water and Wastewater Treatment*; IWA Publishing: London, 2004.
11. *Handbook on Advanced Photochemical Oxidation Processes*. EPA, 1998.
12. Legrini, O.; Oliveros, E.; Braun, A.M. *Chem. Rev.* **1993**, *93*, 671–698.
13. Symons, J.M.; Worley, K.L. *J. Amer. Wat. Works Assn.* **1995**, *87*, 66–75.
14. Bragg, S.A.; Armstrong, K.C.; Xue, Z.-L. *Talanta* **2012**, *97*, 118–123.

15. Yong, L.; Armstrong, K.C.; Dansby-Sparks, R.N.; Carrington, N.A.; Chambers, J.Q.; Xue., Z.-L. *Anal. Chem.* **2006**, *78*, 7582–7587.
16. Schulte, P.; Bayer, A.; Kuhn, F.; Luy, T.; Volkmer, M. *Ozone Sci. Eng.* **1995**, *17*, 119–134.
17. Zepp, R.G.; Faust, B.C.; Holgne, J. *Environ. Sci. Technol.* **1992**, *26*, 313–319.
18. Shelor, C.P.; Campbell, C.C.; Kroll, M.; Dasgupta, P.K; Smith, T.L.; Abdalla, A.; Hamilton, M.; Muhammad, T.W. *Anal. Chem.* **2011**, *83*, 8300–8307.
19. Drouliscos, N.J.; Bowland, J.P.; Elliot, J.I. *Can. J. Anim. Sci.* **1970**, *50*, 113–120.
20. Schultze, M.O.; Elvehjem, C.A.; Hart, E.B. *J. Biol. Chem.* **1936**, *116*, 107–118.

## **PART 7**

**Bismuth-based, disposable sensor for the detection of  
hydrogen sulfide gas**

A version of this chapter was originally published by Samuel M. Rosolina, Thomas S. Carpenter, and Zi-Ling Xue. Only minor revisions were made.

Samuel M. Rosolina, Thomas S. Carpenter, and Zi-Ling Xue. "Bismuth-Based, Disposable Sensor for the Detection of Hydrogen Sulfide Gas." *Anal. Chem.* **2016**, *88*, 1553–1558.

Additional materials for Part 7 are provided in Appendix D.

### **Abstract**

A new sensor for the detection of hydrogen sulfide ( $\text{H}_2\text{S}$ ) gas has been developed to replace commercial lead(II) acetate-based test papers. The new sensor is a wet, porous, paper-like substrate coated with  $\text{Bi}(\text{OH})_3$  or its alkaline derivatives at pH 11. In contrast to the neurotoxic lead(II) acetate, bismuth is used due to its non-toxic properties, as Bi(III) has been a reagent in medications such as Pepto-Bismol. The reaction between  $\text{H}_2\text{S}$  gas and the current sensor produces a visible color change from white to yellow/brown, and the sensor responds to  $\geq 30$  ppb  $\text{H}_2\text{S}$  in a total volume of 1.35 L of gas, a typical volume of human breath. The alkaline, wet coating helps the trapping of acidic  $\text{H}_2\text{S}$  gas and its reaction with Bi(III) species, forming colored  $\text{Bi}_2\text{S}_3$ . The sensor is suitable for testing human bad breath, and is at least two orders of magnitude more sensitive than a commercial  $\text{H}_2\text{S}$  test paper based on  $\text{Pb}(\text{II})(\text{CH}_3\text{COO})_2$ . The small volume of 1.35-L  $\text{H}_2\text{S}$  is important, as the commercial  $\text{Pb}(\text{II})(\text{CH}_3\text{COO})_2$ -based paper require large volumes of 5 ppm  $\text{H}_2\text{S}$  gas. The new sensor reported here is

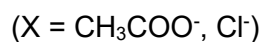
inexpensive, disposable, safe, and user-friendly. A simple, laboratory setup for generating small volumes of ppb-ppm H<sub>2</sub>S gas is also reported.

### **7.1. Introduction**

Hydrogen sulfide gas has a very unpleasant odor even at very low levels (low ppb) and is one of the main contributors to halitosis.<sup>1-3</sup> Humans with bad breath have an average H<sub>2</sub>S concentration of 80 ppb while a healthy individual has an average of 2 ppb in the breath.<sup>2</sup> Aside from being flammable, H<sub>2</sub>S also falls under the category of chemical asphyxiant, along with carbon monoxide and cyanide gases, making it extremely dangerous in mining and related industries. Above 30 ppm, H<sub>2</sub>S begins to saturate the olfactory, making it difficult to recognize the toxic gas, and at 100 ppm is completely undetectable through smell alone. Above 50 ppm, the gas begins to cause loss of motor skills, shock, convulsion, and even death as it prevents the uptake of oxygen in the blood due to strong affinity of the sulfide ion for iron(II/III). Even chronic, low level exposures can lead to irreversible health effects. Because H<sub>2</sub>S is often found in natural pockets underground, there are often dangers associated with industrial drilling and hydraulic fracturing, and even with the use of natural hot springs.<sup>4-7</sup> A simple visual method for its detection would be very valuable in oral health, mining, and other industries.<sup>1-7</sup>

The most common type of H<sub>2</sub>S sensors is electrochemical, using metal oxide semiconductors or conducting polymers.<sup>8-15</sup> Adsorption of sulfide to the

metal oxide causes an increase in electrical resistivity which can be monitored in real time. Unfortunately, such sensors are too expensive for the common consumer and they do not perform consistently with respect to changes in humidity and temperature.<sup>8-11</sup> In addition, many chemicals have affinities for metal oxides, leading to interferences and often requiring the addition of inlet filtration.<sup>8</sup> Electrical devices using metal salts have also been fabricated, capitalizing on the affinity of sulfides for metals such as Cu(II).<sup>12-15</sup> While the detection limits of these sensors may be as low as 100 ppb, the volumes (and thus total moles of H<sub>2</sub>S) are often unspecified.<sup>12-15</sup> Furthermore, the reactions of acidic H<sub>2</sub>S with the metal salts yield acids such as CH<sub>3</sub>COOH or HCl,<sup>13</sup> retarding the reactions of the salts with H<sub>2</sub>S [Eq. 7.1 for examples of Cu(II) salts], and potentially reducing the sensitivity. An attractive alternative would be a sensor with a high surface pH, leading to fast neutralization of acidic H<sub>2</sub>S gas and capturing of the S<sup>2-</sup> ion.



Optical approaches for sulfide analysis have been developed based on sulfide-selective, organic- and organometallic-based dyes<sup>16-19</sup> or nanoparticle-based sensors.<sup>20-22</sup> While these methods are sensitive and accurate, they have been used in liquid media only, making it difficult to detect H<sub>2</sub>S gas. Sarfraz and coworkers have immobilized Cu(CH<sub>3</sub>COO)<sub>2</sub> onto solid substrates initially for

electrochemical H<sub>2</sub>S analysis. The immobilized Cu(CH<sub>3</sub>COO)<sub>2</sub> may also be used for the optical detection of H<sub>2</sub>S gas at as low as 1 ppm. However, this sensitivity required an exposure time of 45 min at an unspecified flow rate.<sup>12</sup>

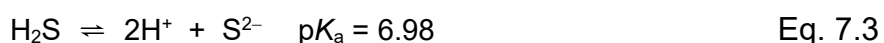
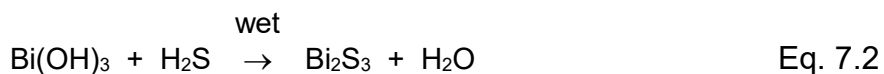
Another widely used H<sub>2</sub>S sensor is commercial lead acetate paper for colorimetric, qualitative detection. These white paper strips turn gray or black in the presence of H<sub>2</sub>S from the formation of black lead sulfide (PbS). Though these commercial lead acetate papers are used worldwide and available for civilian application, it has major disadvantages in addition to those discussed above. First, its limit of detection (LOD), between 5 and 10 ppm H<sub>2</sub>S, is high and is not suitable for bad breath tests. Even with such a high LOD, lead acetate has been recently called “the most sensitive H<sub>2</sub>S indicator reagent.”<sup>23</sup> Second, and possibly the most crucial disadvantage, is its use of lead, a known neurotoxin.<sup>24</sup> Much care is needed when handling the Pb(II)-based sensor. In addition, the disposal of the lead acetate papers is an environmental concern. Despite their toxicity, lead acetate test papers are still commonly used in research labs to identify the presence of hydrogen sulfide,<sup>23,25</sup> and are readily available to the general public.<sup>26</sup> In this work, a novel sensor has been developed using a wet, paper-like substrate coated with bismuth hydroxide Bi(OH)<sub>3</sub> or its derivatives. Bismuth was chosen in place of lead due to its non-harmful properties. In fact bismuth is already used in many consumer products, including medications such as Pepto-Bismol® to treat irritations in the stomach and gastrointestinal tract.

Stone has studied the solubility of Bi<sub>2</sub>S<sub>3</sub> by converting Bi(OH)<sub>3</sub> to BiCl<sub>3</sub> before reacting with H<sub>2</sub>S.<sup>27</sup> Although there have been papers and patents



regarding the use of bismuth compounds to detect H<sub>2</sub>S, none uses alkaline bismuth hydroxide or its derivatives. Instead the earlier studies all used a bismuth salt to detect H<sub>2</sub>S.<sup>28-37</sup> These bismuth salts include bismuth nitrate Bi(NO<sub>3</sub>)<sub>3</sub>, bismuth acetate Bi(OAc)<sub>3</sub>, bismuth chloride/fluoride BiCl<sub>3</sub>/BiF<sub>3</sub>, bismuth phosphate Bi(PO<sub>4</sub>), bismuth citrate, and bismuth carbonate.<sup>28-37</sup> In reacting any of these bismuth(III) salts with H<sub>2</sub>S, at least one product is an acid (HNO<sub>3</sub>, CH<sub>3</sub>COOH, HCl/HF, or H<sub>3</sub>PO<sub>4</sub>), as demonstrated for copper(II) salts in Eq. 7.1. A recommended turbidimetric procedure for H<sub>2</sub>S detection uses Bi(NO<sub>3</sub>)<sub>3</sub>·5H<sub>2</sub>O in manitol solution.<sup>32</sup> It is based on a paper by Field and Oldach that requires scrubbing H<sub>2</sub>S from a gas stream by a caustic solution, followed by addition of Bi(NO<sub>3</sub>)<sub>3</sub> in glacial acetic acid and dilution with water.<sup>33</sup> Dean adopted a similar approach using a NaOH solution to scrub H<sub>2</sub>S from a gas stream, followed by a reaction with a bismuth reagent (1500 ppm of bismuth and 1% gelatin in 4 N acetic acid).<sup>34</sup>

In contrast, our sensor uses alkaline bismuth hydroxide Bi(OH)<sub>3</sub> or its derivatives (Eq. 7.2). Because H<sub>2</sub>S is a weak acid (Eq. 7.3), the use of Bi(OH)<sub>3</sub> or its derivatives quickly and effectively removes H<sup>+</sup> in H<sub>2</sub>S, forming water and shifting the equilibrium in Eq. 7.3 to the product S<sup>2-</sup>. This is critical to the high sensitivity of our sensor.



Another feature of our sensor is that *wet* Bi(III) coating is used, facilitating the trapping of H<sub>2</sub>S gas and enhancing sensitivity to  $\geq 30$  ppb limit of detection for H<sub>2</sub>S gas in a total volume of 1.35 L, which is the typical volume of human breath. Given that bad breath usually contains H<sub>2</sub>S at 80 ppb, our sensor is capable of revealing halitosis. Both the thermodynamic equilibrium shift by using alkaline Bi(III) compounds and enhanced kinetics with the wet sensor surface lead to the high sensitivity of our sensor. The H<sub>2</sub>S sensor reported here has proven to be a simple and inexpensive qualitative detector of H<sub>2</sub>S, even at low ppb concentrations.

## **7.2. Experimental**

### **7.2.1. Reagents and materials**

The following chemicals were used as received: Bi(NO<sub>3</sub>)<sub>3</sub> (Alfa Aesar, Haverhill, MA), Acetone (Histological Grade, Thermo Fisher Scientific, Waltham, MA), NaHS·1.25 H<sub>2</sub>O (iodimetrically determined, Acros Organics, New Jersey), NaOH (Certified ACS, Thermo Fisher Scientific), HCl (Trace Metal Grade, Thermo Fisher Scientific). Amplitude™ Prozorb® (46% cellulose, 54% polyester) by Contec (Osaka, Japan) was cut to 1.5 × 1.5 cm<sup>2</sup> square. Lead acetate test paper dispenser was purchased from Whatman™ and used as directed. A gas cylinder of 50 ppm H<sub>2</sub>S in nitrogen (MESA Specialty Gases and Equipment) was used only for verification purposes. Ultrapure water from a Millipore water purified system ( $\geq 18$  M $\Omega$ ·cm, Barnstead/Thermos Fisher Scientific) was used in all

solutions. All glassware was soaked in 1 M nitric acid bath and thoroughly rinsed with deionized (DI) water before use.

### **7.2.2. Sensor preparation**

$\text{Bi}(\text{NO}_3)_3 \cdot 5\text{H}_2\text{O}$  (0.10 g) was added to 10.0 mL of acetone. This mixture was allowed to stir for 10 min, forming a suspension. The supernatant, now saturated with  $\text{Bi}(\text{NO}_3)_3$ , was filtered and used for sensor preparation. Cut Prozorb ( $1.5 \times 1.5 \text{ cm}^2$  square) was coated with 200  $\mu\text{L}$  of the supernatant. This was performed by pipetting 100  $\mu\text{L}$  increments directly onto the substrate with 2 min in between to allow for air drying. Lastly, 80  $\mu\text{L}$  of 0.1 M aqueous NaOH solution was added to the cut Prozorb coated with  $\text{Bi}(\text{NO}_3)_3$ , making the sensor alkaline and producing  $\text{Bi}(\text{OH})_3$  or its derivatives. Measurements showed pH 11 for the sensor. The sensor was then used immediately or stored under nitrogen at room temperature until use.

### **7.2.3. Laboratory generation of 1.35-L, ppb-ppm $\text{H}_2\text{S}$ gas and its sensing**

Few reports of devices for generating ppb-ppm  $\text{H}_2\text{S}$  gas, especially at small volumes such as 1.35 L, are in the literature.

A 1.35-L glass chamber was designed and prepared in the glass-blowing shop at the University of Tennessee. This volume was chosen to mimic the breath volume of an average human. With a closed top and open bottom, the chamber was designed to seal flatly on the surface of a stir plate, as shown in a

schematic in Figure 7.1. The chamber has two inlets for nitrogen gas and/or deionized water, and one outlet for generated H<sub>2</sub>S. Additional details of the setup, including a photo, and the process to generate H<sub>2</sub>S gas in nitrogen are given in the Appendix D.

Prior to the generation of H<sub>2</sub>S gas, a small open crystallizing dish is filled with 70 mL of HCl solution at pH 1, bubbled with nitrogen gas for 10 min, and placed on the surface of a stir plate. A small vial containing fresh Na<sub>2</sub>S solution (made by dissolving a known amount of NaHS·1.25 H<sub>2</sub>O in pH 11 NaOH solution), and an upright stir bar is then placed in the crystallizing dish holding the HCl solution. The chamber (Figure 7.1A) is placed over top of these containers and sealed tightly to the stir plate using household Vaseline grease. This seal is strong enough to make the entire vessel water tight.

To remove all O<sub>2</sub> and avoid the oxidation of S<sup>2-</sup> to S, the chamber is flushed with nitrogen gas through the two inlets (Figure 7.1A). Next, all inlets and the outlet are closed, and the stir plate is turned on, knocking over the Na<sub>2</sub>S solution into the HCl solution (Figure 7.1B), and generating H<sub>2</sub>S gas (Eq. 7.4).



One inlet is kept sealed, deionized water (previously bubbled with nitrogen gas) is introduced into the chamber through the lower inlet, filling the chamber and pushing the 1.35 L of H<sub>2</sub>S/N<sub>2</sub> gas through the outlet (Figure 7.1C). A hose connected to the outlet directs the gas to the sensor that is pre-moistened with

80  $\mu\text{L}$  of 0.1 M NaOH. A plastic micro pipette tip is firmly sealed to the end of the outlet hose, and funnels the generated gas to a smaller area (roughly a 3 mm diameter) directly onto the surface of the sensor. The generated gas is forced through the sensor by using a porous wire mesh as the sensor support, and by keeping the pipette tip of the outlet hose directly in contact with the sensor. This allows for more interaction between  $\text{Bi}^{3+}$  and  $\text{S}^{2-}$ . The 1.35-L chamber is filled with water after a period of roughly 60 s, at which point the water flow is stopped and the sensor is removed.

Several measures were taken to avoid the loss of analyte before it reached the sensor. At such low concentrations of  $\text{S}^{2-}$  ions, its oxidation prior to weighing and/or after being placed in solution would have an effect on the overall detection. NaHS was always handled under a nitrogen flow to prevent oxidation. All solutions that NaHS was added to were bubbled with nitrogen gas. Despite these measures, some of the generated  $\text{H}_2\text{S}$  may be left in the solution of the chamber.<sup>38,39</sup> *For the tests in this part, it is assumed that the maximum possible amount of  $\text{H}_2\text{S}$ , based on the total volume of 1.35 L and the amount of NaHS used, was generated.*

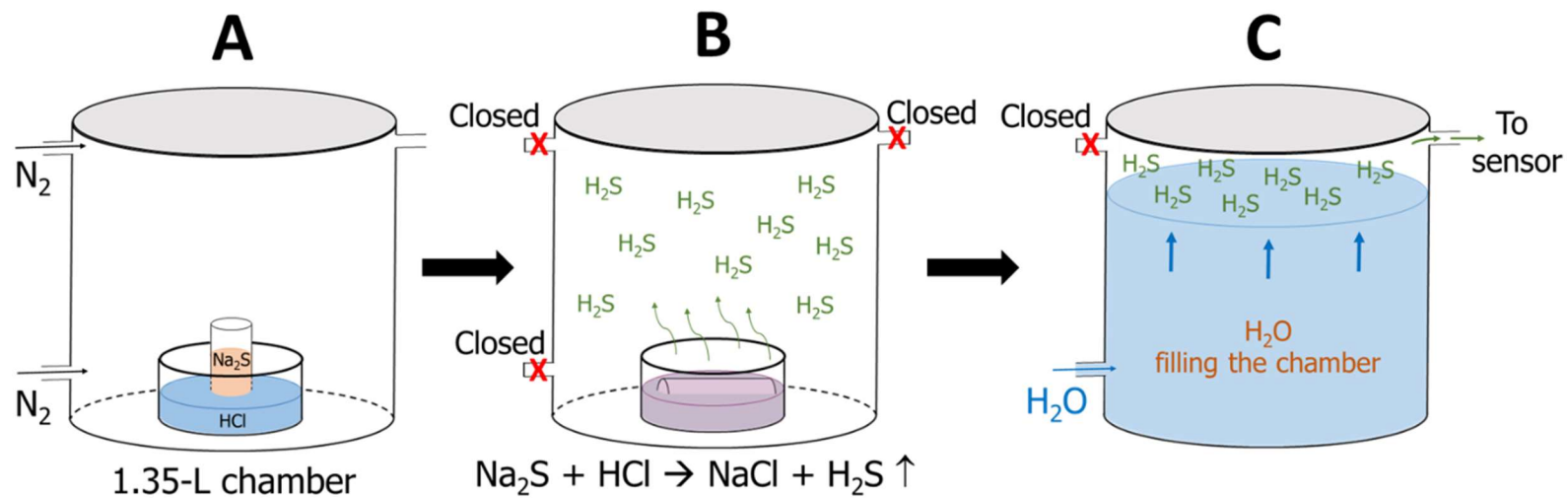


**Figure 7.1.** Schematic of H<sub>2</sub>S gas generation in a 1.35-L vessel: (A) Initial setup; (B) Flipping of the vial containing Na<sub>2</sub>S solution to react with HCl solution; (C) Use of deaerated, deionized water to push out the 1.35 L of H<sub>2</sub>S gas out of the chamber to the sensor.

### **7.3. Results and discussion**

The colorimetric detection here relies on the reaction of sulfide with Bi(III). When H<sub>2</sub>S, a colorless gas, reacts with white Bi(OH)<sub>3</sub> powder, it forms the yellow/brown compound Bi<sub>2</sub>S<sub>3</sub> (Eq. 2). At high concentrations, the color of Bi<sub>2</sub>S<sub>3</sub> is dark to black, while at low concentrations it appears yellow. The contrast of the yellow/black Bi<sub>2</sub>S<sub>3</sub> spot on the white Bi(OH)<sub>3</sub> background is imperative for the sensitivity in naked-eye detection. Dampening the sensor prior to exposure of the analyte enhances the reaction rates and the formation of color Bi<sub>2</sub>S<sub>3</sub>. The ideal substrate for this sensor is one that is absorbent and porous enough to allow gas to pass through and consistently textured to give a large surface area. After numerous trials with different substrates, Prozorb was found to be the best.

We have also tested several Bi(III) complexes including Bi(III)-EDTA, Bi(III)-diethylene triamine pentaacetic acid (DTPA), and Bi(III)-triethanolamine. While the Bi complexes show a better solubility than bismuth hydroxide, and thus a higher Bi(III) concentration on the sensor, their reactions with H<sub>2</sub>S were found to be slower, probably because S<sup>2-</sup> ions need to replace the organic ligands in the process. Thus sensors made with the Bi complexes gave larger spots but lighter in color in tests with NaHS solution (pH 11), and a higher detection limit when performing gas-based tests.

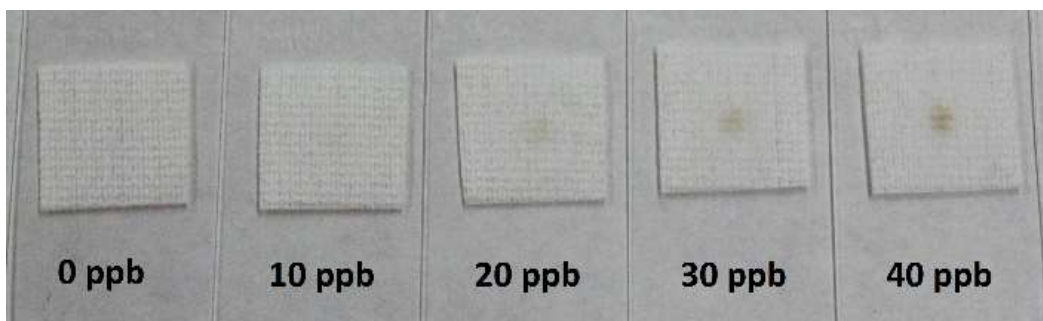
Tests were performed to determine if wetting the sensor using solutions of basic NaHCO<sub>3</sub> would result in the same sulfide detection range as more basic solutions like 0.1 M NaOH. In these tests, which used varying concentrations of

NaHCO<sub>3</sub>, the limits of detection were much higher (above 100 ppb H<sub>2</sub>S) than those using NaOH. This is most likely due to the formation of (BiO)<sub>2</sub>CO<sub>3</sub> which is less reactive to H<sub>2</sub>S than Bi(OH)<sub>3</sub>.

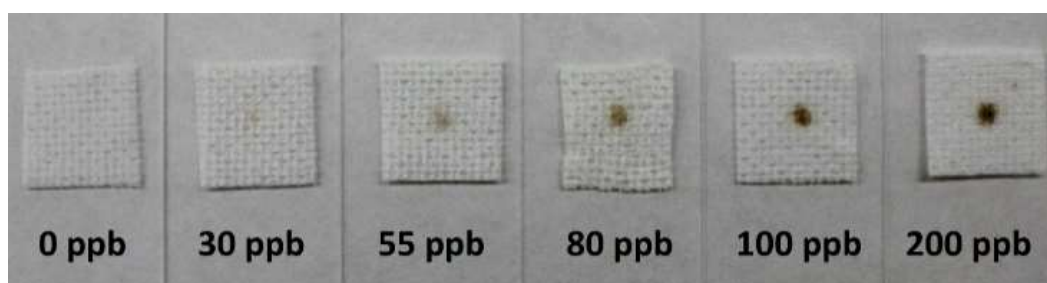
After the verification that the basic Bi(OH)<sub>3</sub> (and its derivatives) resulted in a lower LOD and quicker response times, Bi(III) concentration within the Prozorb substrate was then optimized before tests with H<sub>2</sub>S gas. Volumes of 0, 50, 100, 200, 300, 500, and 1000 μL of Bi(NO<sub>3</sub>)<sub>3</sub>/acetone suspensions were deposited on the Prozorb squares using aliquots of 100 μL with 2 min drying time between depositions. Liquid solutions of NaHS (pH 11) indicated that 200 μL of the Bi(NO<sub>3</sub>)<sub>3</sub>/acetone suspension was optimal; less than 200 μL developed a lighter spot and more than 200 μL showed no clear improvement (Figure D.2 in Appendix D). The Prozorb without the Bi coating remained white when exposed to NaHS. The naked-eye limit of detection is closer to 10 ppb (gas equivalency) when using a volume of 20 μL of the NaHS solution. Sensors discussed below were prepared using the 200 μL of the Bi(NO<sub>3</sub>)<sub>3</sub>/acetone suspension. Solution tests on a batch of newly optimized sensors showed obvious, increasingly dark spots with increasing NaHS concentrations (Figure 7.2).

Figure 7.3 shows six sensors, each of which was exposed to 1.35 L of different H<sub>2</sub>S gas concentrations from our H<sub>2</sub>S generator. The current LOD is 30 ppb (Figure 7.2), based on detection by the naked eye. This is a significant improvement upon the 5-10 ppm detection limit of the commercial lead acetate papers.





**Figure 7.2.** Sensors after being exposed to 20  $\mu\text{L}$  of pH 11 *solutions* of varying NaHS concentrations. Concentrations shown (0–40 ppb  $\text{S}^{2-}$ ) are in terms of *gas equivalency*: Concentrations of  $\text{H}_2\text{S}$  gas in 1.35 L of  $\text{N}_2$  gas.



**Figure 7.3.** Six sensors after being exposed to 0 to 200 ppb  $\text{H}_2\text{S}$  gas.

Given that humans with bad breath have an average H<sub>2</sub>S concentration of 80 ppb,<sup>2</sup> and that the average human breath volume is 1.35 L, our sensor has the appropriate detection limit for halitosis. This was tested in the laboratory by giving a human subject raw onion to eat. After 30 min, the subject blew through a plastic straw onto our sensor which developed a light brown spot, indicating the presence of sulfides.

There are two options with the sensor: (1) Pre-made, alkaline (pH 11), wet sensor stored *under nitrogen* that is ready for use; (2) Sensor with dry Bi(NO<sub>3</sub>)<sub>3</sub> coatings stored *in air* that, after adding the NaOH solution, is ready for use. The Bi(NO<sub>3</sub>)<sub>3</sub> coating on the sensor, before the addition of the basic solution, is stable for weeks without losing sensitivity. Furthermore, longevity tests showed that keeping the pre-made sensors under nitrogen for over a month did not affect the sensitivity in comparison to freshly fabricated sensors. Storing under nitrogen is needed with the pre-made sensor to avoid reactions of CO<sub>2</sub> in air with the base in the sensor, forming CO<sub>3</sub><sup>2-</sup> and perhaps (BiO)<sub>2</sub>CO<sub>3</sub>, reducing sensor sensitivity.

It is interesting to note that, because of Prozorbor's high absorption capacity, the supernatant is readily soaked up, spreading the Bi(NO<sub>3</sub>)<sub>3</sub> coating evenly throughout. This was confirmed by adding 50 μL of 1.0 M NaOH to a dry, coated sensor and placing it in an oven at 70 °C for 10 min. The heating process converted Bi(III) ions to the bright yellow Bi<sub>2</sub>O<sub>3</sub>. The even yellow coloring (Figure 7.4) demonstrated the consistent distribution of Bi(III) throughout the substrate.

It has also been found through several solution tests that, similar to lead acetate test strips, our sensor is capable of detecting many other sulfide species

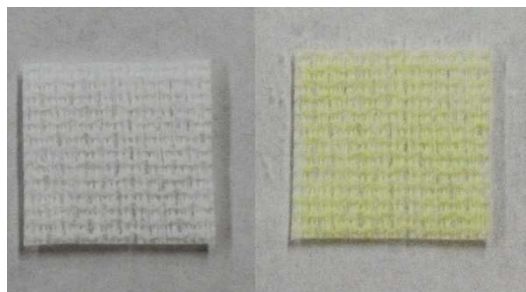


**Figure 7.4.** Test showing that Bi(III) is spread evenly throughout the sensor.

including mercaptans. This increases the usefulness of the sensor in lab and health settings.

Our Bi(III)-based sensor was also evaluated through side by side comparisons with a commercially available lead acetate paper in tests using H<sub>2</sub>S gas, mercaptan solutions, and NaHS solutions. In all tests, our sensor outperformed the lead acetate test strips, and in many cases there was no observable change in the lead acetate test strips, including in exposure to 1.35 L of H<sub>2</sub>S at concentrations between 30 ppb and 5 ppm. For verification purposes, 50 ppm H<sub>2</sub>S was directed from a gas cylinder onto the surface of a damp lead acetate test strip and then onto an optimized Bi(OH)<sub>3</sub> sensor at a flow rate of 89 mL min<sup>-1</sup>. Both sensors immediately developed dark black spots upon exposure, indicating that both sensors respond to H<sub>2</sub>S at high concentrations.

#### **7.4. Conclusion**

In summary, several features of the novel sensor reported herein are unique and some are critical to its high sensitivity: (1) Alkaline coatings to trap

acidic H<sub>2</sub>S gas; (2) Wet coatings to facilitate the kinetics of the reaction between H<sub>2</sub>S and Bi(OH)<sub>3</sub>. In comparison, other reported processes/patents usually use either a solution or a dry salt; (3) Benign bismuth to replace toxic lead; (4) A total volume of 1.35 L of ≥30 ppb H<sub>2</sub>S gas for the naked-eye detection limit, making it suitable for the detection of halitosis. In comparison, reported/patented processes, including testing using lead acetate test papers, often require a much larger volume of ppm-level H<sub>2</sub>S. At a given concentration, a larger volume of the H<sub>2</sub>S gas delivers more reactant H<sub>2</sub>S to the sensor, making it easier for less sensitive sensors to detect H<sub>2</sub>S; (4) A large detection range, including 50 ppb—the current LOD of the US Environmental Protection Agency (EPA) detection method,<sup>40-41</sup> 80 ppb—the average H<sub>2</sub>S concentration qualified as ‘bad breath’ in a typical human breath volume,<sup>2</sup> and 10 ppm—the OSHA Permissible Exposure Limit.<sup>41</sup> Our highly sensitive sensor is thus fast, direct, easy to use, and non-toxic. However, its alkalinity (pH 11) requires care in handling and that the sensor be stored inside an inert gas to avoid neutralization by acidic CO<sub>2</sub> in air. It may be developed into safe, disposable commercial test strips for H<sub>2</sub>S gas which do not currently exist on the market. The increasing depth of color with increasing H<sub>2</sub>S concentrations indicates that this detection may be developed into a semi- or fully quantitative method. The sensor also has the potential for both human bad breath tests and industrial H<sub>2</sub>S detection in, e.g., mining, petroleum, and natural gas industries.

## References

1. U.S. Occupational Safety and Health Administration, *Hydrogen Sulfide in Work Places*  
[https://www.osha.gov/SLTC/hydrogensulfide/hydrogensulfide\\_found.html](https://www.osha.gov/SLTC/hydrogensulfide/hydrogensulfide_found.html)
2. Van Den Velde, S. *J. Dent. Res.* **2009**, *88*, 285-289.
3. Tangerman, A.; Winkel, E.G. *Phosphorus, Sulfur, Silicon and Related Elements.* **2013**, *188*, 396-402.
4. Colborn, T.; Kwiatkowski, C.; Schultz, K.; Bachran, M. *Hum. Ecol. Risk Assess.* **2011**, *17*, 1039-1056.
5. Weinhold, B. *Environ. Health. Persp.* **2012**, *7*, A273-A279.
6. Daldal, H.; Beder, B; Serin, S.; Sungurtekin, H. *Clin. Toxicol.* **2010**, *48*, 755-756.
7. (a) Song, L.; Morris, J.; Hasemyer, D. Fracking Boom Leaves Texans Under a Toxic Cloud. *Bloomberg Business*, February 20, 2014. (b) Neuhauser, A. Toxic Chemicals, Carcinogens Skyrocket near Fracking Sites. *U.S. News & World Report*, October 30, 2014. (c) Hopkins, J.S. High Levels of Dangerous Chemicals Found in Air Near Oil and Gas Sites. *National Geographic*, November 1, 2014.
8. Pandey, S.K.; Kim, K.-H.; Tang, K.-T. *Trends Anal. Chem.* **2012**, *32*, 87-99.
9. Wang, C.; Chu, X.; Wu, M. *Sensor Actuat B.* **2006**, *113*, 320-323.
10. Advani, G.; Nanis, L. *Sensor Actuator.* **1982**, *2*, 201-206.

11. Liu, J.; Huang, X.; Ye, G.; Liu, W.; Jiao, Z.; Chao, W.; Zhou, Z.; Yu, Z. *Sensors*. **2003**, *3*, 110-118.
12. Sarfraz, J.; Ihalainen, P.; Määttänen, A.; Gulin, T.; Koskela, J.; Wilén, C.-E.; Kilpelä, A.; Peltonen, J. *Sensor Actuat B*. **2014**, *191*, 821-827.
13. Virji, S.; Kaner, R.B.; Weiller, B.H. *Inorg. Chem.* **2006**, *45*, 10467-10471.
14. Sarfraz, J.; Määttänen, A.; Törngren, B.; Pesonen, M.; Peltonen, J.; Ihalainen, P. *RSC Adv.* **2015**, *5*, 13525-13529.
15. Sarfraz, J.; Tobjörk, D.; Österbacka, R.; Lindén, M. *IEEE Sens. J.* **2012**, *12*, 1973-1978.
16. Liu, Y.; Feng, G. *Org. Biomol. Chem.* **2014**, *12*, 438-445.
17. Wallace, K.J.; Cordero, S.R.; Tan, C.P.; Lynch, V.M.; Anslyn, E.V. *Sensor Actuat B*. **2007**, *120*, 362-367.
18. Zhang, D.; Jin, W. *Spectrochim Acta A*. **2012**, *90*, 35-39.
19. Adarsh, N.; Krishnan, M.S.; Ramaiah, D. *Anal. Chem.* **2014**, *86*, 9335-9342.
20. Deng, H.-H.; Weng, S.-H.; Huang, S.-L.; Zhang, L.-N.; Liu, A.-L.; Lin, X.-H.; Chen, W. *Anal. Chim. Acta* **2014**, *852*, 218-222.
21. El Sayed, S.; Milani, M.; Licchelli, M.; Martinez-Máñez, R.; Sancenón, F. *Chem. Eur. J.* **2015**, *21*, 7002-7006.
22. Gao, Z.; Tang, D.; Tang, D.; Niessner R.; Knopp, D. *Anal. Chem.* **2015**, *87*, 10153-10160.
23. Tang, Y.-W.; Stratton, C.W. *Advanced Technology in Diagnostic Microbiology*, Springer Science: New York, 2013.
24. Sanderson, H.P. *J. Air Pollut. Control Assoc.* **1966**, *16*, 328-330.

25. A Scifinder search on August 25, 2015 showed that there were at least the following publications since 2010 that relied on lead acetate paper for sulfide detection: (a) Tong, L.P.; Fei, Y.; Yang, H. *Adv. Mater. Res.* **2012**, *395*, 1462-1465. (b) Oguri, T.; Schneider, B.; Reitzer, L. *J. Bacteriol.* **2012**, *194*, 4366-4376. (c) Tellis, R. *Int. J. Biomed. Res.* **2012**, *3*, 174-180. (d) Luksiene, B.; Druteikiene, R.; Peculyte, D.; Baltrunas, D.; Remeikis, V.; Paskevicius, A. *App. Rad. Isot.* **2012**, *70*, 442-449. (e) Myamoto, K.; Hoque, M.; Ogasa, S. *J. Org. Chem.* **2012**, *77*, 8317-8320. (f) Tofalo, R.; Schirone, M.; Torriani, S.; Rantsiou, K.; Cocolin, L.; Perpetuini, G.; Suzzi, G. *Food Microbiol.* **2012**, *29*, 18-26. (g) Tan, T.; Liu, C.; Liu, L.; Zhang, K.; Zou, S.; Hong, J.; Zhang, M. *Bioprocess Biosyst. Eng.* **2013**, *10*, 1363-1373. (h) Binta, M.G.; Baipoledi, E.K.; Nyange, J.C.; Mushi, E.Z. *J. Pet. Enviro. Biotechnol.* **2012**, *3*, 1-5. (i) Sonia, G.A.S.; Lipton, A.P. *Indian J. Geo-Marine Sci.* **2012**, *41*, 348-354. (j) Pagnanelli, F.; Viggi, C.C.; Cibati, A.; Uccelletti, D.; Toro, L.; Palleschi, C. *J. Haz. Mat.* **2012**, *15*, 186-192. (k) Chiarella, G.M.; Cotton, F.A.; Ibragimov, S. A.; Murillo, C. A.; Wilinon, C. C.; Young, M. D. *Polyhedron* **2013**, *58*, 7-12. (l) Saa, L.; Pavlov, V. *Small* **2012**, *8*, 3449-3455. (m) Alvarez, M. T.; Pott, B.-M.; Chavez, G.; Gimenez, A.; Hatti-Kaul, R.; Mattiasson, B. *Int. J. Env. Waste Manag.* **2012**, *9*, 313-324. (n) Amin, A.; Latif, Z. *Pak. J. Bot.* **2013**, *45*, 1437-1442. (o) Zhang, Y.; Weiner, J. H. *BioTechniques.* **2014**, *57*, 208-210. (p) Gong, C.; Liu, X.; Jiang, X. *Poult. Sci.* **2014**, *93*, 702-710. (q) Ma, J.; Wang, L.; Liu, Y. *Acta Agric. Bor.-Occi. Sin.* **2013**, *22*, 168-172. (r) Ji, L.; Liao, Q.; Lu, W.; Wu, L.; Yang, M.;

- Wan, L. *Chin. J. Exp. Trad. Med. Form.* **2013**, *19*, 66-69. (s) Meyer, S.; Smith, S.; Meyer, R.; Howe, J. *Technical Papers of ISA 2012*, 489(ISA 57th Analysis Division Symposium, 2012), a27/1-a27/14. (t) Shafique, U.; Anwar, J.; Salman, M.; Dar, A.; Rehman, R.; Azeem, M.; Ameer, S. *J. Sulfur Chem.* **2011**, *32*, 151-157. (u) Gao, F.; Jia, Y.-Z.; Sun, J.-H.; Jing, Y.; Yao, Y.; Ma, J.; Xia, C.-L. *J. Salt Lake Res.* **2010**, *18*, 22-25. (v) Ugliano, M.; Henschke, P. A. *Anal. Chim. Acta.* **2010**, *660*, 87-91. (w) Zhang, Y; Weiner, J. H. *BioTechniques* **2014**, *57*, 208-210. (x) Kar, S.; Majumdar, R. K.; Chaudhuri, M. K. *J. Geol. Soc. India.* **2014**, *84*, 35-40.
26. [http://www.amazon.com/Precision-Laboratories-Lead-Acetate-paper/dp/B001DBH4DQ/ref=sr\\_1\\_3?ie=UTF8&qid=1440613832&sr=8-3&keywords=lead+acetate#product-description-iframe](http://www.amazon.com/Precision-Laboratories-Lead-Acetate-paper/dp/B001DBH4DQ/ref=sr_1_3?ie=UTF8&qid=1440613832&sr=8-3&keywords=lead+acetate#product-description-iframe), accessed on August 26, 2015.
27. Stone, G.C. *J. Amer. Chem. Soc.* **1896**, *18*, 1091-1091.
28. ZoBell, C.E.; Feltham, C.B. *J. Bacteriol.* **1934**, *28*, 169-176.
29. Pacheco and Mello recommended the use of a culture media containing suspended, water-insoluble bismuth carbonate to detect H<sub>2</sub>S. Pacheco, G.; Mello, J.T., *C.R. Séances Soc. Biol. Ses. Fil.* **1932**, *110*, 131-132.
30. Clarke, P.H. *J. Gen. Microbiol.* **1953**, *8*, 397-407.
31. Wilson, W.J.; Blair, E. M.M. *J. Hygiene*, **1927**, *26*, 374-391.
32. Patterson Jr., G.D.; Pappenhagen, J.M. *Sulfur in Colorimetric Determination of Nonmetals*, D.F. Boltz, J.A. Howell eds., (*Chemical Analysis*, P. J. Elving, J.D. Winefordner, I. M. Kolthoff, Vol. 8, 2<sup>nd</sup> ed.) Wiley, 1978, Ch. 12, pp.



463-527.

33. Field, E.; Oldach, C.S. *Industrial and Engineering Chemistry, Analytical Edition*, **1946**, *18*, 665-667.
34. Dean, G.A. *Analyst*, **1966**, *91*, 530-532.
35. Ghosh, A.K.; Banerjee, N.N. Hydrogen Sulfide Detector Tubes, Indian patent, IN 110409 19690809, 1969.
36. Sinclair, R.A.; Glasspoole, E.A., US Patent 4,019,865, H<sub>2</sub>S Indicator, 4/26/1977. This patent uses Bi(NO<sub>3</sub>)<sub>3</sub> or bismuth subnitrate and needs a flow of 1 ppm H<sub>2</sub>S for *one day*.
37. Yoshimura, M.; Nakayama, K.; Ohara, N.; Takehara, N.; Yoshida, A., WO 2007/052635 A1, Method for Rapid Detection of Oral Bacterium, 10/31/2006.
38. Carroll, J.J.; Mather, A.E. *Geochim. Cosmochim. Acta*. **1994**, *53*, 1163-1170.
39. Kendall, J.; Andrews, J.C. *J. Am. Chem. Soc.* **1921**, *43*, 1545–1560.
40. US EPA's *Current H<sub>2</sub>S Detection Method*. February 11, 2000, <http://www.epa.gov/ttn/emc/promgate/m-16.pdf>
41. OSHA Permissible Exposure Limits: [http://www.osha.gov/dts/chemicalsampling/data/CH\\_246800.html](http://www.osha.gov/dts/chemicalsampling/data/CH_246800.html)

## **PART 8**

### **Concluding remarks**

While the work described in this dissertation can have many applications, the central focus is on the detection of environmental toxins. Parts 2, 3, and 4 of this work are based on newly updated regulations concerning the allowed concentrations of elemental impurities within active pharmaceutical ingredients (API) and excipients. With the new guidelines come new requirements for detection methods, which the work herein attempts to address using electroanalytical chemistry. These studies will eventually be combined into one technique that will detect many of the regulated elements simultaneously. Part 2 concerns the direct quantification of cadmium and lead, two of the most toxic heavy metals, in solutions containing pharmaceutical components using anodic square-wave stripping voltammetry. With the assistance of a bismuth codeposition, detection of the metals can be performed individually or simultaneously, in either water or 95/5 DMSO/water solutions. This work marks the first time that heavy metals have been analyzed in DMSO solutions using anodic stripping voltammetry (ASV).

In the next part, ASV was used to detect the catalytic metal palladium in pharmaceutical matrices. The novel use of this method is important for several reasons. First, palladium is included in the new international regulations concerning impurities in pharmaceuticals and excipients and can have adverse health effects on patients. Second, residual palladium may lead to unwanted side reactions during subsequent steps in synthesis, lowering the yields of final products. Third, a consistent loss of palladium throughout the multi-step synthesis of APIs could quickly become costly. Similar to the previous study,

palladium can be detected in the presence of API and excipients dissolved in either water or 95/5 DMSO/water solutions. Unlike the work with cadmium and lead, bismuth is not required for the detection of palladium in aqueous pharmaceutical matrices. In the DMSO solutions, bismuth codeposition is still required. This study also included cadmium and lead in both media showing that all three metals, along with bismuth, can be detected simultaneously.

Part 4 of this dissertation focuses on the detection of mercury in aqueous solutions containing dissolved API and excipients. The results of this work indicate the potential of ASV as a method that can meet the new pharmaceutical regulation requirements. Bismuth is not required for the analysis of mercury in the pharmaceutical matrices, making it simple to use. However due to differing electrolyte requirements mercury cannot be detected simultaneously with cadmium, lead or palladium. To the best of our knowledge, this is the first time mercury has been analyzed in solutions containing pharmaceutical ingredients.

The fifth part of this dissertation concerns the trace analysis of hexavalent chromium, a strong oxidizer and known carcinogen, in aqueous solutions. Using a glassy carbon electrode modified with single-walled carbon nanotubes coated with a pyridinium/sol-gel thin film, the electrochemical sensor yields a detection limits of 0.3 ppt (parts per trillion) and exhibits high selectivity and precision. The film thickness was optimized based on iridescence observations: both uniformity of color as well as the color itself. The electrode surface was further characterized via scanning electrode microscopy.

Two novel methods for the pretreatment of whole blood were developed and optimized based on the Fenton reaction, as reported in Part 6 of this dissertation. One method utilizes a synthesis microwave, and is capable of mineralizing a sample within 6 min. The second method uses an inexpensive laboratory oven over a period of 5 h, allowing for a fast option and an inexpensive option. Post-treatment samples were analyzed using ASV, and the results were validated through comparison with ICP-OES (inductively coupled plasma–optical emission spectroscopy). The analyses indicated that the methods were highly effective and capable of being exploited in laboratory and medical settings.

The final part of this collection of work, Part 7, describes the development of a simple, disposable, bismuth-based optical sensor for the detection of hydrogen sulfide ( $\text{H}_2\text{S}$ ), a gas that is dangerous at high concentrations and is also the main contributor to bad breath, in low concentrations. Alongside the sensor, a system for generating low concentrations of  $\text{H}_2\text{S}$  gas at a set volume of 1.35 L (the volume of an average human's breath) was also created. Through the use of alkaline  $\text{Bi}(\text{OH})_3$ , the sensor is able to trap the  $\text{H}_2\text{S}$  gas, which is a weak acid, and react with it immediately to form the yellow/brown  $\text{Bi}_2\text{S}_3$ . The lowest concentration visible with the naked eye was determined to be 30 ppb, exhibiting a detection range that includes the current LOD of the US Environmental Protection Agency (EPA) detection method, the average  $\text{H}_2\text{S}$  concentration qualified as 'bad breath' in a typical human breath volume, and the OSHA Permissible Exposure Limit.

## **APPENDICES**

## Appendix A

Appendix A provided additional materials for Part 2.

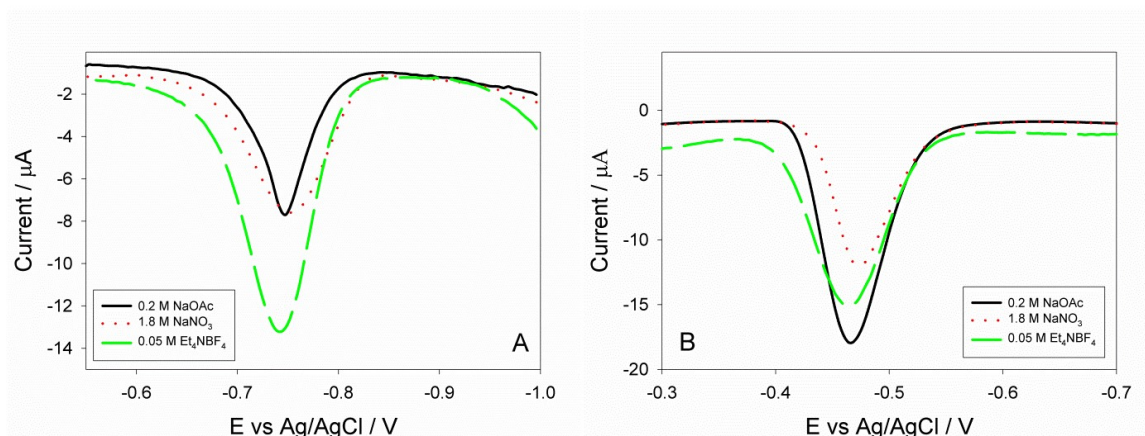


**Figure A.1.** Voltammograms depicting the supporting electrolyte's effect on the sensitivity of detecting Cd(II) (A) and Pb(II) (B) in aqueous solutions. Electrolytes tested were 0.2 M NaOAc (black solid line), 1.8 M NaNO<sub>3</sub> (red dotted line), and 0.05 M Et<sub>4</sub>NBF<sub>4</sub> (green dashed line). The best electrolyte (0.05 M Et<sub>4</sub>NBF<sub>4</sub>) was chosen through the comparison of Cd(II) and Pb(II) peak areas, both at concentrations of 50 μg L<sup>-1</sup>.

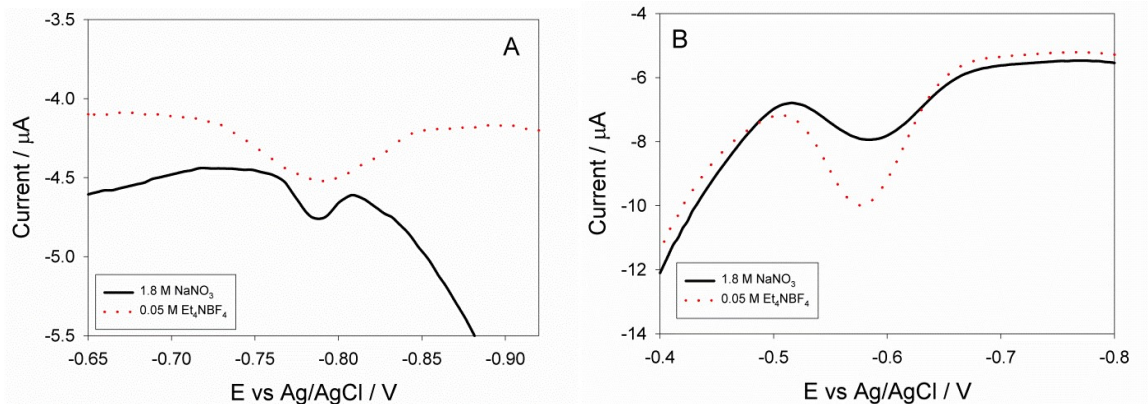


**Figure A.2.** Voltammograms depicting the supporting electrolyte's effect on the sensitivity of detecting Cd(II) (A) and Pb(II) (B) in 95/5 DMSO/water solutions. Electrolytes tested were 1.8 M NaNO<sub>3</sub> (black solid line) and 0.05 M Et<sub>4</sub>NBF<sub>4</sub> (red dotted line). The best electrolyte (0.05 M Et<sub>4</sub>NBF<sub>4</sub>) was chosen through the comparison of Cd(II) and Pb(II) peak areas, both at concentrations of 50 µg L<sup>-1</sup>.

## A.1 Apparent recoveries

### A.1.1. Apparent recoveries of [Pb(II)] and [Cd(II)] in the presence of 1000 mg L<sup>-1</sup> caffeine (aqueous solution)

An aqueous solution containing 1000 mg L<sup>-1</sup> caffeine [and 0.05 M Et<sub>4</sub>NBF<sub>4</sub>, 2.5 mg L<sup>-1</sup> Bi(III)] was spiked to 10.0 µg L<sup>-1</sup> Pb(II) and 15.0 µg L<sup>-1</sup> Cd(II). The sample was treated as an unknown, and standard addition was performed with simultaneous spiking of both metals between each analysis to added concentrations of 5.0, 10.0, 20.0, 30.0, 50.0, and finally 80.0 µg L<sup>-1</sup>. By placing the initial concentrations at [M(II)] = 0, the analyses produced the linear regression  $y = 0.0206x + 0.2348$  ( $R^2 = 0.999$ ) for Pb(II) and  $y = 0.0102x + 0.1645$  ( $R^2 = 0.998$ ) for Cd(II) (Figure A.3). Calculating the initial “unknown”



concentration of the metals gave  $11.4 \mu\text{g L}^{-1}$  Pb(II) and  $16.2 \mu\text{g L}^{-1}$  Cd(II) with apparent recoveries of 114% and 108%, respectively.

In another test, Cd(II) was detected in a new aqueous 1000 ppm caffeine solution ( $0.05 \text{ M Et}_4\text{NBF}_4$ ), using a different electrode, three months after making the calibration curve of Cd(II) in the presence of caffeine. The solution was spiked to  $2.5 \mu\text{g L}^{-1}$  Bi(III) and  $20 \mu\text{g L}^{-1}$  Cd(II) before being analyzed in triplicate. The average peak area fell within the error bars, giving a concentration of  $22 \pm 0.4 \mu\text{g L}^{-1}$  Cd(II), and an apparent recovery of 111%.

#### ***A.1.2. Apparent recoveries of [Pb(II)] and [Cd(II)] in 95/5 DMSO/H<sub>2</sub>O solutions***

A 95/5 DMSO/H<sub>2</sub>O solution containing  $1000 \text{ mg L}^{-1}$  ketoprofen [ $0.05 \text{ M Et}_4\text{NBF}_4$ ,  $10.0 \text{ mg L}^{-1}$  Bi(III)] was spiked to  $5.0 \mu\text{g L}^{-1}$  Pb(II) and  $25.0 \mu\text{g L}^{-1}$  Cd(II). Standard addition was performed with simultaneous spiking of both metals between each analysis to added concentrations of 10.0, 20.0, 25.0, 40.0 and finally  $50.0 \mu\text{g L}^{-1}$  (Table A.1). At this point, the  $[\text{Pb(II)}]_{\text{initial}}$  was treated as an unknown by placing it at  $[\text{Pb(II)}] = 0$ . The Pb(II) curve produced a linear regression of the equation  $y = 0.0022x + 0.0101$  ( $R^2 = 0.997$ ), and calculating the  $[\text{Pb(II)}]_{\text{initial}}$  concentration gave  $4.59 \mu\text{g L}^{-1}$  and an apparent recovery of 91.8%.

**Table A.1.** Calibration curve for Cd(II) and Pb(II) with 1000 mg L<sup>-1</sup> caffeine in 95/5 DMSO/H<sub>2</sub>O

<b>[Cd(II)] / μg L<sup>-1</sup></b>	<b>A<sub>p</sub> (Cd Peak Area) / μVA</b>	<b>A<sub>p</sub>'</b>	<b>[Pb(II)] / μg L<sup>-1</sup></b>	<b>Pb Peak Area / μVA</b>
25.0	0.007677	24.47	5.0	0.01298
35.0	0.02915	35.72	15.0	0.03001
45.0	0.05527	44.67	25.0	0.05183
50.0	0.07464	49.90	30.0	0.06602
65.0	0.1497	65.05	45.0	0.1006
75.0	0.2152	74.94	55.0	0.1213

Due to the non-linear nature of Cd(II) in the presence of sulfide impurities in the DMSO, the initial concentration cannot be calculated through extrapolation, as is the case for linear calibrations in standard addition. We have thus developed a method to derive the concentration of Cd(II) solution by addition of standards.

In this approach, the logarithmic regression (Eq. A.1) was obtained first from a set of standards (Table A.1, Figure A.4).

$$A_p = 5.006e^{-6}[Cd(II)]^{2.478} + 6.144e^{-3} \quad \text{Eq. A.1}$$

$R^2 = 0.999$ ;  $A_p$  = peak area

The lowest Cd(II) concentration here was 25.0  $\mu\text{g L}^{-1}$ , the detection limit. It should be noted that the logarithmic regression in Eq. A.1 depends on [Pb(II)]. That is, the three parameters in Eq. A.1 are functions of [Pb(II)].

Eq. A.2 is then converted into a *linear* form by using  $A_p'$  in Eq. A.2, giving Eq. A.3.

$$A_p' = \left( \frac{A_p + 6.144e^{-3}}{5.006e^{-6}} \right)^{\frac{1}{2.478}} \quad \text{Eq. A.2}$$

$$A_p' = [\text{Cd(II)}] \quad \text{Eq. A.3}$$

Since Eq. A.3 is linear, we have used it in conjunction with standard addition to determine the unknown [Cd(II)] in a solution. In the example below, initial concentrations of Cd(II) and Pb(II) were recovered through standard addition and the use of Eq. A.3 in the case of Cd(II).

A 95/5 DMSO/H<sub>2</sub>O solution containing 1000 mg L<sup>-1</sup> ketoprofen [0.05 M Et<sub>4</sub>NBF<sub>4</sub>, 10.0 mg L<sup>-1</sup> Bi(III)] was spiked to 5.0  $\mu\text{g L}^{-1}$  Pb(II) and 40.0  $\mu\text{g L}^{-1}$  Cd(II), which were treated as [Pb(II)]<sub>initial</sub> and [Cd(II)]<sub>initial</sub>, respectively. Standard addition was performed with simultaneous spiking of both metals between each analysis to added concentrations of 10.0, 20.0, and 30.0  $\mu\text{g L}^{-1}$  (Table A.2). The Cd peak area ( $A_p$ ) was then individually transposed into  $A_p'$  using Eq. A.2 and the data are given Table A.2. In other words, the calibration of the previous Cd(II) standards was used here to calculate  $A_p'$ . Plotting [Cd(II)]<sub>added</sub> vs.  $A_p'$  produced a linear regression (Figure A.5,  $R^2 = 0.999$ ) which, through extrapolation, was used to

calculate  $[\text{Cd(II)}]_{\text{initial}}$ . This calculation gave  $[\text{Cd(II)}]_{\text{initial}}$  of  $39.8 \mu\text{g L}^{-1}$  and an apparent recovery of 99.5%. The  $[\text{Pb(II)}]:[\text{Cd(II)}]$  ratios here were different from the previous calibration in Table A.1, but within the small range of the concentrations of both metal ions tested, the effects were negligible.

**Table A.2.** Standard addition for Cd(II) and Pb(II) with  $1000 \text{ mg L}^{-1}$  ketoprofen in 95/5 DMSO/H<sub>2</sub>O

$[\text{Cd(II)}]_{\text{added}} / \mu\text{g L}^{-1}$	$A_p$ (Cd Peak Area) / $\mu\text{VA}$	$A_{p'}$	$[\text{Pb(II)}]_{\text{added}} / \mu\text{g L}^{-1}$	Pb Peak Area/ $\mu\text{VA}$
0.00	0.08011	51.23	0.00	0.01881
10.0	0.1461	64.44	10.0	0.04954
20.0	0.2306	77.00	20.0	0.08407
30.0	0.3425	90.02	30.0	0.1195

Standard addition of Pb(II) in this study also produced a linear regression (Figure A.6), yielding  $[\text{Pb(II)}]_{\text{initial}} = 5.15 \mu\text{g L}^{-1}$  and an apparent recovery of 97.1%.

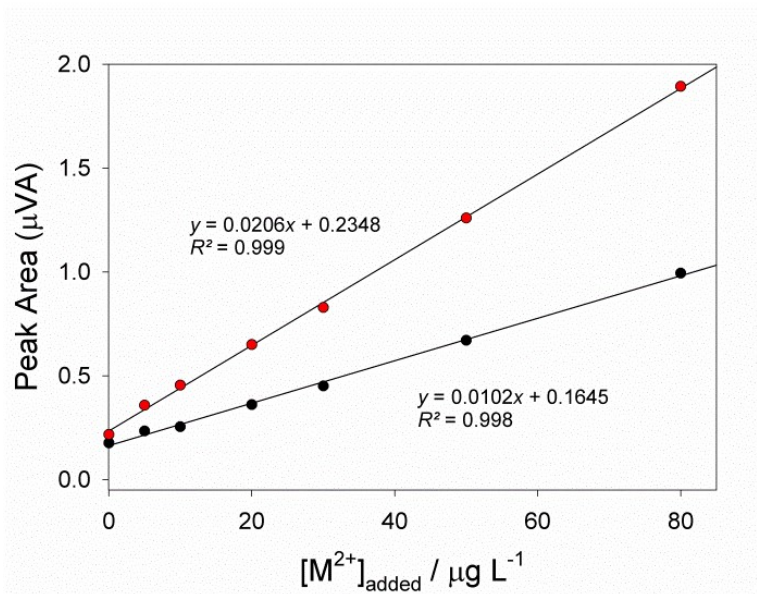


**Figure A.3.** Simultaneous standard additions of Cd(II) (black) and Pb(II) (red) in an aqueous solution containing 1000 mg L<sup>-1</sup> caffeine, 0.05 M Et<sub>4</sub>NBF<sub>4</sub>, and 2.5 mg L<sup>-1</sup> Bi(III).

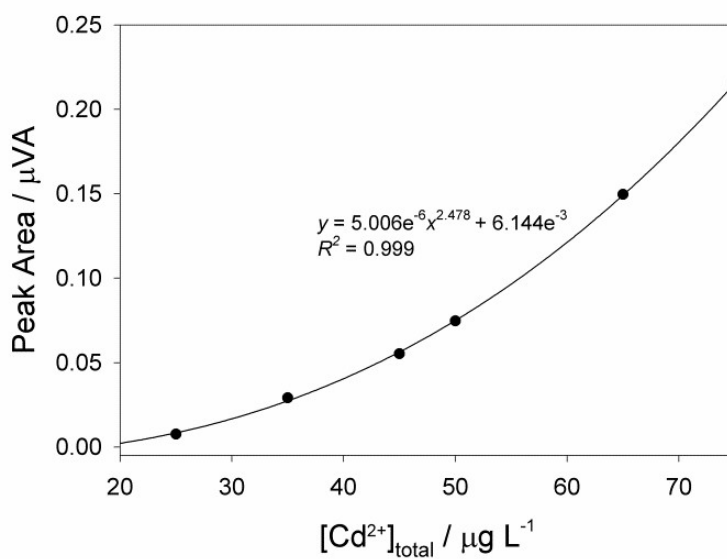


**Figure A.4.** Calibration plot of Cd(II) in the presence of increasing Pb(II), 1000 mg L<sup>-1</sup> ketoprofen, 0.05 M Et<sub>4</sub>NBF<sub>4</sub>, and 10.0 mg L<sup>-1</sup> Bi(III), in 95/5 DMSO/H<sub>2</sub>O.

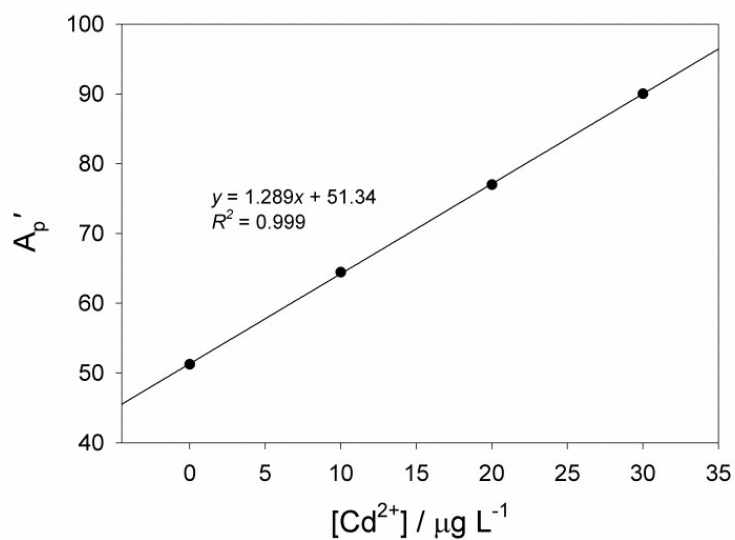


**Figure A.5.** Linearized Cd(II) standard addition calibration, using Eq. A.3, through simultaneous standard additions of Cd(II) and Pb(II) in 95% DMSO containing 1000 mg L<sup>-1</sup> ketoprofen, 0.05 M Et<sub>4</sub>NBF<sub>4</sub>, and 10.0 mg L<sup>-1</sup> Bi(III).

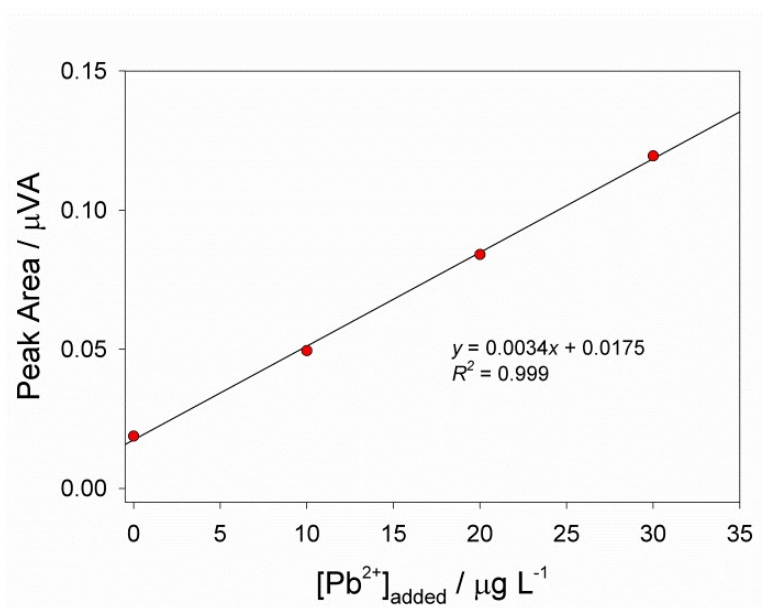


**Figure A.6.** Linear regression of Pb(II) through simultaneous standard additions of Cd(II) and Pb(II) in 95% DMSO containing 1000 mg L<sup>-1</sup> ketoprofen, 0.05 M Et<sub>4</sub>NBF<sub>4</sub>, and 10.0 mg L<sup>-1</sup> Bi(III).

## Appendix B

Appendix B provided additional materials for Part 3.

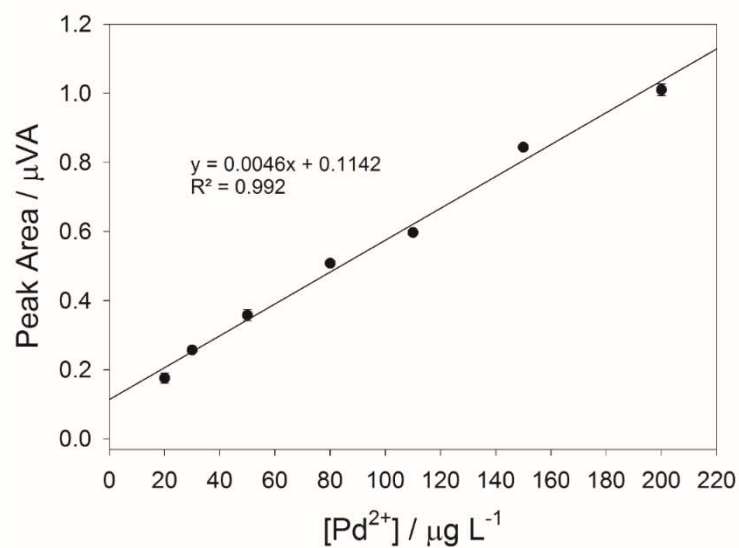


**Figure B.1.** Linear regression for the analysis of Pd(II), codeposited with Bi(III) (10 mg L<sup>-1</sup>) in 95% DMSO/5% water.

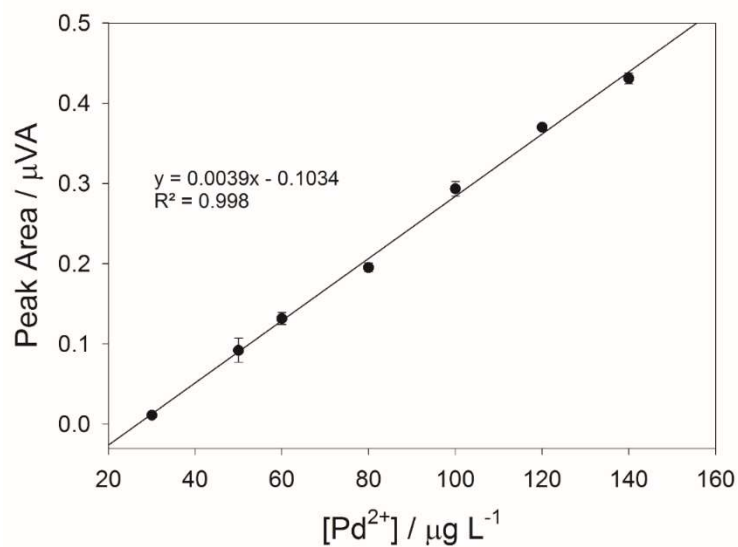


**Figure B.2.** Linear regression for the analysis of Pd(II) in aqueous solutions in the presence of 1000 mg L<sup>-1</sup> caffeine. No Bi(III) codeposition was used.

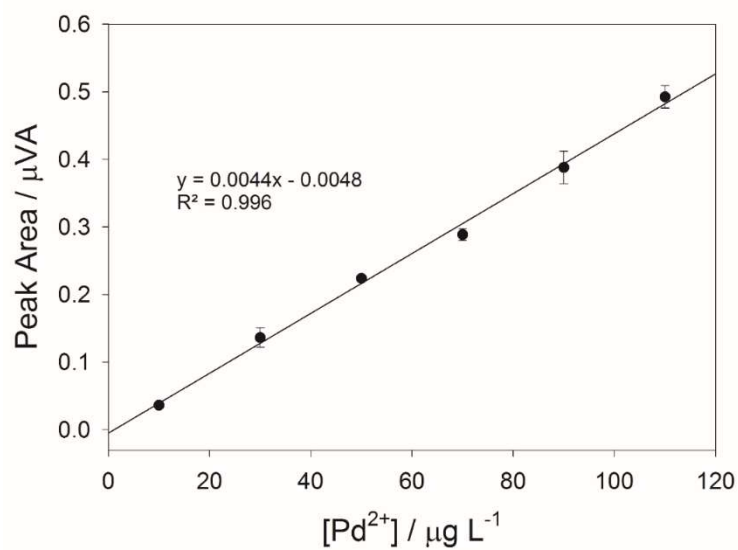


**Figure B.3.** Analysis of Pd(II), codeposited with 10 mg L<sup>-1</sup> Bi(III) in 95/5 DMSO/water in the presence of 1000 mg L<sup>-1</sup> ketoprofen.



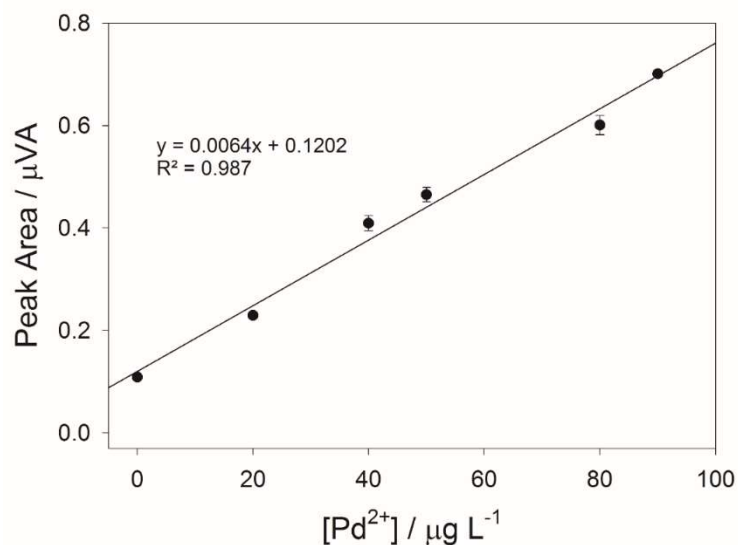


**Figure B.4.** Recovery of Pd(II) (original concentration of 20 μg L<sup>-1</sup>) through the standard addition method in an aqueous solution containing 1000 mg L<sup>-1</sup> caffeine. No Bi(III) codeposition was used.

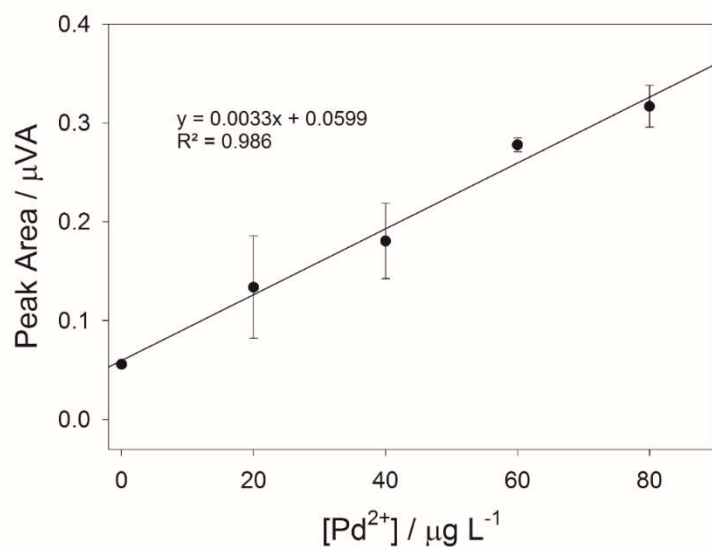


**Figure B.5.** Recovery of Pd(II) (original concentration of 20 μg L<sup>-1</sup>) through the standard addition method in a 95/5 DMSO/water solution containing 1000 mg L<sup>-1</sup> ketoprofen. The Pd(II) was codeposited using Bi(III).

## Appendix C

Appendix C provided additional materials for Part 4.

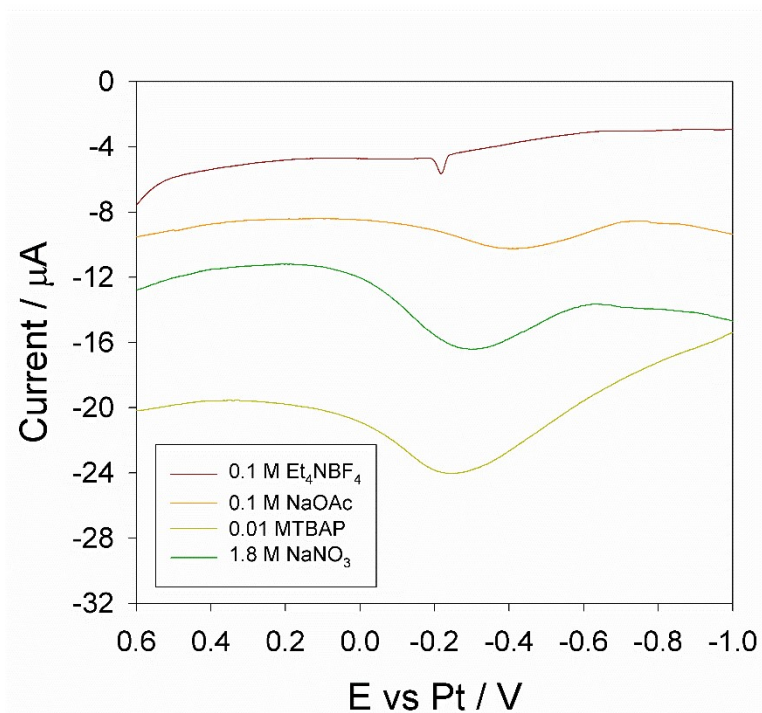


**Figure C.1.** Voltammograms depicting the supporting electrolyte's effect on the Hg(II) peak. The best electrolyte (0.01 M TBAP) was chosen through the comparison of the Hg(II) peak area at concentrations of  $100 \mu\text{g L}^{-1}$ .

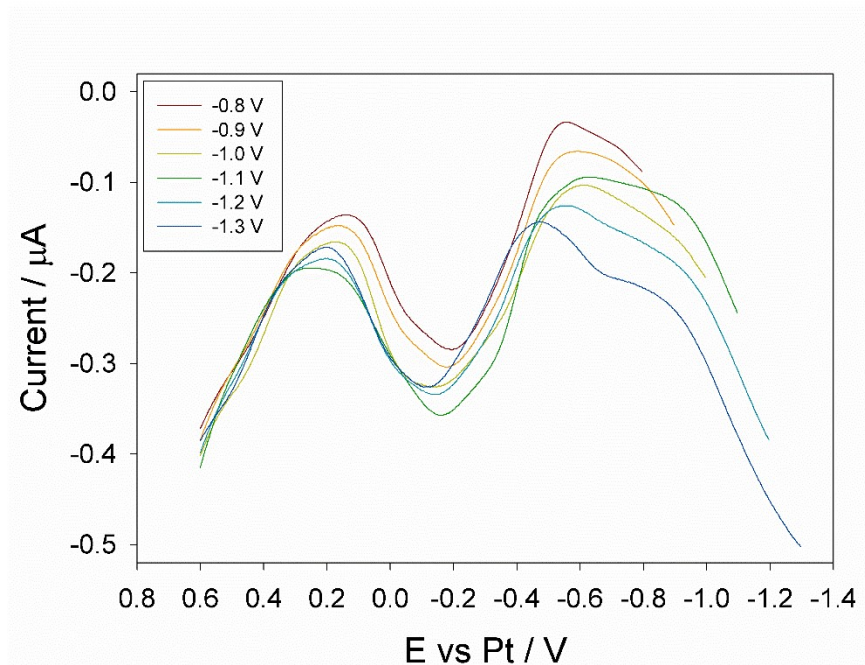


**Figure C.2.** Voltammograms collected from preconcentration potential optimization studies.

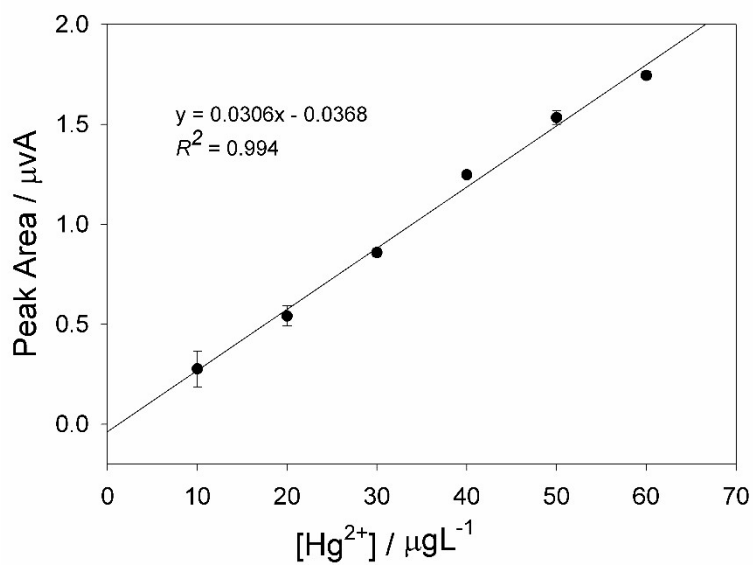


**Figure C.3.** Standard additions of  $\text{Hg}(\text{II})$  in an aqueous solution containing  $1000 \text{ mg L}^{-1}$  caffeine.

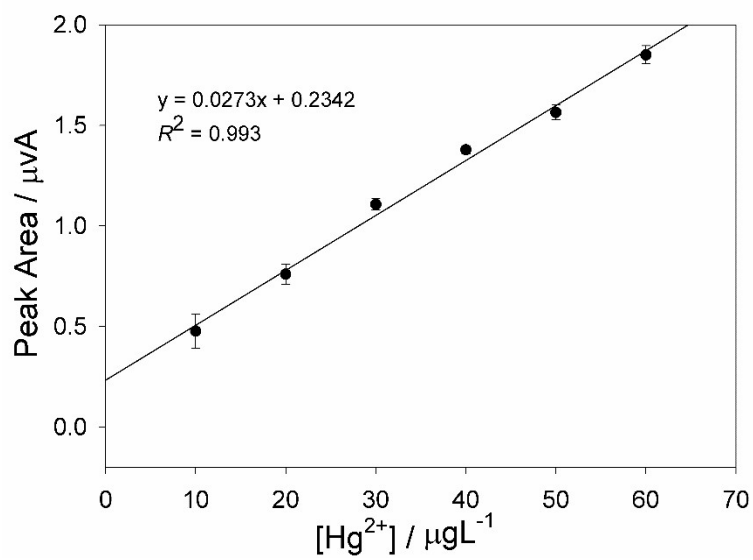


**Figure C.4.** Standard additions of Hg(II) in an aqueous solution containing  $1000 \text{ mg L}^{-1}$  lactose.

## Appendix D

Appendix D provided additional materials for Part 7.

### ***D.1. Laboratory Generation of 1.35-L, ppb-ppm H<sub>2</sub>S Gas and Its Sensing***

Few reports of devices for generating ppb-ppm H<sub>2</sub>S gas, especially at a small volume of 1.35-L, have been reported in the literature.

A 1.35-L glass chamber was made in the glass-blowing shop at the University of Tennessee. This volume was chosen to mimic the breath volume of an average human. With a closed top and open bottom, the chamber was designed to sit flat on a stir plate (Figure D.1, **A**). The chamber has one outlet for the generated gas (Figure D.1, **E**), one inlet used for nitrogen gas, followed by water (Figure D.1, **D**), and another inlet attached to a small, internal capillary used for bubbling nitrogen gas (Figure D.1, **C**).

Prior to generation of H<sub>2</sub>S gas, a small container is filled with 70 mL of HCl solution at pH 1. A loosely capped vial containing a NaHS solution and an upright stir bar is then placed, standing, in the container holding the acidic solution. The chamber (Figure D.1, **A**) is placed over top of these containers and sealed tightly to the stir plate using household Vaseline grease. This seal is strong enough to make the entire vessel water tight. To remove all oxygen and avoid the oxidation of S<sup>2-</sup> to S, reaction chamber **A** is flushed with nitrogen gas through hose **D**, and the acidic solution is bubbled through the internal capillary attached to hose **C** for 10 min. The ultrapure DI water in container **B** is simultaneously bubbled with nitrogen gas as well.

A sensor, previously dampened with 80  $\mu\text{L}$  of 0.1 M NaOH, is placed on a wire mesh as the sensor stand (Figure D.1, **F**). A plastic micro pipette tip has been firmly attached and sealed to hose **E** and funnels the generated gas to a smaller area (roughly a 3 mm diameter) directly onto the surface of the sensor. This pipette tip is held so that it is in direct contact with the sensor. The nitrogen gas is clamped off at hose **D** and lowered to a very slow flow through hose **C**. The stir plate is then turned on at a high rate, knocking the vial of the NaHS solution into the HCl solution and forming  $\text{H}_2\text{S}$  gas (Eq. 7.4). At this point the water (also bubbled with  $\text{N}_2$ ) of container **B** is allowed to slowly travel into the reaction chamber **A** via hose **D** using gravitational flow. As chamber **A** is filled with water, it pushes out the generated  $\text{H}_2\text{S}$  gas through hose **E** onto the sensor at **F**. Direct contact between the pipette tip of hose **E** and the sensor at **F** forces the gas through the sensor, allowing for more interaction between  $\text{Bi(III)}$  and  $\text{S}^{2-}$ . The acidity of solution in the container is enough that even when diluted to 1.35 L after mixing, the pH is still 3.

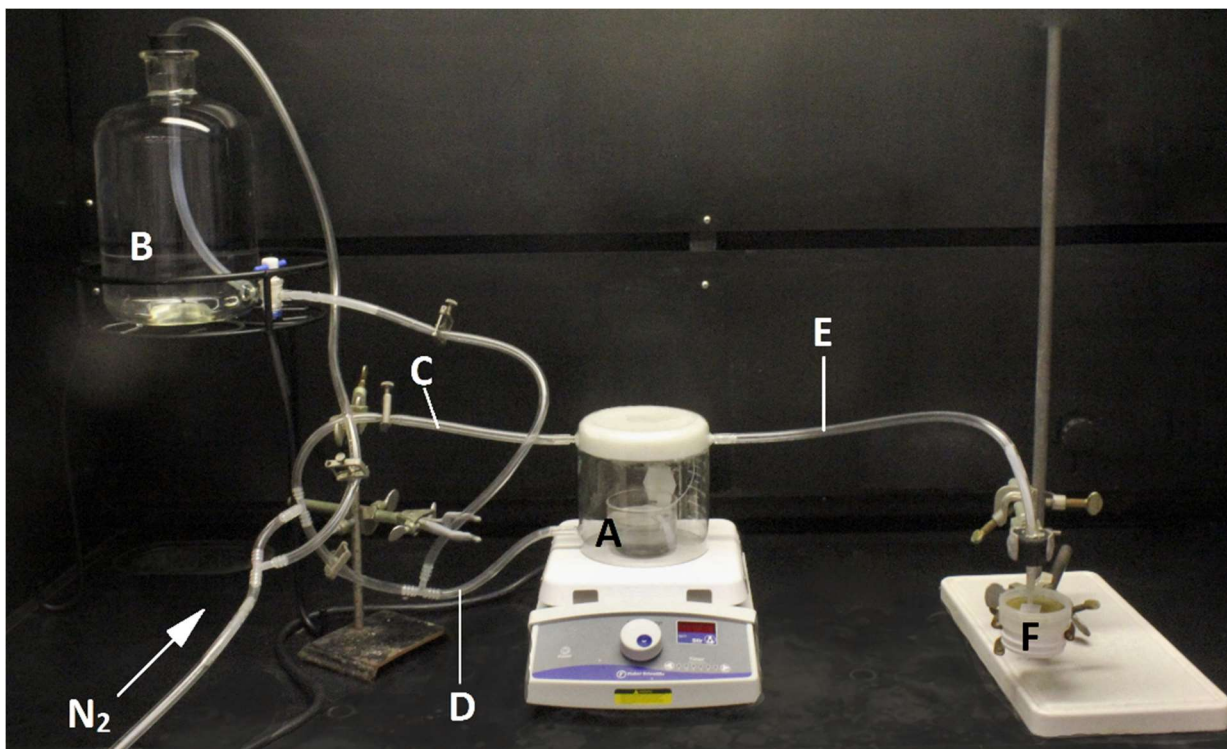


**Figure D.1.** The system to generate H<sub>2</sub>S gas. **A:** Reaction chamber; **B:** Water container; **C:** N<sub>2</sub>-inlet hose; **D:** Water-inlet hose; **E:** Gas-outlet hose; **F:** Wire mesh as the sensor stand.

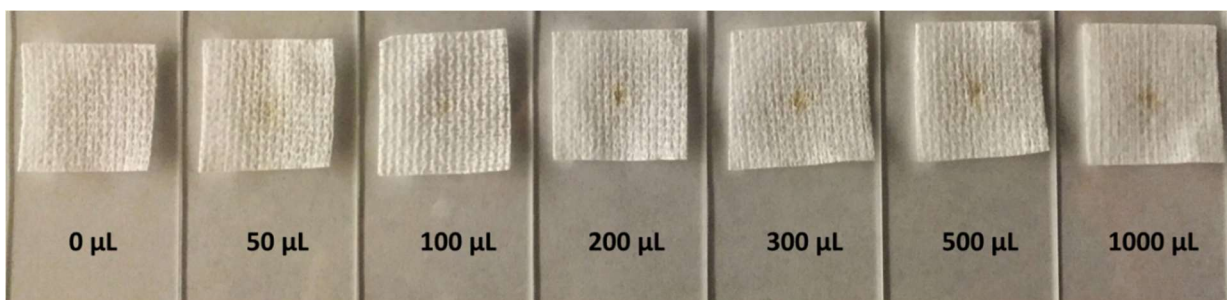


**Figure D.2.** Volumes of 0, 50, 100, 200, 300, 500, and 1000 μL of Bi(NO<sub>3</sub>)<sub>3</sub>/acetone suspensions were deposited on the ProzorB squares. Note no spot development for the ProzorB containing no Bi.

## VITA

Samuel M. Rosolina was born on February 10, 1988 and grew up in the mountains of northeast Tennessee, which shaped his appreciation for the outdoors and cultivated his love of science. In 2010 he received his bachelor's degree in chemistry at Berea College in Kentucky. After graduating, he travelled to a sustainable community in Washington state to perform research on biomass gasification applications before taking an extra semester to intern at Eastman Chemical Company where he worked with novel polymer products. He entered the chemistry Ph.D. program at UTK in January 2011, joining the Xue analytical lab in May of the same year. Sam's research and interests have revolved around the development of simple, inexpensive sensors and methods to detect environmental toxins.